DE NOVO EXPRESSION AND FUNCTION OF THE EPITHELIAL MUCIN MUC1 ON T CELLS

by

Jessica Candelora Kettel

B.S. in Microbiology, The Ohio State University, 1996

Submitted to the Graduate Faculty of

School of Medicine in partial fulfillment

of the requirements for the degree of

Doctor of Philosophy

University of Pittsburgh

2003

UNIVERSITY OF PITTSBURGH

FACULTY OF SCHOOL OF MEDICINE

This dissertation was presented

by

Jessica Candelora Kettel

It was defended on

August 29th 2003

and approved by

Timothy M. Carlos, MD
Associate Professor, Department of Medicine

JoAnne Flynn, Ph.D.
Associate Professor, Department of Molecular Genetics and Biochemistry

Rebecca Hughey, Ph.D.
Associate Professor, Department of Medicine

Penelope Morel, MD
Associate Professor, Departments of Immunology and Medicine

William Ridgway, MD
Associate Professor, Department of Medicine

Olivera J. Finn, Ph.D.
Dissertation Director
Professor, Department of Immunology

DE NOVO EXPRESSION AND FUNCTION OF THE EPITHELIAL MUCIN MUC1 ON T CELLS

Jessica Candelora Kettel, PhD

University of Pittsburgh, 2003

MUC1 has conventionally been studied as an epithelial cell surface molecule. Its glycosylation and expression change when those cells are transformed into adenocarcinomas. These changes have led to focus on MUC1 as a tumor antigen and also its role in adhesion to blood vessels and signaling within the tumor cell. The recent discovery that T cells also express MUC1 on their surface extends the physiological role of MUC1, with the possibility that functions observed in tumors may be reproduced on T cells.

Expression of MUC1 on T cells was first characterized in terms of timing, location and structure. T cells activated both *in vivo* and *in vitro* express MUC1. Expression *in vitro* is maintained over long time periods as the T cell population acquires the memory phenotype. Activated T cells induced to polarize by inflammatory conditions focus MUC1 expression to their leading edge, the sensory compartment of polarized T cells. Reactivity with glycosylation-sensitive antibodies and induction of glycosyltransferases indicates that the glycosylation of MUC1 on T cells is similar to that on normal epithelial cells.

A MUC1-negative T cell line was transfected with MUC1 cDNA and used as a model to investigate consequences of MUC1 expression on the T cell surface. Interaction of $MUC1^+$ T cells with resting or activated endothelial cells revealed that MUC1 aids in adhesion under both normal and inflammatory conditions. Analysis of interactions with individual adhesion molecules demonstrated MUC1 specific enhancement of binding to ICAM-1 but inhibition of

binding to E-selectin. Phosphorylation of the MUC1 intracytoplasmic tail is constitutive but decreases upon interaction with activated endothelium. MUC1 expression on T cells is also associated with differential phosphorylation of proteins in the molecular weight ranges of 39 kDa, ~80 kDa and 190 kDa, with the ~80 kDa band identified as β-catenin.

While human T cells express MUC1 on their surface upon activation, this does not appear to be a characteristic of mouse T cells from the human MUC1 transgenic mouse model. However, as recent work indicates that mouse T cells express mouse Muc-1 after activation, human and mouse T cells may similarly depend on MUC1 for normal functioning.

ACKNOWLEDGMENTS

"Be anxious for nothing, but in everything by prayer and supplication, with thanksgiving, let your requests be made known to God; And the peace of God, which surpasses all understanding, will guard your hearts and minds through Christ Jesus."

written by Paul the apostle in 60-61 A.D. during his imprisonment in Rome.

I wanted to start my Acknowledgments with this verse as it has been my prayer since I decided to become a Christian believer in 1998. Through the many ups and downs of graduate school I've found that my oftentimes tenuous hold on peace has grown, and there are many people God has blessed my life with whom I'd like to thank.

Olja, your kindness and generosity are an inspiration to me. I hope to be as welcoming to others as you have been to me and my husband since I first met you. At times when I felt I was more of a burden to your lab than a help you reassured me and I can't express my appreciation enough. My committee members have been always ready with assistance, ideas and guidance throughout my project and I thank you for your willingness and time. The members, past and present, of the Finn lab have made coming to school each day fun and encouraging. To mention each person's touch on my life would take more space than I have here but each has been a blessing to me in different ways.

My parents, Judy & Steve Anderson, Debby & Nick Candelora, Mary & Leonard Kettel, and siblings Nicole Candelora, James & Connie Candelora deserve a salute for supporting my continuous schooling with only occasional inquiries about when I'd be done. Your sustaining love has been bedrock for me, thank you. I'd also like to thank the many friends who have listened to me, prayed for me and reminded me when I needed it that there is more to life than

graduate school. Finally, my husband Michael whose encouragement and support are the most appreciated as they have been present despite the numerous demands my schooling has made on you. Never once have you complained about bringing me food during late work nights, picking me up after midnight from lab or my bringing work home. You amaze me and I'm so thankful to be married to you.

With much appreciation,

Jessica C. Kettel

TABLE OF CONTENTS

LIST OF TABLES

LIST OF FIGURES

1.0 INTRODUCTION

1.1 MUC1 Structure

MUC1 is expressed both as a transmembrane and a secreted glycoprotein. Though it is encoded as a single molecule, the type I transmembrane form is a heterodimer (Figure 1.0-1). The two proteins that make up MUC1 differ greatly in size with most of MUC1 larger fragment being composed of a tandemly repeated 20 amino acid sequence PDTRPAPGSTAPPAHGVTSA. This serine, threonine and proline rich sequence can be repeated up to 100 times in a single MUC1 molecule, commonly occurring between 41-85 times (1, 2). This region is referred to as VNTR for variable number of tandem repeats.

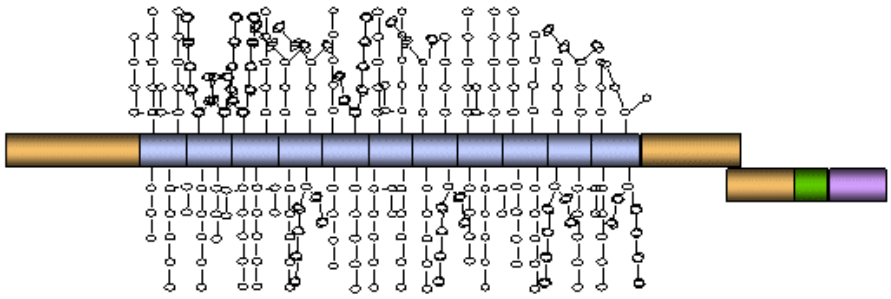

Figure 1.0-1 Structure of MUC1. The 72 amino acid cytosolic tail is shown in purple. The 28 amino acid transmembrane domain is shown in green. The VNTR region is shown in blue while the remaining extracellular portions of MUC1 shown in tan. The extensive O-linked glycosylation in the VNTR region is indicated with the stick figures.

The biosynthesis of MUC1 proceeds via distinct steps (3). The newly synthesized protein receives several N-glycans adjacent to its transmembrane region following co-translational transfer of high-mannose glycans during synthesis in the endoplasmic reticulum. Within 1 –2 minutes, while still in the endoplasmic reticulum, MUC1 undergoes proteolytic cleavage. Ligtenberg et al (4) showed in 1992 that the 2 cleavage products remain non-covalently associated so that the smaller transmembrane fragment anchors the larger piece. A proteolytic cleavage site, FRPG/SVW, located 65 amino acids upstream of the transmembrane domain was

identified recently (5). After cleavage, the precursors move through the Golgi where the N-glycans become more complex and O-glycosylation is started on the VNTR region. O-glycosylation increases the molecular weight dramatically within the first 30 minutes of synthesis. MUC1 becomes partially sialylated on its O-linked oligosaccharides before leaving the Golgi as a premature form. Completely and incompletely sialylated MUC1 are both expressed on the cell surface (6). Trafficking of MUC1 to the cell surface is thought to be controlled by at least two signals, one contained in Cys-Gln-Cys motif at the junction of the MUC1 cytoplasmic tail and transmembrane domains, and a second in the extracellular domain but outside of the VNTR region (7).

To become fully sialylated the premature form recycles several times from the cell surface to the trans-Golgi and back to the surface. Complete sialylation occurs within 3 hours (3). The recycling of MUC1 is constitutive so that even after full sialylation a mature MUC1 molecule will complete 10 cycles before being lost approximately 24 hours after synthesis. MUC1 on the surface of normal cells is completely sialylated, while on tumor cells the surface MUC1 is a combination of completely and incompletely sialylated molecules. It was suggested that this is due to greater abundance of MUC1 on tumor cells and/or less efficient sialylation process compared to normal cells (6).

NMR studies using peptides composed of one to three tandem repeats have shown that as the number of repeats increases the structure of MUC1 becomes more ordered. Indeed, intrinsic viscosity measurements indicate that the peptide composed of three repeats has a rod-like structure (8), suggesting that MUC1 on the cell surface would project outwards rather than exist in a globular shape. Further NMR studies established that in each repeat the immunodominant APDTR sequence exists on a protruding knob-like structure on the MUC1 backbone (9). When

multiple repeats are examined, the overall effect is a rod with evenly spaced knobs throughout the entire VNTR region. Most antibodies against MUC1 bind to this epitope making it immunodominant on the native MUC1 molecule (10).

Because of the large number of repeats in the VNTR region, MUC1 can extend 300-500 nm above the cell surface, towering over other cell surface molecules. Twenty-five percent of the amino acids in the VNTR region are either serine or threonine that can be O-glycosylated. On either side of the VNTR region are several degenerate repeats (11, 12). Recently, Engelmann, et al. provided genetic evidence of variation in the 20 amino acid sequence within the VNTR domain (12). By sequencing PCR products followed by minisatellite variant repeat analysis of the 5' and 3' peripheral areas of the VNTR region in 33 samples taken from normal and cancerous cells, they found that the same sequence variation consistently occurred in the same repeats, indicating that the variation predates the duplication event that has led to the elongated VNTR domain. The proline (triplet code, cca) in position 13 of the tandem repeat sequence PDTRPAPGSTAPPAHGVTSA could be altered to glutamine (caa), alanine (gca) or threonine (aca), possibly generating an additional glycosylation site. The other location of sequence change is in the immunodominant epitope, APDTR, in which the DT (gacacc) is substituted with ES (gagagc). This was the most commonly seen sequence variation within the diverse population studied. However, in only four of the 24 repeats sequenced from each of 33 samples was this variation found in the majority of samples. This particular variation within the immunodominant peptide sequence could be regarded as a source of additional epitopes with immunogenic potential; nevertheless, since this mutated (ES) sequence is less commonly seen than the conserved DT sequence found in the majority of repeats, one should expect the majority

of responses to be directed towards the highly conserved and overwhelmingly abundant tandem repeat sequences.

The smaller subunit (~ 20 kDa) of MUC1 contains a short extracellular portion, a transmembrane region and a short intracellular tail. In its extracellular domain is one site for N-linked glycosylation (2, 13). The transmembrane region carries cysteines that may be used for fatty acid acetylation to help anchor MUC1 in a cell's membrane (11). In the cytosolic tail are potential sites of phosphorylation and intracellular protein binding that prompted research into the possibility that MUC1 could be a signaling molecule (reviewed in section 3.1.2). This is especially of interest because the exact function of MUC1 is still being deciphered.

Alternative splicing of MUC1 mRNA can lead to multiple forms being expressed by a single cell type. When the full-length cDNA and genomic organization of MUC1 were initially published they showed that two different amino terminal signal sequences could be produced. The longer form, referred to as MUC1/A has an additional 27 base pairs when compared to MUC1/B (11, 13). Whether MUC1/A or MUC1/B was produced depends on whether a guanine or adenine is present 8 nucleotides downstream of exon 1, in the first intron. When guanine is present, the longer MUC1/A is synthesized and the number of repeats is higher. Conversely, when adenine is present the shorter isoform MUC1/B is made and there are fewer repeats (14). In 2001 Obermair et al, looking at cervical carcinoma cells, found two novel MUC1 splice variants (15). These were shorter than the variants described for normal MUC1 and were named MUC1/C and MUC1/D. Both are a result of alternative splice acceptor sites when joining exons one and two. Splice variants of MUC1 lacking the VNTR region (MUC1/Y, MUC1/X, and MUC1/Z) have also been reported. MUC1/Y transcripts and protein were found in primary

breast cancer tissue (16). MUC1/X (17) and MUC1/Z (18), both larger than MUC1/Y by 18 amino acids, were reported in cancer cell lines.

Soluble MUC1 is found in human milk (19, 20) and in barely detectable amounts in the serum of healthy men and women (21, 22). This form may be produced when a splice donor site downstream of the VNTR region is not used during transcription, allowing translation of a stop codon prior to the transmembrane region (13). In 1996 a monoclonal antibody was generated against this novel out peptide sequence (23). With this antibody, soluble MUC1 was detected in supernatant of a cancer cell line and in sera of cancer patients. However, mouse mammary epithelial cells transfected with full-length human MUC1 in which alternative splicing could not occur (24), still produced soluble MUC1 lacking the cytosolic tail. This supports a second mechanism that that MUC1 might be released from the surface of cells by proteolytic cleavage (25). TACE (TNFα converting enzyme) is considered the likely protease responsible for the cleavage (26). Other potential mechanisms for producing soluble MUC1 are cleavage by external proteases or simple dissociation of the heterodimeric complex. The involvement of external proteases is not likely given that addition of proteolytic inhibitors has no effect on amounts of shed MUC1 (27). Simple dissociation seems unlikely as well, given that MUC1 remains a stable heterodimer during repeated recycling through the cell for further glycosylation and sialylation (6, 14). Furthermore, when a mutated form of MUC1 that lacks the site of initial proteolytic cleavage is expressed as a single protein, it is still released from the cell (4).

1.2 MUC1 Glycosylation

Because of the differences in MUC1 glycoforms expressed on normal and cancerous epithelium, there has been a great effort to understand MUC1 O-linked glycosylation. The majority of MUC1 glycosylation occurs in the VNTR region on the two serines and/or three

threonines in each repeat. The most common carbohydrate addition to one of these amino acids is a core 2 structure (Figure 1.0-2B), an N-acetyl galactosamine that has a galactose branching from its third carbon and N-acetyl glucosamine branching from its sixth carbon. In normal MUC1 these branches are elongated and effectively cloak the peptide backbone. Only a minor fraction of normal MUC1 glycosylation consists of just core 1 additions (28). The core 1 structure (Figure 1.0-2A) is an N-acetyl galactosamine that has only the galactose branching from its third carbon, no addition to carbon 6. This yields a less effective cloaking of the peptide backbone and is predominantly seen on the tumor form of MUC1.

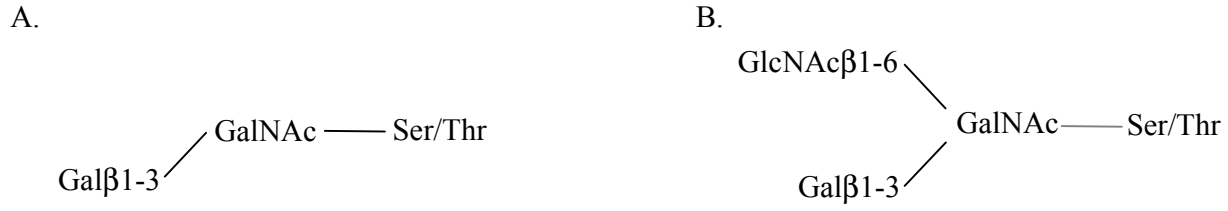

Figure 1.0-2 Core structures in MUC1. Core 1 (A) is common to the tumor form of MUC1 while core 2 (B) is common to the normally glycosylated form of MUC1.

While N-linked glycosylation occurs at known consensus sites, O-linked glycosylation motifs have not been identified. However human GalNAc transferases responsible for initiating O-linked glycosylation on MUC1 have been studied *in vitro* (29) and the *in vivo* products analyzed (30) using recombinant enzymes and MUC1 peptides. Regardless of whether the peptide contained one or five repeats [PDTRPAPGSTAPPAHGVTSA], *in vitro* only three of the five Ser/Thr sites per repeat were glycosylated. No glycosylation was seen on the Ser in GVTSA or Thr in DTR. Interestingly, the enzyme kinetics varied for the site being glycosylated, *e.g.* GalNAc-Transferase2 (T2) being the fastest of the transferases tested to glycosylate ST in GSTAP but slowest on T in GVTSA (29). Examining human milk however, all five potential sites were glycosylated *in vivo* with an average of 2.7 sites per repeat (30). The discrepancy between *in vitro* and *in vivo* work could be attributed to additional GalNAc transferases working

in vivo and an enhancing effect of previous glycosylation on subsequent glycosylation. This effect was demonstrated with a recombinant GalNAc-T4 that could glycosylate Ser in GVTSA and Thr in PDTR but only if the peptide had been previously O-glycosylated (31). Furthermore, transferases GalNac-T1, -T2 and -T3 glycosylated *in vitro* single MUC1 tandem repeat peptides at 0 – 4 sites. There were distant and neighboring effects on subsequent glycosylation, as well as enzymatic competition between transferases and core synthesizing enzymes that could help explain the MUC1 glycosylation differences between normal and cancer cells (32).

Subsequent to receiving the initial GalNAc on a serine or threonine (referred to as Tn antigen), galactose can be added by the core 1 β3-galactosyltransferase to make the core 1 disaccharide Galβ1-3GalNAc (also called T antigen). This can be a precursor to the branched core 2 O-glycan, Galb1-3(GlcNAcβ1-6)GalNAcα1-Ser/Thr. Other core structures can be found on MUC1 (28) and this will vary by cell type and differentiation state. However, the most common core type is the core 2 formed by adding galactose to carbon 3 and GlcNac to carbon 6 from the initially added GalNAc. These branching saccharides on carbons 3 and 6 can in turn be elongated. Fucose can also be added to subterminal and internal GlcNAc in α4 and α3 linkages. In cancerous cells expressing MUC1 the saccharide chains added to Ser/Thr do not extend beyond the core-type level (core 1 disaccharides accumulate) and sialylated glycans are more common than neutral glycans, in contrast to MUC1 from normal cells. This is attributed to lack of core 2 specific β-6-N-acetylglucosaminyltransferase activity (C2GnT) and an increase in α3 and/or α6-sialyltransferase activity. The latter terminates elongation of core 1 disaccharides by adding sialic acid to carbon 3 or carbon 6 of galactoses. In contrast to the short trisachharides (NeuAcα2-3Galβ1-3GalNAc and NeuAcα2-6(Galβ1-3)GalNAc) commonly seen on tumor MUC1, normal cells would synthesize long polylactosamine-type chains (up to 16

monosaccharides have been observed in human milk MUC1) (28). Additional studies are continuing to explore this highly dynamic regulation of O-glycosylation (33, 34).

1.3 Trafficking of T cells

The trafficking of T cells to sites within the body allows the immune system to specifically target its defenses. Endothelium at inflammatory sites express particular adhesion molecules that allow recruitment of T cells activated within secondary lymphoid organs that also express unique endothelial adhesion molecules (35-42). The inflammatory trafficking process can be broken down into sequential major steps, beginning with T cell adhesion to vascular walls (38, 40-42). First is the tethering and rolling of T cells at a slower speed along the sides of blood vessels. Villous projections from the T cell surface express adhesion receptors that contact ligands on the lumen walls to slow T cell transit through the vessel. These initial interactions predominantly involve selectins which can bind with high tensile strength in an easily reversible and transient manner to their ligands, carbohydrate structures presented by a variety of proteins. L (leukocyte) -selectin is utilized by T cells while E (endothelial) - and P (platelet) -selectins are employed by inflamed endothelium.

Having slowed down the T cell, the next step in trafficking involves further interactions with other molecules on the vessel wall. Activating factors such as chemokines on the endothelial surface act through G protein-coupled receptors on the T cell. Signaling by these receptors rapidly activates integrin adhesion molecules already present on the T cell surface to enhance their binding capacity. This leads to the third step in trafficking, the firm arrest of T cells to the wall of the blood vessel which allows the T cell to better resist shear forces exerted by blood flow. Integrins vital to leukocyte arrest are LFA-1 (Lymphocyte Function-associated antigen; $\alpha L\beta 2$; CD11a-CD18), Mac-1 ($\alpha M\beta 2$; CD11b-CD18), VLA-4 ($\alpha 4\beta 1$) and $\alpha 4\beta 7$ (42,

43). These bind to members of the immunoglobulin supergene family (IgSF) of receptors. Intercellular adhesion molecules -1 (ICAM-1; CD54) and -2 (ICAM-2; CD102) bind to the LFA-1 and Mac-1 β2 integrins; vascular cell adhesion molecule-1 (VCAM-1; CD106) binds to VLA-4; mucosal addressin cell adhesion molecule-1 (MAdCAM-1) binds to α4β7 (36, 38, 40, 44). Arrest mediated by the integrins and their receptors is reversible but on a much longer time scale (occurring over minutes), than rolling interactions (occurring over seconds). As a result the T cell can return to the bloodstream unless signaled to initiate the final step of trafficking, transendothelial migration into tissue. Migration occurs at junctions between endothelial cells in a process involving other adhesion molecules (42, 45) in a manner still being elucidated.

1.4 Adhesion molecules on endothelium

1.4.1 Selectin family

On the endothelial cell surface are multiple adhesion molecules whose expression and regulation help direct the accumulation of leukocytes. The three members of the selectin family all participate in lymphocyte trafficking into inflammatory sites. The selectin family is responsible for the initial attachment and rolling along the surface of endothelial cells and selectin expression is limited to the vasculature and leukocytes. (46, 47). L-selectin (CD62L) is expressed on microvilli of monocytes, granulocytes and majority of lymphocytes. P-selectin (CD62P) and E-selectin (CD62E) expression occur on the endothelial surface but only after activation by inflammatory cytokines which translocate P-selectin from secretory granules and induce E-selectin expression. Because of this regulation, only inflamed tissues will provide these important leukocyte recruiting molecules.

The genes for all three selectins are found in a ~300kb gene cluster on human chromosome one (48). The selectins are type I transmembrane proteins (Figure 1.0-3) that share significant homology in the extracellular regions (46). The transmembrane and cytoplasmic regions have the least homology, reflecting individualized intracellular trafficking. The most conserved domain is the lectin binding region, suggesting that the selectins bind similar ligands, carbohydrate structures on sialylated and fucosylated glycoproteins, though there are defined differences in ligands for each selectin (49-53). Each selectin has a different number of repeating complement regulatory (CR) homology domains, thus extending each a different distance above the cell surface (51). Selectins contain sites for N-linked glycosylation which can account for greater than 30% of their mass (54).

Figure 1.0-3 Structure of selectins. Selectins consist of an N-terminal lectin domain (red), an epidermal growth factor (EGF) domain (orange) followed by differing numbers of consensus repeats with homology to complement regulatory (CR) proteins (green): nine for P-selectin, six for E-selectin or two for L-selectin, a transmembrane domain (blue) and a cytoplasmic domain (purple).

1.4.2 E-selectin

E-selectin interaction with MUC1 discussed later in this work warrants a closer look at this selectin. Cloning of the single gene encoding E-selectin (55) revealed the sequence of domains illustrated in Figure 1.0-3, with six repeated CR motifs. The 3' untranslated region contains sequence associated with molecules transiently expressed in response to inflammation. The 610 amino acid sequence indicates a type I transmembrane protein that would be cleaved to 589 amino acids with an expected mass of 64kD. Eleven putative sites for N-linked glycosylation as well as other possible post-translational modifications lead to larger actual size of the molecule, around 100 -115kD. The cytosolic tail contains six serines and two tyrosines

available for interaction with intracellular proteins. Message for E-selectin can be detected in IL-1 activated human endothelial cells within an hour of stimulation, peaking after 2-4 hours and declining to baseline levels by approximately 24 hours. Protein expression on the cell surface correlates with message. The protein and message are quickly degraded suggesting that high turnover also contributes to regulating E-selectin expression (55).

In the hopes of blocking harmful inflammatory responses, there has been a focus on examining the ligand binding structure of E-selectin. Using the tetrasaccharide selectin ligand sialyl Lewis X (sLe^x; α-D-Neu5Ac-[2,3]-β-D-Gal-[1,4]-[α-L-Fuc-(1,3)]-β-D-GlcNAc-O-$[CH_2]_8$ COOMe) Erbe et al mapped a finite region of E-selectin's lectin domain vital to recognizing carbohydrates (56). A β–sheet within the lectin domain and a pair of nearby loops contain amino acids whose positively charged side chains are required for recognizing sLe^x, probably via interacting with the sialic acid carboxylate group. This work was later substantiated with crystal structure studies (57, 58) showing the three dimensional structure of E-selectin's lectin and EGF domains. Following deglycosylation of these domains, which does not interfere with binding, the amino acids essential for ligand recognition were determined to be in the lectin region nearby bound calcium. This places them in close approximation with the sialic acid and fucose structures of bound sLe^x. Similar studies looking at the lectin domain of P-selectin showed that its binding relied on some amino acids in the same region; however, there were subtle disparities in binding due to differences within the lectin domain. Chimeric P- and E-selectin molecules showed that carbohydrate binding specificity was contained completely within the lectin domain, as a result the lectin domain is sufficient to discriminate between counter-receptors (53). More recent studies examining binding by E-selectin to sLe^x show that sialylation and sulfation at position three of the galactose in sLe^x enhances binding and that the position of fucose in the

tetrasaccharide is important (59). This is consistent with the indispensable activity of fucosyltransferase VII (FucTVII) in generating selectin ligands (46, 51, 60).

The conservation of E-selectin's cytosolic region across species indicates that it plays a role in the function of E-selectin on endothelium. Using anti-E-selectin antibody Lorenzon et al showed that binding E-selectin without cross-linking led to transient increases in intracellular calcium levels in activated endothelial cells. Similarly, actin reorganized into stress fibers upon antibody binding while anti-sLe^x antibodies inhibited neutrophil mediated actin reorganization (61). When activated endothelial cells bound leukocytes, the distribution of E-selectin switched from diffuse to clustered in areas around bound leukocytes and the tail became associated with the actin cytoskeleton. Actin associated proteins filamin, α-actinin, paxillin, vinculin and focal adhesion kinase (FAK) were co-purified with E-selectin isolated from activated endothelial cells (62). This E-selectin mediated association with cytoskeletal proteins and cytoskeletal rearrangement is important to the ability of the endothelial cell to resist mechanical stress due to the tethered leukocyte in the blood stream.

1.4.3 Immunoglobulin gene superfamily (IgSF) adhesion molecules

In addition to members of the selectin family, five molecules in the immunoglobulin gene superfamily (IgSF) act in adhering leukocytes to endothelium: platelet-endothelial cell adhesion molecule-1 (PECAM-1; CD31), MAdCAM-1, VCAM-1, ICAM-2, and ICAM-1 (36, 37, 40, 63, 64). While MAdCAM expression is fairly limited to endothelium of mucosal tissues, the remaining members are found on endothelium throughout the body. MAdCAM-1, PECAM-1 and ICAM-2 are constitutively expressed on endothelium while VCAM-1 expression is induced and ICAM-1 expression is upregulated by inflammatory cytokines. The essential module in the structure of these molecules is the immunoglobulin (Ig) domain, the number of which varies for

each. The size of these adhesion molecules ranges from the smallest, ICAM-2 having core protein size of 29 kD to the largest, PECAM-1 with a core protein size of 80kD. Each protein contains sites for N-linked glycosylation that increase its molecular weight. MAdCAM-1 is unique in that it also contains a mucin-like region that is extensively O-glycosylated.

Members of the IgSF that bind to integrins, MAdCAM-1, VCAM-1, ICAM-2 and ICAM-1, contain two disulfide bonds in Ig domain 1 that aid in uniting the integrin binding region (65). The second Ig domain helps adjust domain 1 for binding integrins and extends it above the cell surface. Both the protein and crystal structures of the two N-terminal domains of integrin binding IgSF members appear similar; however MAdCAM-1 and VCAM-1 use a flat surface of Ig domain 1 to present a key acidic amino acid for integrin binding while the ICAM's use a more jutting surface (65). This is a reflection of the different integrins each pair can bind. ICAM's bind to the β2 integrins: ICAM-2 to LFA-1 and ICAM-1 to LFA-1 and Mac-1. MAdCAM-1 binds to α4β7, in addition to its selectin binding property via the mucin–like region. VCAM-1 can bind to α4β7 as well but is a much stronger receptor for VLA-4 (α4β1) (37, 40, 63). Unlike the integrin binding members, PECAM-1 is a homotypic adhesion molecule in the IgSF. Its expression on endothelium is localized at cell-cell junctions and it likely binds to PECAM-1 expressed on leukocytes to aid not only adhesion but also transmigration (64).

1.4.4 Intercellular Adhesion Molecule-1 (ICAM-1)

ICAM-1 is a well characterized adhesion molecule critically important in the adherence of leukocytes to endothelium. Cloning of the gene and cDNA placed it in the IgSF of adhesion receptors (66-69). It is encoded in seven exons over a 12kbp stretch with no indications of alternative splicing. ICAM-1 has five of the IgSF characteristic immunoglobulin domains, each encoded in a distinct exon. These extracellular domains are followed by a 24 amino acid

transmembrane region and short cytosolic tail of 28 amino acids. The core protein is 55kDa but eight N-linked glycosylation sites are differentially used by various cell types to heavily glycosylate ICAM-1 in the Ig domains 2-4. As a result the final protein ranges in size from 80-114 kDa, though endothelial ICAM-1 has less heterogeneity (67). On the cell surface ICAM-1 is expressed as a homodimer via hydrophobic areas in the transmembrane and third Ig domain. The dimeric form of ICAM-1 is a stronger ligand for the integrin LFA-1 than the monomeric form (70). Expression of dimerized ICAM-1 was also observed during crystal structure studies on ICAM-1's Ig domains 1 and 2 (71, 72).

Expression of ICAM-1 is regulated at multiple levels and differs among cell types. The 5' regulatory region contains various cis-acting elements (66). Binding sites for three transcription factors as well as two different transcription start sites complete with consensus TATA boxes are found upstream of the translation initiation sequence. Choice of transcription start sites varies between different cells and inductive agents. A variety of signal transduction pathways can upregulate and downregulate ICAM-1 expression Cytokine induction and steady state levels of ICAM-1 expression occur partially at the transcriptional level with the κB enhancer being the most important element (69). The effects of inflammatory cytokines on endothelium have been extensively studied (73). Tumor necrosis factor α (TNF α) and interleukins 1 α and 1β have been shown to upregulate ICAM-1 on human umbilical vein cells (HUVEC) in a manner dependent on protein synthesis (74). Post-transcriptional regulation of ICAM-1 is a minor component but can occur through mRNA stabilization, post-translational modifications and proteolytic cleavage from the cell surface (69).

ICAM-1 was the first member of the IgSF shown to bind to an integrin despite not having the typical Arg-Gly-Asp (RGD) motif present in most integrin ligands (67, 68, 75, 76). It binds

to two members of the β2 subfamily, LFA-1 and Mac-1. These are both found on leukocytes and the structure of ICAM-1 may allow binding to both at the same time (69). Each binding site is on a separate Ig domain, with LFA-1 binding to the N-terminus of Ig domain 1 and Mac-1 binding to Ig domain 3. Interestingly, N-glycosylation within the two sites of Ig domain 3 inhibits Mac-1 binding so that cell binding to ICAM-1 is increasingly LFA-1 dependent as the size of N-glycan chains increase (77). Conservation of the LFA-1 binding site between species points to LFA-1 being a very important *in vivo* ligand (69). The crystal structures of ICAM-1's two N-terminal Ig domains show that the negatively charged glutamate critical to binding LFA-1 is exposed on either side of the dimerized ICAM-1 so that the ligand binding regions are on opposite faces of ICAM-1. This structure implied that the ICAM-1 homodimer can bind a similarly dimerized LFA-1 (71, 72) and is specially fit to resist distortion due to stress forces.

Signaling by ICAM-1 does occur despite its lack of inherent tyrosine kinase activity or binding of Src family kinases. However, establishing the definite mechanism is complicated by the large range of studies conducted using a wide variety of ICAM-1 expressing cells and ICAM-1 ligands (74, 78). Cross-linking ICAM-1 with ligand expressing cells or antibodies can each initiate signaling in endothelial cells of the pulmonary, nervous and peripheral circulatory systems as well as endothelial lines. In HUVEC, cross-linking ICAM-1 leads to activation of the MAP kinases ERK1 and ERK2, but not Jun amino-terminal kinase (JNK), and to activation of the activator protein-1 (AP-1) transcription factor, but not NFκB activity (74). Endothelial surface protein and chemokine expression are affected downstream of ICAM-1 binding. Lawson et al showed that anti-ICAM-1 antibody cross-linking induced ERK-1 and the AP-1 transcription factor activity in HUVEC and led to increased VCAM-1 expression (79). Also in HUVEC,

synthesis and secretion of the chemokines IL-8 and RANTES was induced via activation of ERK1 and ERK 2 following ICAM-1 cross-linking (80).

1.5 Adhesion molecules on T cells binding to endothelium

1.5.1 Selectin-counter receptors

The selectin counter-receptors on T cells are used to bind E-selectin and P-selectin expressed on activated endothelium. These selectin receptor structures are presented on proteins which have undergone post-translational modifications (glycoproteins, proteoglycans, glycolipids (51) and sialomucins (42)). Required fucosylation and sialylation indicate that fucose and α-2,3-linked sialic acid are universally used by endothelial selectins (47, 51, 81, 82). The well established and much studied α2,3sialylated, α1,3 fucosylated tetrasaccharide, sLe^x, can bind all selectins, but is not sufficient to confer binding to a selectin. Specificity of cell-cell interactions is imparted by individual proteins presenting the glycan counter-receptor structures and this aids in directing leukocyte trafficking. Diverse proteins presenting carbohydrate structures may alternatively space or combine them to impart an unique three dimensional arrangement for binding specificity, or modifications may occur to the protein itself. For example, P-selectin ligands must contain sulfation though this is not required for E-selectin ligands (51).

A great deal of what is known concerning the carbohydrate structures recognized by selectins has come from study of the P-selectin glycoprotein ligand-1 (PSGL-1) (46), a sialomucin believed to be the primary ligand for P-selectin on leukocytes and expressed on all T cells (46, 47, 81, 83). PSGL-1 was identified in 1992 as a ligand for P-selectin (83) and later as a ligand for E-selectin (84, 85). However, expression of this protein alone is not enough to endow selectin-mediated cell adhesion. Studies of the structural requirements for P-selectin binding

showed a necessity for fucose, sialic acid and O-linked glycosylation, while N-linked glycans were unnecessary (83, 84). Co-transfection of PSGL-1 with specific glycosyltransferases showed that binding to both P- and E-selectin required core 2 O-linked glycans to be sialylated and fucosylated (86). In addition to these carbohydrate structures, tyrosine sulfation on the N-terminus of the protein backbone of PSGL-1 is required for binding to P-selectin (87, 88) but not to E-selectin (86). Given the variety of factors influencing selectin binding of PSGL-1 it's been proposed that selectin binding to counter-receptors is based on a three-dimensional structure rather than a linear recognition site (47). Extensive analysis of PSGL-1 expressed by a myeloid cell line showed that most of the O-linked saccharides have a core 2 motif and are a combination of neutral and sialylated structures. Only 14% are α-1,3-fucosylated and contain sLe^x (89), a fairly small amount given the PSGL-1 dependency of P-selectin binding (51, 81, 83). X-ray crystallography of P- and E-selectin in complex with sLe^x or PSGL-1 has illustrated some of the molecular interactions occurring with selectin counter-receptors (90). On P- and E-selectin the binding site for sLe^x is highly conserved but P-selectin has neutral amino acids in that region while those of E-selectin are charged. Both selectins bind sLe^x in a comparable orientation and with predominantly electrostatic interactions. While the galactose of sLe^x interacts with identical amino acids of P- and E-selectin, the sialic acid residue and fucose of sLe^x participate differently so that contacts with E-selectin are more extensive. P-selectin has vital contacts with sulfated tyrosines that are not seen with E-selectin. These differences between P- and E-selectin are conserved across species and point to their importance in bestowing selectin-ligand binding specificity.

Synthesis of the selectin counter-receptors require activity of different glycosyltransferase enzymes expressed in the Golgi apparatus of a T cell. They are categorized based on the type of

sugar each adds to its substrate. Depending on the type, relative amounts, location of enzymes expressed and substrates available, a cell can express a broad diversity of glycan products (81). The enzymes core 2 β1,6-N-acetylglucosamine transferase (core 2 GlcNAcT; C2GnTase) and α(1-3) fucosyltransferase-VII (FucT-VII) are involved in generating carbohydrate structures on T cells for endothelial selectin binding (46, 81, 82, 86). Synthesis of P-selectin counter-receptors is dependent on core 2 GlcNAcT activity (84, 86, 87) but less so for the E-selectin counter-receptors, for structural reasons not yet defined (81, 91). In contrast, FucT-VII is absolutely required for synthesis of both E- and P-selectin counter-receptors on cell surface glycoproteins (60, 81, 82, 92, 93). Interestingly, lower levels of activity are required to make P-selectin ligands as compared to E-selectin ligands in T lymphoblasts (93). The presence of α2-3-sialic acid also determines binding of selectins to counter-receptors. Of the six sialyltransferases only ST3Gal-IV has been determined important to E- and P-selectin binding (49). The regulation of expression of glycosyltransferase enzymes in T cells is influenced by their cytokine environment during activation, which then leads to differences in expression of endothelial selectin counter-receptors and ability to subsequently migrate (94-99).

1.5.2 Integrins

Integrins are transmembrane cell surface adhesion molecules composed of non-covalently interacting α and β chains. These form metalloprotein heterodimers, expressed on cells throughout the human body, which can be categorized based on which β chain is used. A separate categorization method divides the integrins into two groups depending on whether their α chain contains the I (inserted or interactive) domain (100). This ~200 amino acid I domain contains a metal ($Mg2^{+}$ or $Mn2^{+}$) binding site and, in cooperation with the bound metal (101), functions as the chief ligand binding site for I domain containing integrins. The 19 α chains and

eight β chains so far identified are known to form 24 or 25 different integrins (100, 102, 103). Of these, the four members of the β2 family, LFA-1, Mac-1, αdβ2 (CD11d/CD18) and αXβ2 (CD11c/CD18; p150,95) along with the β7 family are all exclusively expressed on leukocytes (102, 104, 105). Different leukocytes express different combinations of integrins and expression changes as the cells develop and migrate throughout their life cycle.

The structure of integrins (Figure 1.0-4) has shed light on how their ligand binding occurs and is regulated (102-104). The N-termini of both the α and β chains extend above the cell surface and form a globular head that is linked to the plasma membrane by the stalks of each chain. The α chain contains at its N-terminus seven repeating 60 amino acid stretches that fold into a β-propellor structure which contains $Ca2^{+}$ binding sites. β2 integrins belong to the group of integrins that contains the metal ($Mg2^{+}$ or $Mn2^{+}$) binding I domain and it is located in the third repeat of the β-propellor region of the α chain. Interestingly, recent studies with LFA lacking the I domain have shown that it is not required for expression of the heterodimer on the cell surface and deletion of the I domain locks LFA-1 in the active conformation, suggesting that the I domain also regulates conversion between high and low affinity states (106). The mechanism of how divalent cation binding affects cell adhesion is not yet clear but involves metal coordinating residues within the I domain that shift between ligand bound and unbound forms of integrins. This corroborates the physiological importance of cations to integrin mediated cell adhesion (102, 103). The β2 chain contains an I-like domain, which has a similar metal binding site as the α chain I domain. This I-like domain is situated closely to the α chain I domain and also is important to ligand binding. Following the transmembrane portions, β2 integrins have short cytosolic tails that lack intrinsic enzyme activity but do have sequences important for interaction with intracellular proteins used in linking to the cytoskeleton and signaling (α-actinin,

talin, filamin, vinculin, Rack1 (104, 107)). The tail GFFKR motif is believed to serve as a hinge that keeps integrins in a low affinity conformation until an activating signal is received by a T cell to switch to a high affinity shape (104).

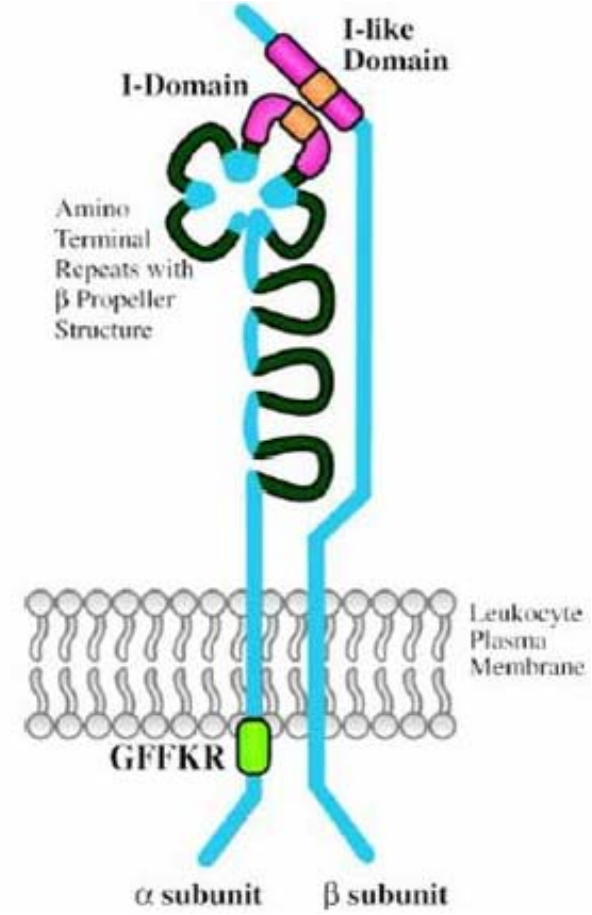

Figure 1.0-4 Features of β2 integrins. The αβ heterodimeric structure is common to all integrins. The α chain includes seven extracellular N-terminal homologous repeats organized into a β propeller structure. The α chain I domain is shown in *pink* with the embedded MIDAS (metal ion-dependent adhesion site) motif in *orange*, and the β chain I-like domain with MIDAS motif is shown in corresponding fashion. The GFFKR sequence (*green*) in the cytoplasmic tail of the α subunit is involved in heterodimer assembly and regulation of ligand recognition. The heterodimer is illustrated in the "closed" or inactive state that undergoes tertiary and quaternary changes in response to inside-out signals. From (104), reproduced with permission of AM SOC FOR BIOCHEMISTRY & MOLECULAR BIOL via Copyright Clearance Center.

T cells have to be able to freely circulate through the blood and then quickly adhere to endothelium at inflamed sites. Integrins, especially the β2 integrin LFA-1 and β1 integrin very late antigen-4 (VLA-4), are critical to this lymphocyte function. Integrins on the lymphocyte surface are kept in an inactive, low affinity conformation. Chemokines presented on inflamed

endothelium mediate signaling through the lymphocytes to activate integrins in a manner still being illuminated (108). The ability to bind to ligand involves both structural changes to the integrin heterodimer as well as changes in cell surface distribution. The I domain of the α chain undergoes conformational changes when the integrins bearing them are activated, going from a closed/inactive shape to an open/active shape that alters the entire integrin conformation (101). Additional evidence of conformational regulation of LFA-1 binding activity comes from studies manipulating the divalent cation environment (removing calcium, adding magnesium) to activate binding to ICAM-1 and from studies effecting intracellular signaling to integrins by activating other cell surface receptors (100, 104). The inside-out signaling path(s) to activate β2 integrins has not been fully mapped but include cytohesin-1, GRP-1, the small GTPase Rho, protein kinase Cs, Rack1 (receptor for activated PKC), and MARCKS (myristolated alanine-rich C kinase substrate) (104, 107).

Changes in cell surface distribution leading to clustering of LFA-1 causes increased avidity for its ligand. In the inactive state LFA-1 is anchored to the cell cytoskeleton. Upon release LFA-1 can laterally move and form clusters on the cell surface increasing avidity for ICAM-1 (100, 107). Clustering is mediated by a number of intracellular molecules, including signaling proteins (SLAP 130, GTPase Rap-1, the Rac-1 GEF protein Vav-1) and cytoskeletal proteins (α-actinin, talin vinculin, filamin). The cytosolic protease calpain that cuts many cytoskeletal proteins is also vital to clustering. In T cells, activation of the cell through a variety of stimuli (T cell receptor, extracellular calcium, chemokines) leads to clustering on the cell membrane. It has been shown that the density of ligand influences whether affinity or avidity is most important in cell adhesion. Studying chemokine mediated lymphocyte arrest *in vitro* and *in vivo*, Constantin et al showed that when ICAM-1 is available at high density then high affinity

LFA-1 is sufficient for adhesion despite lack of mobility (108). It is when ligand is at low density that mobility of LFA-1 is crucial to adhesion. The distinction could be made by inhibiting phosphatidylinositol 3-OH kinase which regulates LFA-1 mobility but not affinity (108). It seems that physiological ligand binding by integrins is likely not mediated exclusively through changes in affinity or avidity but by both.

In addition to inside-out signaling regulating integrin function, integrins can also mediate outside-in signaling to alter gene transcription via Jun activating domain binding protein 1 (JAB1) and stabilizing mRNA transcripts (105, 109). LFA-1 on primary T cells can mediate outside-in signaling to organize the F actin cytoskeleton and enhance binding to ICAM-1; both conformational alterations and clustering were required. Though the mechanism behind this has yet to be mapped out, (110) LFA-1 has been linked to phosphorylation of intracellular proteins. Rodriguez-Fernandez et al showed in T cells that LFA-1 activation by monoclonal antibodies or by binding to ICAM-1 led to phosphorylation of focal adhesion kinase (FAK) and proline-rich tyrosine kinase 2 (PYK-2) (111), as detected in anti-phosphotyrosine immunoprecipitates from T cell lymphoblasts. Activation of FAK and PYK-2 also occurred in response to LFA-1 binding ICAM-1 in a cytoskeletal dependent manner, as evident from interference by actin and tubulin disrupting agents. These findings were concomitant with cell morphology switching from spherical to a polarized appearance.

Intracellular signals generated by LFA-1 in response to binding to ICAM-1 embody a range of intracellular changes such as phosphorylation of phospholipase Cγ1, phospholipids hydrolysis, PKC activation, intracellular calcium mobilization and serine and tyrosine kinase activation (111, 112). Since integrins have no catalytic activity they use a number of different non-receptor kinases that include FAK, PYK-2, c-Src, Abl and Syk (112). In T cells, “cross-

talk" between integrins has been demonstrated and is further evidence of the ability of integrins to mediate outside-in signaling. In this process integrins can modulate each others' adhesive function. Porter et al showed that activation of LFA-1 by ICAM-1 binding decreased α4β1 ability to bind to VCAM-1 and fibronectin (113). α5β1 binding was also decreased but to a lesser degree. Interestingly, activation of the β1 integrins did not modulate LFA-1 binding to ICAM-1 indicating a specific inhibition by LFA-1 rather than a common mechanism following integrin activation. The β1 integrins could modulate each other in that blocking α4β1 integrin binding enhanced α5β1 binding. Investigating the mechanism for the observed cross-talk eliminated changes in β1 integrin expression, redistribution or conformation (113). Further exploration of the regulation of β1 integrins by LFA-1 used the I domain-deleted LFA-1. This constitutively active form activated both α4β1 and α5β1 through clustering of β1 integrins and not by increasing their affinity. The need for clustering in activating β1 integrins but not for inhibiting β1 integrins might be due to different expression levels of LFA-1 and the interaction with intracellular mediators of cross-talk (106). Much work remains to be done to identify the molecules involved in LFA-1 cross talk but protein kinase C and calmodulin-dependent kinase II have been implicated in β1- β1 and β3 – β1 integrin cross-talk (102). Clearly the outside-in signaling by integrins is complicated by the cell type studied, range and expression level of integrins displayed and of cytosolic mediators but clarifying the pathways involved will greatly aid in understanding how T cells respond to extracellular signals to alter their function.

1.6 Polarization of T cells During Interactions with Endothelium

Shifting from a spherical to polarized morphology is a required initial step prior to T cell migration through endothelium. It allows T cells to produce cell body movement from internal

cytoskeletal forces (114). During this process the cell forms two compartments, the leading edge (contacts the endothelial surface) and the trailing edge (uropod extending above the T cell body). On the leading edge are active integrins (β1 and β2), chemokine receptors, and ganglioside GM3-enriched rafts. Within the cytosol nearby the leading edge are polymerized actin filaments, Rho GTPases, the protein kinase FAK and vinculin, α-actinin, talin. The uropod surface displays adhesion molecules ICAM-1, -2 -3 and PSGL-1, CD 43, 44, and ganglioside GM1-enriched rafts. Within it are the ERM family of proteins (ezrin, radixin, moesin), motor protein myosin II, the Golgi apparatus, the microtubule organizing center (MTOC) and protein kinase C (114-117). These differentially localized components are indicative of the unique roles of the leading edge and uropod. The leading edge acts as a sensory organ to respond to polarizing stimuli and guide migration of the T cell. The uropod acts as an adhesive structure to facilitate interactions with other cells.

Presentation of chemokine to T cells and subsequent polarization and migration was investigated by Pelletier et al who showed that SDF1α bound to fibronectin and this bound chemokine could induce polarization of Jurkat cells (118). Migration assays indicated that a distinct edge of SDF1 α was needed to orient the cells in a particular direction. A uniform SDF1 α concentration still allowed directed migration, despite the absence of gradient, but in whatever direction the cell happened to polarize. Pelletier et al proposed that matrix bound chemokine is still functional for inducing polarization. Consistent with this idea, the polarized chemokine receptors were detected along the leading edge at the basal surface of the cells contacting fibronectin (118). Nieto et al also reported that chemokine receptors on polarized cells are located on the flattened cell-substratum contact area and that polarization of chemokine receptors to the leading edge relies on integrin mediated cell adhesion (119).

Localization of ICAM-1 and -3 on the uropod would recruit additional lymphocytes. del Pozo et al describe the upward projection of the uropod above the cell bodies of adherent T cells and the subsequent attachment of additional T cells to the elevated uropod (120). Following binding of a cell at the uropod the adherent T cell could then migrate and carry the attached cell(s) with it. This was observed not only with *in vitro* stimulated PHA lymphoblasts but also with cells activated *in vivo* ($CD45RO^+$ cells isolated from PBL, tumor infiltrating lymphocytes and lymphocytes from the synovial fluid of rheumatoid arthritis patients) (120).

Cell polarization occurs via chemokines produced by different leukocytes and by endothelial cells, and their subsequent signaling pathways (121). Chemokines bind to a family of heterotrimeric G-protein-linked heptahelical receptors that are expressed in various combinations on different leukocytes. Complex signaling pathways initiated by the heterotrimeric G proteins are still being mapped but include protein serine/threonine and tyrosine kinases, adenyl cyclase, phospholipases A, C, D, the phosphatidylinositol 3-kinase (PI3K) lipid kinase, the Rho family of small GTPases and intracellular second messengers (calcium, cyclic AMP and phosphoinositides) (114).

Chemokine signaling ultimately results in complete rearrangement of the T cell's cytoskeleton to quickly switch from a spherical non-motile phenotype to an elongated bell-shaped polarized morphology (114). Central to this is concentrating F-actin filament distribution to primarily the leading edge rather than symmetrically dispersed around the cell body. The rigid tubulin cytoskeleton is also moved during polarization. Whereas the MTOC is adjoining the nucleus in spherical T cells, upon polarization the MTOC slips into the uropod and its splayed connected microtubules fold up into a narrow packed arrangement that allows the T cell increased malleability. This form confers greater ability of the T cells to maneuver through

constricted spaces, e.g. between endothelial cells (122) but plays no role is generating the uropod. In contrast, myosin II is vital to uropod formation as a myosin-disrupting agent completely prevents its formation and cell polarization (121). The ERM protein radixin is also with myosin II in the uropod neck, differing from moesin which is adjacent to the distal end of the uropod. There moesin associates with the cytosolic tails of CD 44 and ICAM-3, but not ICAM-1, linking them to the cytoskeleton and facilitating their movement to the uropod during polarization (123).

1.7 Hypotheses, Specific Aims & Rationale

Hypothesis 1:

MUC1 expressed by T cells is used to prevent and/or aid adhesion to blood vessels and thus modulate migration into tissues. Because of this role it is expressed on the surface of activated but not resting T cells in the normally glycosylated form. The location of MUC1 on the T cell surface changes as it shifts from an anti-adhesive to a pro-adhesive role, moving to the leading edge so as to be the first contact point with inflamed endothelium.

Specific Aim 1:

Determine when T cells express MUC1, where on the surface MUC1 is localized and the type of glycosylated form of MUC1 expressed on the surface of human T cells.

Rationale:

As the role of a T cell changes so do the molecules on its surface. Naïve T cells express adhesion molecules that specifically direct them to secondary lymphoid tissue where they can be activated. Upon activation the spectrum of adhesion molecules changes so that the cells can home in on inflammatory sites. Transitioning to a memory T cell population, the surface again contains a unique set of molecules. Knowing at what stage(s) T cells are expressing MUC1 may

help in understanding its role. In addition, MUC1 has been shown on tumor cells to both bind adhesion molecules and prevent cell-cell adhesion, the latter effect removed by capping MUC1. The location of MUC1 on the T cell surface, whether dispersed or localized to a particular area, is likely to alter the adhesion properties of the cell.

MUC1 can be expressed in different forms depending on the extent of glycosylation. The form found throughout the body on epithelial surfaces is glycosylated with long branched chains of sugars on the majority of the molecule's extracellular portion. In contrast, when MUC1 expressing cells alter glycosylation enzyme activities the glycosylation of MUC1 changes such that the sugar chains attached are much shorter. The differences between these two forms of MUC1 would affect how the MUC1-bearing cell interacts with other cells. In addition, cancer vaccines using MUC1 as an antigen specifically target the underglycosylated form of MUC1. For these reasons it is important to determine which form of MUC1 is expressed on activated human T cells.

Hypothesis 2:

MUC1 on T cells interacts with one or more molecules on the surface of blood vessels as a means to initiate adhesion. Upon interaction with a ligand MUC1 signals to the T cell via phosphorylation of its cytosolic tail and association with intracellular signaling proteins.

Specific Aim 2:

Determine if MUC1 on T cells affects their interactions with endothelial adhesion molecules and if there are changes in protein phosphorylation occurring within the T cell, to the MUC1 cytosolic tail and/or other proteins, during interaction with endothelium.

Rationale:

Cell surface molecules enable the T cell to interact with and adhere to endothelium in the context of appropriate ligands. Most T cell adhesion molecules project only a small distance above the cell. MUC1, with its elongated rod-like structure, stretches above the cell surface and would be the first molecule of the T cell to make contact. The results of this contact would likely play an initial role in the homing of a T cell to an immunologically active site. Furthermore, phosphorylation and association with intracellular proteins, observed in MUC1 expressing tumor cells, may also be occurring in activated MUC1 expressing T cells in response to interaction with endothelium. The role of MUC1 in adhesion and signaling would be important not only to understanding T cell biology but also in the hopes of manipulating T cell trafficking.

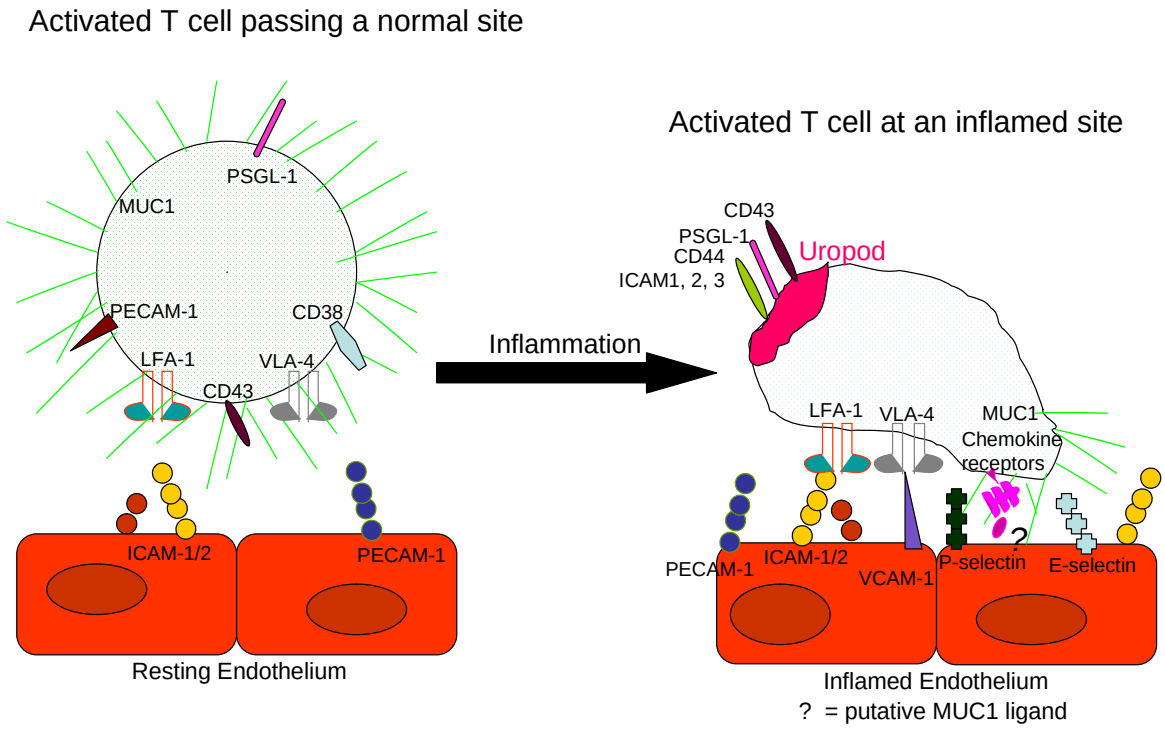

Figure 1.0-5 Model of activated MUC1 expressing T cell interacting with endothelium in a normal or inflamed site, illustrating the hypotheses guiding specific aims 1 and 2.

Hypothesis 3:

In vivo manipulation of T cell MUC1 would affect the ability of T cells to reach inflammatory sites. As observed in humans, T cells from MUC1 transgenic mice should express MUC1 on their cell surface following activation and thus be susceptible to blocking MUC1 with antibodies. Failure to express MUC1 would indicate either inability of mouse T cells to express the human transgenic MUC1 or an intrinsic difference between mouse and human T cells.

Specific Aim 3:

Determine expression of human MUC1 on the surface of MUC1 transgenic mouse T cells following activation and document any differences in the mouse model from human T cell expression of MUC1.

Rationale:

An *in vivo* model is necessary to best study the effect of MUC1 on T cell migration. Mouse Muc-1 and human MUC1 have a homologous structure but differ in size, sequence, and the number of repeats in the extracellular region. The mouse system cannot be used however because there are no reliable reagents such as anti-Muc-1 antibodies commercially available to study mouse Muc-1. In order to take advantage of the numerous reliable well-characterized human MUC1 reagents, the human MUC1 transgenic mouse model (124) could be used. It has been documented to express human MUC1 on the same epithelial surfaces where MUC1 is seen in humans. Due to its fidelity in reproducing human MUC1 expression on epithelium, this model should be ideal to study the role of MUC1 on T cells via *in vivo* manipulation of the T cell MUC1. Additionally, this transgenic mouse is used in many cancer vaccine studies. Any differences seen between the mouse and human T cell would be relevant to comparisons made between humans and mice in numerous immune research studies.

2.0 FORM AND PATTERN OF MUC1 EXPRESSION ON T CELLS

Hypothesis 1:

MUC1 expressed by T cells is used to prevent and/or aid adhesion to blood vessels and thus modulate migration into tissues. Because of this role it is expressed on the surface of activated but not resting T cells in the normally glycosylated form. The location of MUC1 on the T cell surface changes as it shifts from an anti-adhesive to a pro-adhesive role, moving to the leading edge so as to be the first contact point with inflamed endothelium.

Specific Aim 1:

Determine when T cells express MUC1, where on the surface MUC1 is localized and the type of glycosylated form of MUC1 expressed on the surface of human T cells.

Rationale:

As the role of a T cell changes so do the molecules on its surface. Naïve T cells express adhesion molecules that specifically direct them to secondary lymphoid tissue where they can be activated. Upon activation the spectrum of adhesion molecules changes so that the cells can home in on inflammatory sites. Transitioning to a memory T cell population, the surface again contains a unique set of molecules. Knowing at what stage(s) T cells are expressing MUC1 may help in understanding its role. In addition, MUC1 has been shown on tumor cells to both bind adhesion molecules and prevent cell-cell adhesion, the latter effect removed by capping MUC1. The location of MUC1 on the T cell surface, whether dispersed or localized to a particular area, is likely to alter the adhesion properties of the cell.

MUC1 can be expressed in different forms depending on the extent of glycosylation. The form found throughout the body on epithelial surfaces is glycosylated with long branched chains of sugars on the majority of the molecule's extracellular portion. In contrast, when MUC1

expressing cells alter glycosylation enzyme activities the glycosylation of MUC1 changes such that the sugar chains attached are much shorter. The differences between these two forms of MUC1 would affect how the MUC1-bearing cell interacts with other cells. In addition, cancer vaccines using MUC1 as an antigen specifically target the underglycosylated form of MUC1. For these reasons it is important to determine which form of MUC1 is expressed on activated human T cells.

This part has been modified from :

Isabel Correa, Tim Plunkett, Anda Vlad, Arron Mungul, Jessica Candelora-Kettel, Joy M. Burchell, Joyce Taylor-Papadimitriou & Olivera Finn. 2003. **Form and pattern of MUC1 expression on T cells activated *in vivo* or *in vitro* suggests a function in T-cell migration**. Immunology 108: 32-41.

SUMMARY

MUC1 is a transmembrane mucin that is expressed on ductal epithelial cells and epithelial malignancies and has been proposed as a target antigen for immunotherapy. The expression of MUC1 has recently been reported on T and B cells. In this study we demonstrate that following activation *in vivo* or activation by different stimuli *in vitro*, human T cells expressed MUC1 at the cell surface. However, the level of expression in activated human T cells was significantly lower than that seen on normal epithelial cells or on breast cancer cells. In contrast, resting T cells do not bind MUC1-specific monoclonal antibodies (mAb), nor is MUC1 mRNA detectable by RT-PCR or Northern blot analysis in these cells. The profile of activated T cell reactivity with different MUC1-specific antibodies suggested that the glycoform of MUC1 expressed by the activated T cells carried core 2-based O-glycans, as opposed to the core 1

structures that dominate in the cancer-associated mucin. Confocal microscopy revealed that MUC1 was uniformly distributed on the surface of activated T cells. However, when the cells were polarized in response to a migratory chemokine, MUC1 was found on the leading edge rather than on the uropod where other large mucin-like molecules on T cells are trafficked. The concentration of MUC1 at the leading edge of polarized activated human T cells suggests that MUC1 could be involved in early interactions between T cells and endothelial cells at inflammatory sites.

2.1 INTRODUCTION

The human epithelial mucin, MUC1, is a heavily O-glycosylated type I transmembrane glycoprotein expressed at the luminal surface of most glandular epithelial tissues. Expression of MUC1 is increased in many epithelial malignancies, notably breast, pancreatic and ovarian cancers as well as in a proportion of colonic and lung cancers (for review see (125). The extracellular domain of MUC1 consists largely of tandemly repeated sequences of 20 amino acids with approximately 100 amino acids 5' to this region and 180 amino acids 3', followed by a transmembrane domain and cytoplasmic tail (2). The number of tandem repeats (TR) in the MUC1 allele can vary between 25 and 100. Each of the TR contains 5 potential O-glycosylation sites, and the glycoforms produced by cancer cells can differ from those expressed by normal tissues (126).

There have been reports of humoral and cellular immune responses to MUC1 in multiparous women and in patients with cancer (127-132). These data, together with the high level of expression in tumor cells, have led to a focus on MUC1 as a potential target for tumor immunotherapy. Several MUC1-derived cytotoxic T cell (CTL) epitopes have been identified

(133-136) and immunization with vectors expressing the full length molecule or with peptides, have shown protection against MUC1-expressing tumors in mouse models (136, 137). However, in transgenic mouse models, where MUC1 is expressed as a self-antigen, it is more difficult to demonstrate immune responses against MUC1 (138-140), suggesting a degree of immunological tolerance. The degree of tolerance to a self-antigen is expected to be dependent on the level and location of expression of the self-antigen.

Although the expression of MUC1 was originally thought to be restricted to epithelial tissues, recent work has suggested that MUC1 is also expressed by T and B cells (141-143). MUC1 expression on T cells has been documented through several experimental techniques: via immunohistochemistry (144), flow cytometry (141, 142, 145-148), RT-PCR (141, 142, 146, 148), Northern blotting (142) and confocal microscopy (148). Most studies have shown MUC1 expression only on activated and not resting T cells (141, 145, 146, 148). The expression of MUC1 on such cells has implications both for immune tolerance and autoimmunity. We therefore sought to investigate in detail the expression of MUC1 in human T cells documenting both the level and duration of expression, the distribution of MUC1 on the T cell surface and the specific form of the glycoprotein expressed.

Our data demonstrate that MUC1 is expressed by T cells activated both *in vivo* and *in vitro*, but that the level of expression is low. MUC1 on chronically stimulated T cells is co-expressed with the memory phenotype marker CD45RO. The profile of reactivity of the T cell glycoprotein with MUC1-specific antibodies indicates that the O-glycans added to the core protein are extended core 2-based structures as seen in many normal tissues, rather than the truncated predominantly core 1-based structures added to mucin produced by tumor cells. Moreover, confocal microscopy revealed that MUC1 expression on T cells is dispersed over the

entire cell surface until polarization, at which point MUC1 becomes confined to the leading edge of the T cell.

2.2 MATERIALS AND METHODS

2.2.1 Cells and tissues

All samples were obtained after acquiring informed consent from the study participants and according to Ethics Committee Guidelines. Peripheral blood was obtained from healthy volunteers, patients with breast cancer and a patient with rheumatoid arthritis, or as a leukopheresis research product from the Central Blood Bank (Pittsburgh, PA). Peripheral blood mononuclear cells (PBMC) were isolated from whole blood by Ficoll/Paque (Amersham Pharmacia Biotech, Uppsala, Sweden) density gradient centrifugation. The synovial fluid was obtained by sterile needle aspiration from the acutely inflamed knee joint of a patient with active rheumatoid arthritis. The human breast cancer tissue was obtained from a patient at the time of primary surgery.

All cell lines (Jurkat, BT-20, DM6, DM6-MUC1) were grown in RPMI supplemented with 10% fetal bovine serum, 1% L-glutamine and 1% penicillin/streptomycin. The 22 repeat MUC1-EGFP fusion construct (Figure 2.0-1) was cloned into the pLNCX2 (Clonetech) retroviral vector and then transfected into an amphotrophic packaging cell line by Dr. Andrea Gambotto. MUC1-EGFP expression is under control of the CMV promoter and the vector contains a neomycin resistance gene. Jurkat cells were resuspended in retroviral supernatant containing 8 μg/ml polybrene. Cells were then aliquoted 2 ml/well to 24 well plate, centrifuged at 1,000 x g for 1 hour at room temperature and incubated at 37^{o}C overnight. The next day (day 2) 1 ml/well

of retroviral supernatant was replaced with new retroviral supernatant containing 8 μg/ml polybrene and centrifugation was repeated. Cells were incubated overnight and the day 2 procedure repeated on day 3. On day 4 the cells were transferred to a tissue culture flask and grown in medium supplemented with 1 mg/ml G418.

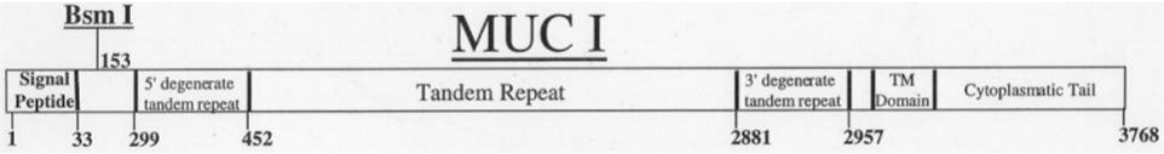

Figure 2.0-1 MUC1-EGFP construct transduced into Jurkat cells. This diagram shows the restriction enzyme site used to insert the enhanced green fluorescence protein (EGFP) sequence in the N terminal region.

Antibodies

The monoclonal antibody (mAb) mouse anti-human CD3 (UCHT1), and mouse anti-human MUC1 mAbs HMFG1, HMFG2 and SM3 were obtained from the Cancer Research UK Hybridoma and Monoclonal Antibody Facility. Other MUC1-specific mAbs were: 232A1 (a gift from Dr. J. Hilkens, the Netherlands Cancer Institute, Amsterdam, the Netherlands); mAb 12C10 (obtained from Dr. R.B. Acres, Transgene, Strasbourg, France), mAb VU-3-C6 (obtained from Dr. J. Hilgers, Department of Obstetrics and Gynecology, Academisch Ziekenhuis, Vrije Universiteit, Amsterdam, The Netherlands). Remaining anti-MUC1 antibodies were obtained from ISOBM TD4 International Workshop on Monoclonal Antibodies against MUC1 (10). In some experiments, biotinylated HMFG1 and 12C10 were used. Phycoerythrin (PE)-labeled mouse anti-human CD69, fluorescein isothiocyanate (FITC)-labeled mouse anti-human CD25, unlabeled isotype control mouse immunoglobulin G1 (IgG1), PE-labeled anti-human CD45RO, PE-labeled isotype control mouse immunoglobulin G2a (IgG2a) and PE-labeled anti-human CXCR4 antibodies were purchased from Becton-Dickinson Pharmingen (San Jose, CA). Polyclonal rabbit anti-chicken spectrin antibody was a gift from Dr. Elizabeth Repasky (Roswell

Park Cancer Institute, Buffalo, NY). Alexa secondary antibodies and rhodamine phalloidin were purchased from Molecular Probes (Eugene, OR).

2.2.2 Activation of human T cells *in vitro*

PBMC were cultured (1 x 10^6 cells/well in a 24 well plate) in RPMI-1640 supplemented with 10% fetal calf serum (FCS), 2mM L-glutamine, 50μM β-mercaptoethanol (RPMI-10% FCS) and stimulated with phytohaemaglutinin (PHA; Abbot-Murex, Dartford, UK) at 1μg/ml or immobilized anti-CD3 mAb. Plates were incubated with 0.5ml of purified anti-CD3 mAb [10μg/ml in phosphate-buffered saline (PBS)] for 2 hours at 37^{o}C. The plates were then washed three times with PBS and blocked with RPMI-10% FCS before use. Alternatively, PBMC in Fig. 4 were incubated in AIM V medium (Gibco, Carlsbad, CA), supplemented with 10% human serum (Cellgro, Herndon, VA) and 1% L-glutamine, in the presence of PHA **(**1 μg/ml; Sigma, St. Louis, MO) and 20 U/ml interleukin-2 (IL-2) (Dupont, Wilmington, DE). For antigen-specific activation *in vitro*, PBMC in RPMI-10% FCS were stimulated in a mixed lymphocyte reaction (MLR). Responder PBMC (1.5 x 10^6 cells/well of a 24-well plate) were co-cultured with irradiated (2000 rads) allogeneic stimulator cells (responder:stimulator ratio of 1:1) for at least 6 days. Cells from short-term MLR were purified by Ficoll-Paque centrifugation before staining. For chronic stimulation of T cells, PBMC were stimulated with irradiated allogeneic PBMC in AIM V-human serum medium containing 20 U/ml IL-2 (Dupont, Wilmington, DE). Three to five days after stimulation, half of the medium from each well was replaced with new medium containing fresh IL-2. The stimulation was repeated every 7 days.

2.2.3 Flow cytometric analysis

Cells were stained with anti-MUC1 mAb HMFG1, HMFG2, SM3, 12C10 or 232A1, followed by FITC-conjugated rabbit anti-mouse immunoglobulins (Dako, High Wycombe, UK). When biotinylated antibodies were used, binding was detected with streptavidin-PE (Southern Biotechnologies, Birmingham, AL). Cells were also stained with directly conjugated antibodies to CD3, CD25, and CD69. For staining of chronically stimulated T cells**,** cells were stained with mouse anti-human MUC1 mAb MF06 or isotype control mouse antibody, followed by a secondary antibody, goat anti-mouse Alexa488. Cells were then fixed for 10 minutes at room temperature in 1% paraformaldehyde and empty binding sites of the goat anti-mouse secondary antibody were blocked with unlabelled mouse isotype control antibody. Cells were finally stained with directly PE-conjugated isotype control or PE-conjugated anti-CD45RO mAb. Anti-MUC1 staining of BT-20, DM6 and DM6-MUC1, resting T cells, activated T cells, MUC1-EGFP Jurkat cells was done according to the procedure used with chronically activated T cells.

Staining for SDF1α receptor was done with anti-CXCR4-PE after a 30 minute incubation of MUC1-EGFP transduced Jurkat cells with SDF1α (PeproTech, Rocky Hill, NJ), (0, 2, 5, 10, 20, 50, 100 150, 300 ng/ml) in fibronectin coated wells. MUC1-EGFP Jurkat cells exposed to the range of SDF1α were also analyzed to detect Enhanced Green Fluorescence Protein (EGFP) fluorescence. Samples were analyzed using an XL Flow Cytometer (Beckman-Coulter, High Wycombe, UK) and WinMDA software (Scripps Research Institute, La Jolla, CA) or a FACSCalibur flow cytometer (Becton Dickinson, San Jose, CA) and FlowJo 3.2 software (Tree Star, Inc., San Carlos, CA). Dead cells were excluded on the basis of forward and side light scatter.

2.2.4 Confocal immunofluorescence microscopy

PHA-activated T cells were separated from dead cells by Ficoll-Paque gradient centrifugation and cultured overnight on fibronectin (Sigma, St. Louis, MO)-coated 4-well chamber slides (Nalge Nunc, Naperville IL). To induce polarization we added CCL5 (Regulated on Activation, Normal, T-cell Expressed, and Secreted; RANTES) chemokine (10 ng/ml, Sigma, St. Louis, MO) to the cells 30 minutes prior to staining. Following chemokine treatment the cells were fixed in 2% paraformaldehyde for 10 minutes at room temperature and then washed extensively in PBS containing 10% FCS. Indirect surface staining for MUC1 was performed using the mouse anti-human MUC1 mAb HMPV and Alexa488 labeled goat anti-mouse as a secondary antibody. Following the MUC1 staining, cells were fixed again and then permeabilized with 0.2% Triton X-100 for 10 minutes at room temperature. Intracellular staining was performed with rhodamine to stain the actin filaments or polyclonal rabbit anti-chicken spectrin followed by a red fluorescent Alexa546 goat anti-rabbit secondary antibody. Following staining, cells were immediately analyzed by confocal laser microscopy at the University of Pittsburgh Center for Biological Imaging Facility, using a Leica TCS NT confocal LSM microscope (Rockleigh, NJ). Images were collected as serial sections using (unless otherwise indicated) the x100 objective. Images are shown as either individual sections or as projections of stacked images.

MUC1-EGFP Jurkat cells were cultured 30 minutes at 37^{o}C on fibronectin coated 4-well chamber slides. Polarization was induced by adding 10 ng/ml SDF1α for 30 minutes. Cells were then fixed and permeabilized in 0.1% Triton X-100 in 2% paraformaldehyde for 15 minutes at room temperature. Cells were rehydrated with 5 washes of PBS containing 0.1% Triton X-100 then washed with PBS containing 0.5% bovine serum albumin, 0.15% glycine. Non-specific

binding was blocked by first incubating in 4% normal goat serum for 45 minutes at room temperature. Intracellular staining was performed with polyclonal rabbit anti-chicken spectrin followed by a red fluorescent Alexa546 goat anti-rabbit secondary antibody. Following staining, cells were analyzed by confocal laser microscopy at the University of Pittsburgh Center for Biological Imaging Facility, using the Olympus Fluoview Confocal microscope.

2.2.5 Fluorescent microscopy

Fluorescent images were collected of untransduced Jurkat and MUC1-EGFP transduced Jurkat in the absence or presence of SDF1α. Cells were activated overnight in 1 μg/ml PHA and 50 ng/ml PMA. The next day they were placed on fibronectin-coated glass slides in the presence or absence of 50 ng/ml SDF1α for 30 minutes at 37^{o}C. After fixing in 2% paraformaldehyde 15 minutes at room temperature the cells were stained with Hoescht dye to color the nuclei blue. Images were obtained with an Olympus Provis fluorescent microscope in the Center for Biologic Imaging, University of Pittsburgh.

2.2.6 Live cell microscopy

Human microvascular endothelial cells (HMVEC) (Cambrex; Walkersville, MD) were grown to 70% confluency on 4-chambered coverglasses (Nalge Nunc; Naperville, IL) in EGM-2-MV HMVEC medium. MUC1-EGFP transduced Jurkat cells were resuspended at 2 x 10^{7} cells /ml in PBS and 50 μl was added to each chamber of HMVEC containing 300ul HMVEC medium. Images were collected at 30 second intervals over 15 minutes on the Nikon 300 Eclipse inverted microscope with a Harvard Apparatus (Holliston, MA.) heated stage adapter. Multidimensional data sets were processed and avi files were generated through MetaMorph Software from Universal Imaging Corporation (Downington, PA).

2.2.7 Reverse Transcription-Polymerase Chain Reaction

Total RNA was prepared using Trizol reagent (Gibco BRL) according to the manufacturer's instructions. cDNA was generated from total RNA using the reverse transcription-polymerase chain reaction (RT-PCR) kit (Stratagene, La Jolla, CA), according to the manufacturer's instructions (in all experiments 10μg total RNA was used to generate cDNA). The cDNA was subsequently amplified using MUC1-specific primers 5'-GCCAGCCATAGCACCAAGACTG-3' and 5'AGCCCCAGACTGGGCAGAGAA-3'. These primers correspond to a sequence 3' of the TR encoded by exons 2 and 5 and would result in the amplification of a 446bp fragment from RNA and a 838bp fragment from genomic DNA. For the semi-quantitative RT-PCR, cDNA was diluted as indicated before the PCR amplification and the same primer set was used. In other experiments, the following primer sets were also used: 5'-TCTCAAGCAGCCAGCGCCTGCCTG-3' and 5'-TCCCCAGGTGGCAGCTGAACC-3' to yield a 331bp product, and 5'-GCCAGCCATAGCACCAAGACTG-3' with 5'-TGAAGAACCTGAGTGGAGTGG-3' to yield an 816bp product.

2.2.8 Northern Blotting

Total RNA was extracted from cells using Trizol reagent (Gibco) according to manufacturer's instructions. RNA (10 μg/lane) was run on a 1% agarose, 2.2M formaldehyde gel and then transferred onto optimized nylon membrane and fixed. The membrane was pre-hybridized for 1hr at 65°C in hybridization buffer (1%BSA, 0.25M SDS, 0.25M disodium hydrogen orthophosphate, 0.25M sodium dihydrogen orthophosphate-1-hydrate). Probes (20ng) were labeled using random primers and the MegaPrime kit (Amersham Pharmacia Biotech), following manufacturer's instructions. Probes were hybridized to the blot overnight at 65°C.

Membranes were washed for 1hr in buffer A (0.08M sodium phosphate, 2mM EDTA, 5% BSA, 10% SDS) at 65°C, and then twice in buffer B (0.16M sodium phosphate, 4mM EDTA, 4% SDS) for 1hr at 65°C and then exposed to a phosphor screen (Amersham Pharmacia Biotech). Screens were exposed overnight at room temperature and visualized using a TYPHOON 8600 scanner system (Molecular Dynamics, Little Chalfont, UK). Blots were stripped in a solution of 0.06 x saline sodium citrate (SSC), 10mM EDTA and 0.1% SDS at 100°C for 10 minutes and then reprobed as described above.

To verify the expression of MUC1 mRNA in normal human tissues, a multiple tissue-expression array (Clonetech, Basingstoke, UK) containing RNA from normal human tissues was hybridized with the MUC1 probe, as described above.

2.2.9 Probes

The following probes were used: MUC1, seven tandem repeats; C2GnT1, 950-bp *Pst*I fragment; C2GnT2, 1234-bp *Eco*RI fragment; C2GnT3, 1361-bp *Eco*RI-*Bam*HI fragment; 18S from Ambion (Austin, TX)

2.3 RESULTS

2.3.1 Expression of MUC1 on T cells activated *in vivo*.

MUC1 expression on human T cells was investigated using MUC1-specific mAbs and flow cytometry. The mAbs used in all experiments on T cells were HMFG1, HMFG2 SM3, HMPV and MF06, all of which react with repetitive epitopes in the TR domain (149). mAbs 232A1 and 12C10, which bind to epitopes outside of the TR region and therefore should react with all glycoforms, were also used.

Previously published work on the expression of MUC1 on T cells has employed *in vitro* methods of activation. We sought to determine if this observation was true also for T cells activated *in vivo*. To examine this issue, an aspirate from an acutely inflamed joint of a patient with rheumatoid arthritis was obtained, and MUC1 expression was ascertained by HMFG1 binding and flow cytometric analysis. As shown in Figure 2.0-2, more than 10% of the T cells from the aspirate were HMFG1-positive, while no staining was observed on T cells from the patient's blood. The percentage of positive cells detected by 12C10 is lower and this is due to not picking up low MUC1 expressing T cells that HMFG1 can detect because it binds multiple times per molecule while 12C10 binds only once per MUC1 molecule. Similar results were obtained with a joint aspirate from a patient with osteoarthritis (data not shown). This indicates that T cells taken from a site of an active immune response, i.e. activated *in vivo*, also express MUC1.

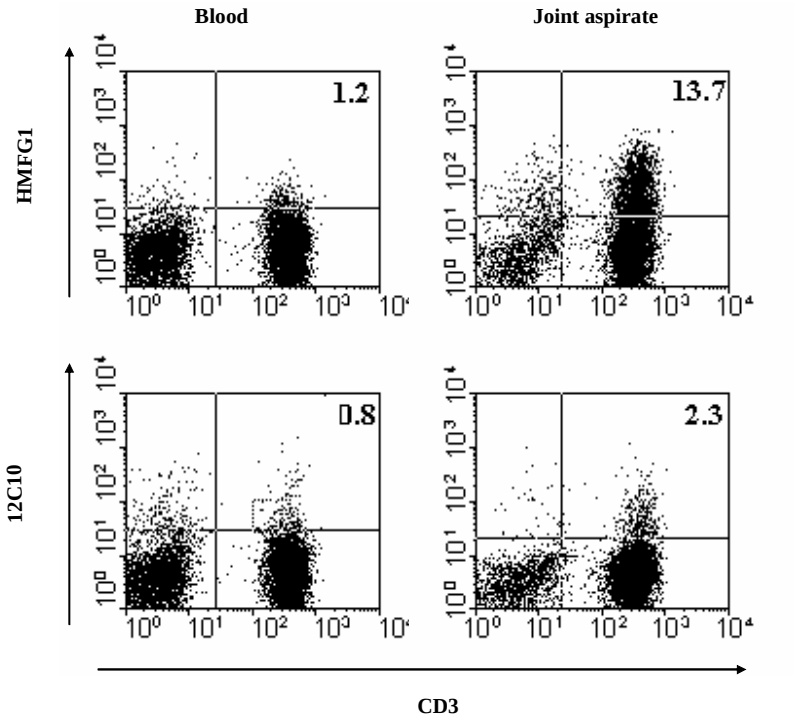

Figure 2.0-2 Expression of MUC1 on T cells activated *in vivo*. Peripheral blood mononuclear cells (PBMC) from blood or a joint aspirate of a patient with rheumatoid arthritis were stained with the indicated antibodies and analyzed by flow cytometry. Numbers indicate the percentage of gated cells in the quadrant.

2.3.2 Reactivity of MUC1 specific antibodies with human T cells activated *in vitro*

We were interested in documenting the reactivity of a variety of different antibodies on T cells to see if there would be differential binding depending on the activation state of the T cell or the epitope of the antibody. To do this we selected a broad panel of antibodies from the 1997 workshop characterizing the epitopes of known anti-MUC1 antibodies (10). These were first tested on MUC1 expressing tumor cells (BT-20) that make the underglycosylated form of MUC1 and on MUC1 transfected cells (DM6-MUC1) that make the glycosylated form of MUC1. Table 2.0-1 lists the antibodies and the mean fluorescent intensities of each cell line after flow cytometric staining. Comparison with parental DM6 cells is given to show MUC1 specific reactivity. The majority of antibodies showed reactivity with both BT-20 and MUC1-transfected

DM6 cells, though some antibodies showed a tendency to react better with one or the other cell type.

Table 2.0-1 Antibodies used to analyze MUC1 expression on BT-20, DM6 and MUC1 transfected DM6 cell lines. Epitopes listed are from (10). [+]Mean fluorescence intensity (MFI) detected by flow cytometry is given in parentheses. *Normalized MFI calculated as the ratio of anti-MUC1 antibody MFI to isotype control antibody MFI. The starred antibodies were used in Figure 2.0-3 and Figure 2.0-4.

Antibody	Epitope	BT-20	DM6	DM6-MUC1
☆ SH1	Le^x	12* (44)[+]	1 (4.02)	3 (11)
BW835	Carbohydrate?	298 (1289)	2 (5.94)	251 (1199)
27.1	Carbohydrate?	748 (3231)	10 (41.15)	929 (4430.36)
☆ KC4	Carbohydrate?	255 (937)	1 (7.8)	27 (118)
Ma695	Sialic acid dependent.	582 (3811)	6 (35.82	573 (5229)
HH6	BG a or A type 1	22 (80.6)	1 (7.2)	6 (25)
43	Galactose dependen/Tn (+TAP-2), H-type	59 (1042)	13 (62.84)	60 (256)
☆ FH6	SLe^x	120 (2108)	5 (22.06)	6 (19)
☆BCRU-G7	GalB1-3GlcNAc?	1 (11.49)	7 (34)	15 (65)
☆ 7539MR	Carbohydrate?.	326 (1378)	3 (11)	639 (3132)
☆ 115D8	Sialic acid dependent	354 (1498)	4 (15)	846 (4143)
VU-3-C6	GVTSAPDTRPAP	323 (1394)	11 (43.9)	458 (2186)
BC4E549	TSAPDTRPAP	884 (3818)	3 (13)	720 (3434)
VU-11-D1	TSAPDTRP	80 (346)	1 (4)	186 (885)
VU-11-E2	TSAPDTRP	160 (692)	2 (7)	361 (1724)
☆ VU-3-D1	SAPDTRPAP	180 (448)	3 (10)	294 (1404)
BC3	APDTR	25 (140)	2 (9.57)	39 (287)
E29	APDTRP	401 (1750)	1 (5.77)	300 (2548.35)
VA2	APDTRPA	59 (257)	2 (9.6)	160 (761
Sec1	APDTRPAP	14 (59.72)	1 (5.85)	10 (50.85)
214D4	PDTR	11 (49)	4 (15.15)	8 (40)
VU-12-E1	PDTRPAP	227 (982.22)	2 (7.83)	257 (1364)
b-12	PDTRPAP	293 (1921)	2 (14)	98 (895.32)
GP1.4	PDTRPAPGS	474 (3103)	6 (36.83)	609 (5556)
Mc5	DTRPAP	629 (2717	5 (19)	311 (1483)
Va1	TRPAP	28 (123)	4 (14)	87 (414)
M38	PAPGSTAPPAHG	774 (3342)	1 (5.34)	258 (1232)
MF11	PPAH	919 (3971)	7 (26.11)	930 (4437)
BCP7	HGVST	4 (18.49)	1 (5)	5 (42.1)
SMA-1	Unknown (Non-VNTR)	3 (14.45)	1 (6.9)	1 (10.26)
12C10	Unknown (Non-VNTR)	176 (1153)	5 (27.66)	368 (3309)
HH14	Unknown (Non-VNTR)	1 (5.32)	1 (6.31)	1 (7.18)
M29	Unknown (Non-VNTR)	57 (373)	4 (15)	638 (3132)

From this panel we selected antibodies (SH1, KC4, FH6, BCRU-G7, 7539MR, 115D8 and VU-3-D1) reactive to the VNTR region that showed this preferential binding towards the different forms of MUC1 and used them to stain resting and activated T cells. Other antibodies not used here may be useful in future studies. As expected, resting T cells did not express MUC1

detectable by any of these antibodies covering a range of epitopes (10). Antibodies that showed a preference for the normal form of MUC1 (Figure 2.0-3), show higher overall reactivity with activated T cells than do the antibodies which prefer the tumor form of MUC1 (Figure 2.0-4). In addition to the antibodies from Table 2.0-1 other anti-MUC1 antibodies with desired characteristics were later obtained and used in subsequent experiments (SM3, HMFG1, 232A1, MF06, HMPV). Staining of activated T cells by SM3, an exquisitely specific tumor MUC1 antibody agrees with previous results (Figure 2.0-5) (150).

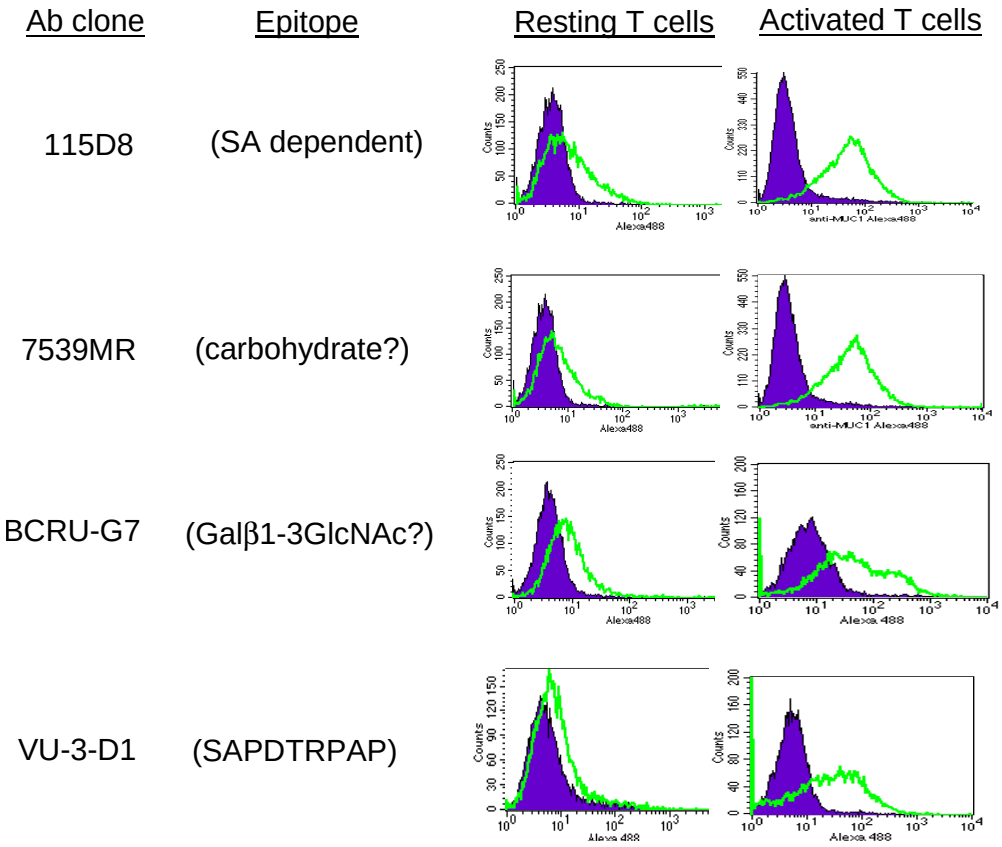

Figure 2.0-3 Resting and PHA activated human T cells stained by anti-MUC1 antibodies with preference towards the normal form of MUC1, followed by Alexa488 labeled goat anti-mouse antibody. Shaded histograms are isotype control antibody fluorescence, open histograms are anti-MUC1 antibody fluorescence. Epitopes listed are from (10).

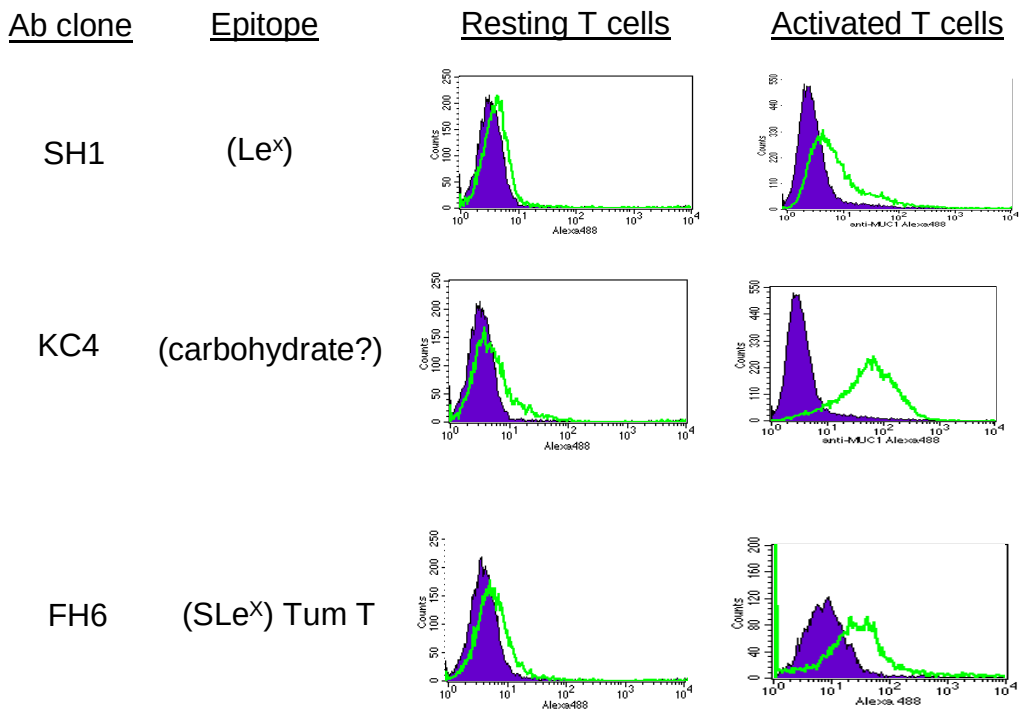

Figure 2.0-4 Resting and PHA activated human T cells stained by anti-MUC1 antibodies with preference towards the tumor form of MUC1, followed by Alexa488 labeled goat anti-mouse antibody. Shaded histograms are isotype control antibody fluorescence, open histograms are anti-MUC1 antibody fluorescence. Epitopes listed are from (10).

Flow cytometric analysis of human T cells with multiple anti-MUC1 mAbs showed that none bound to resting T cells and most bound to activated T cells (Figure 2.0-3; Figure 2.0-4; Figure 2.0-5). mAb HMFG1, HMPV and MF06 reproducibly bound to activated T cells and were used in further experiments. Staining of activated T cells with mAb 232A1 was detectable, but the fraction of cells recognized by this antibody was low (Figure 2.0-5).

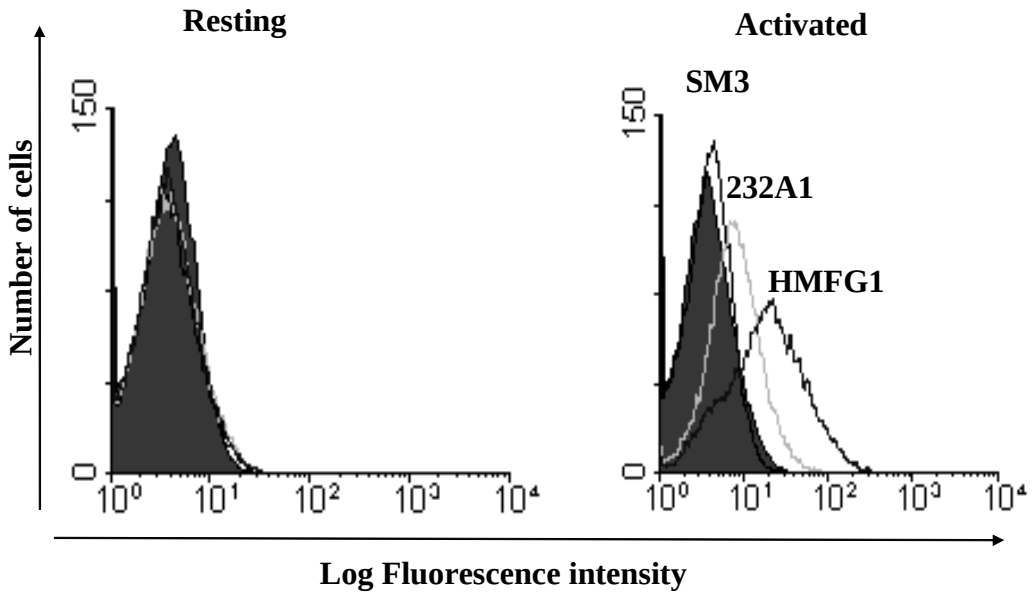

Figure 2.0-5 Expression of MUC1 on activated T cells. Resting and phytohaemagglutinin (PHA)-activated T cells were stained using different MUC1-specific monoclonal antibodies (mAbs) followed by fluorescein isothiocyanate (FITC)-labeled rabbit anti-mouse immunoglobulin.

To increase the intensity of signal, 12C10 and HMFG1 mAbs were biotinylated and streptavidin-PE was used for detection. Staining of T cells with HMFG1 was demonstrable 24 hours after *in vitro* activation with immobilized anti-CD3 mAb, and after 4 days more than 90% of cells were stained by the antibody (Figure 2.0-6). Staining with biotinylated 12C10 mAb (also an IgG1 like HMFG1) was also seen, but at a much lower level than that for HMFG1 (Figure 2.0-6). Staining for the activation marker CD69, indicated that MUC1 expression was a later event than CD69 expression during T cell activation (Figure 2.0-6). Expression of MUC1 on activated T cells was similar on both $CD4^+$ and $CD8^+$ T cells (data not shown).

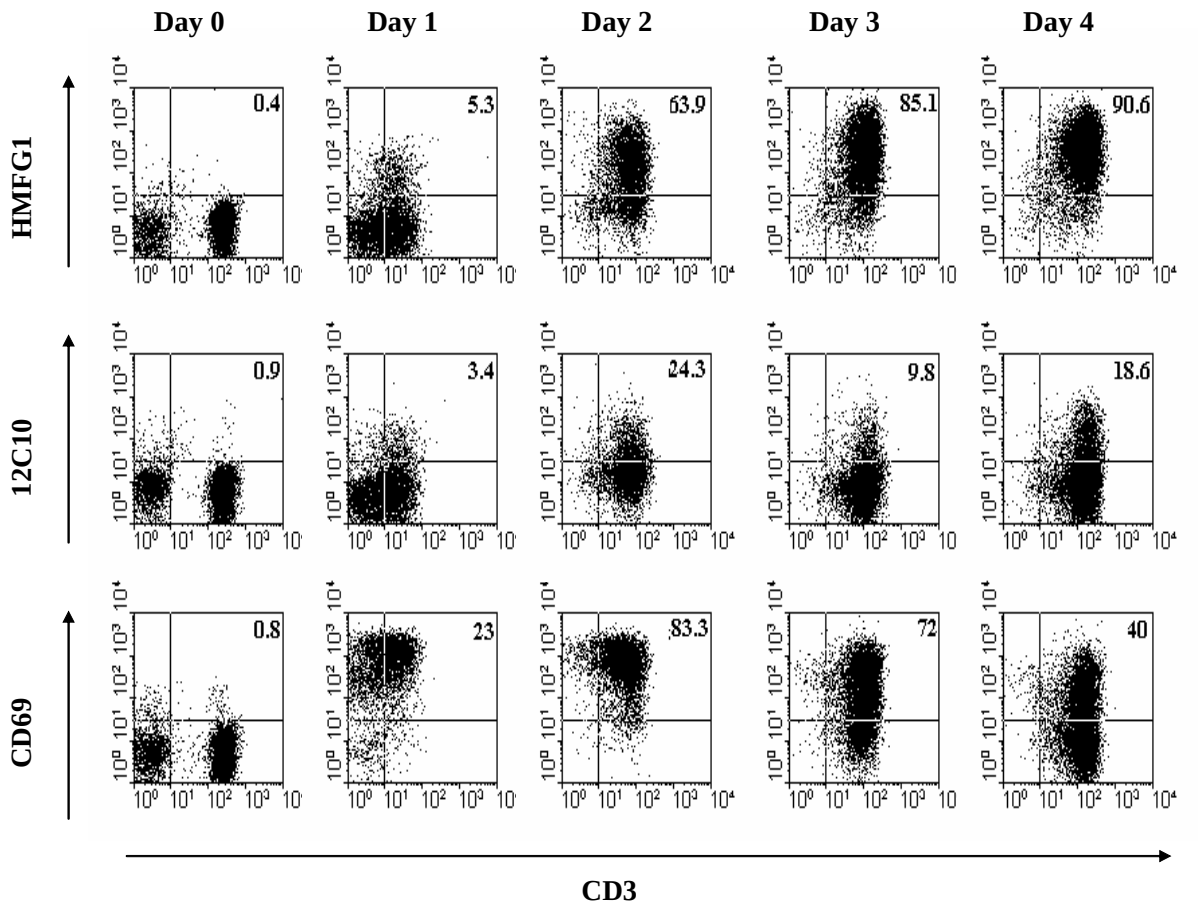

Figure 2.0-6 Expression of MUC1 on activated T cells. Unstimulated peripheral blood mononuclear cells (PBMC) (day 0) or PBMC stimulated with anti-CD3 mAb for the indicated periods of time were stained with anti-CD3-FITC, in combination with anti-CD69-PE, HMFG1-biotin or 12C10-biotin, and analyzed by flow cytometry. Numbers indicate the percentage of gated cells in the quadrant.

The above experiments utilized potent polyclonal stimuli that might not be considered physiological, and in further studies we examined MUC1 expression by T cells stimulated by alloantigens in an MLR. After 6 days in culture with allogeneic stimulator cells, approximately 25% of responding T cells stained with HMFG1 mAb (Figure 2.0-7A). The pattern of HMFG1 staining mirrored the expression of the activation marker CD25. There was no significant staining of the non-stimulated T cells from the same donor. Cells repeatedly stimulated every 7 days over a 1 month period demonstrated persistent MUC1 expression. During this chronic

stimulation T cells acquired the memory phenotype, gaining expression of CD45RO, which was co-expressed with MUC1 on the majority of T cells (Figure 2.0-7B).

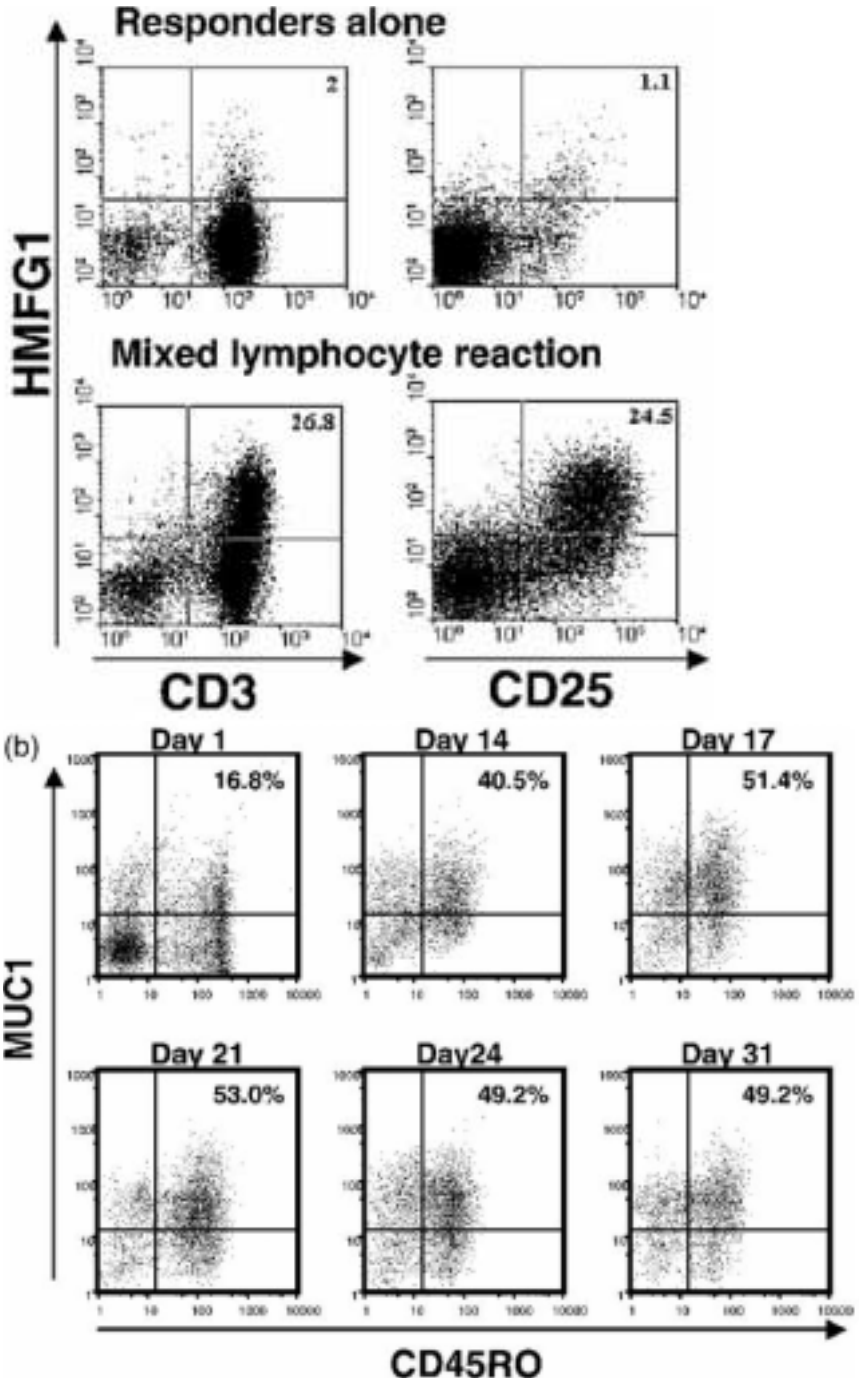

Figure 2.0-7 Expression of MUC1 on activated T cells in a mixed lymphocyte reaction. (A.) Responder PBMC, incubated for 6 days in the presence or absence of irradiated allogeneic stimulator cells, were stained with HMFG1-biotin, in association with CD3-fluorescein isothiocyanate (FITC) or CD25-FITC and analyzed by flow cytometry. Numbers indicate the percentage of gated cells in the quadrant. (B.) Cells activated with allogeneic PBMC every 7 days for a month were stained for CD45RO and MUC1 (MF06 monoclonal antibody) then analyzed by flow cytometry.

2.3.3 Differential distribution of MUC1 on the surface of activated and polarized T cells

The distribution of MUC1 on the surface of T cells was studied by confocal microscopy using the MUC1-specific mAb HMPV. Activated, non-polarized T cells displayed MUC1 evenly over the entire surface (Figure 2.0-8A). When these cells were then exposed to the chemokine RANTES they responded predictably by changing morphologically and assuming a polarized shape needed for migration, with a leading edge and a trailing edge (uropod). In these polarized cells MUC1 was immediately sequestered to one of the poles (Figure 2.0-8B). By staining for spectrin (in red), which is a known marker of the T cell uropod (151, 152), and for MUC1 (in green), we were able to determine that MUC1 is concentrated opposite the uropod and on the leading edge of the T cell (Figure 2.0-8B).

A. Non-polarized B. Polarized

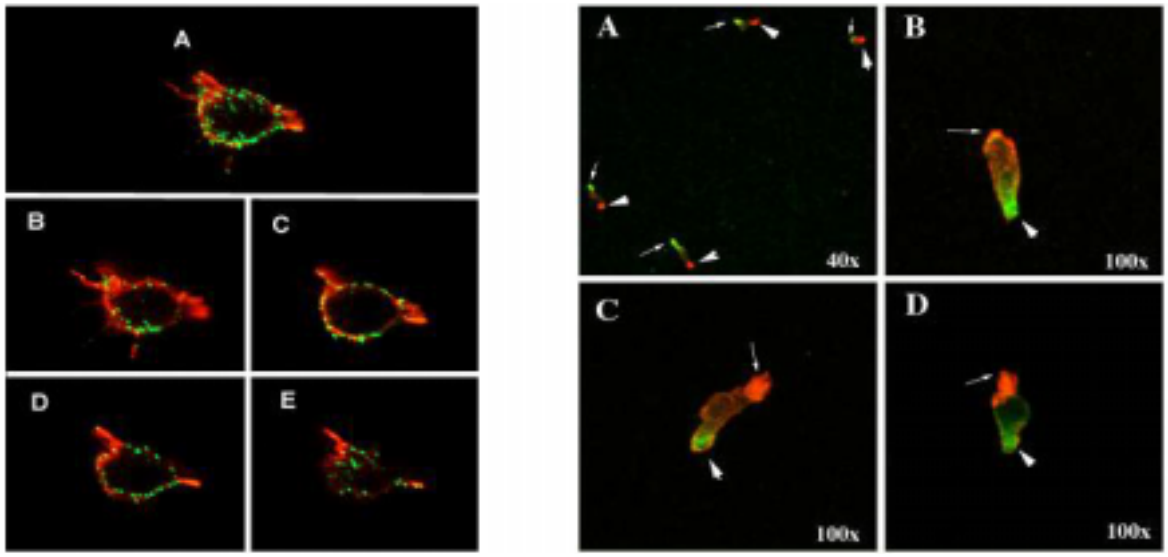

Figure 2.0-8 Analysis by confocal microscopy of MUC1 on activated T cells. (A. Non-polarized) Activated T cells were stained for MUC1 (green) and then counterstained for actin (red). The top image shown in (A. Non-polarized) represents a projection of eight images acquired as 0.5-μm-thick scanned sections, four of which are shown in b–e. Magnification is 100x. (B. Polarized) Activated T cells adherent to fibronectin-treated slides were treated with regulated on activation, normal, T-cell expressed, and secreted (RANTES) chemokine prior to staining for MUC1 (green; thick arrows). Cells were then permeabilized and stained for spectrin (red; thin arrowheads), a marker for uropods. The magnification of the top-left image in (B. Polarized) is 40x. The magnification of remaining images b–d is 100x. These confocal microscopy images are projections of 16 stacked sections through the cells.

For further study of polarization of MUC1 to the leading edge of T cells we decided to generate a model MUC1 expressing T cell line with which we could watch the movement of MUC1. The use of fluorescent MUC1 would allow observation of MUC1 movement. Jurkat cells were transduced with a MUC1-EGFP vector and positively selected. Flow cytometry of unstained cells looking at just EGFP fluorescence (Figure 2.0-9) shows that the MUC1-EGFP transduced Jurkat cells are expressing EGFP.

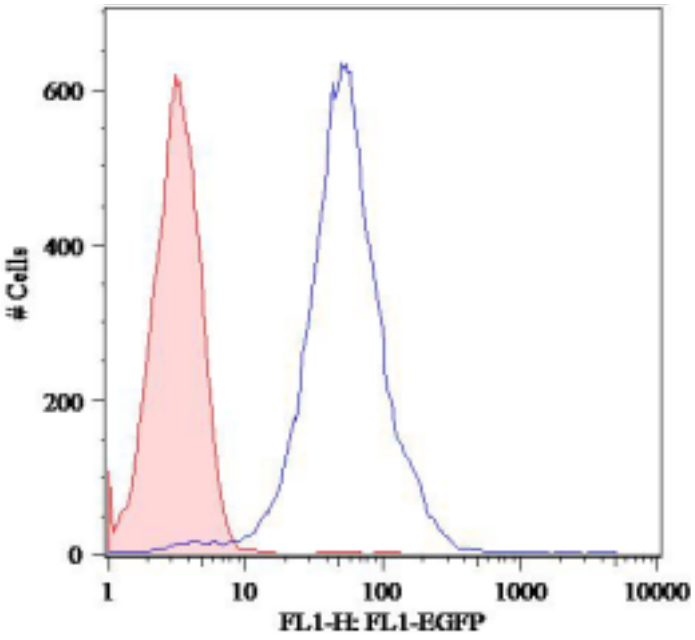

Figure 2.0-9 Fluorescence of EGFP from MUC1-EGFP transduced Jurkat cells. After transduction and positive selection, MUC1-EGFP Jurkat cells were analyzed by flow cytometry in the absence of antibody staining. Shaded histogram is the fluorescence of untransduced Jurkat cells. Open histogram is the fluorescence of MUC1-EGFP transduced Jurkat.

However, EGFP fluorescence could be detected through the cell membrane from MUC1-EGFP that is not expressed on the cell surface. It is also possible that expression of the construct could have been altered in some way that results in EGFP expression without full-length MUC1 protein. Flow cytometry staining was done on intact transduced Jurkat cells using an antibody reactive to the VNTR region to verify surface expression of MUC1 (Figure 2.0-10). Fluorescent

microscopy demonstrating MUC1-EGFP expression also indicates successful transduction of the Jurkat cells (Figure 2.0-11).

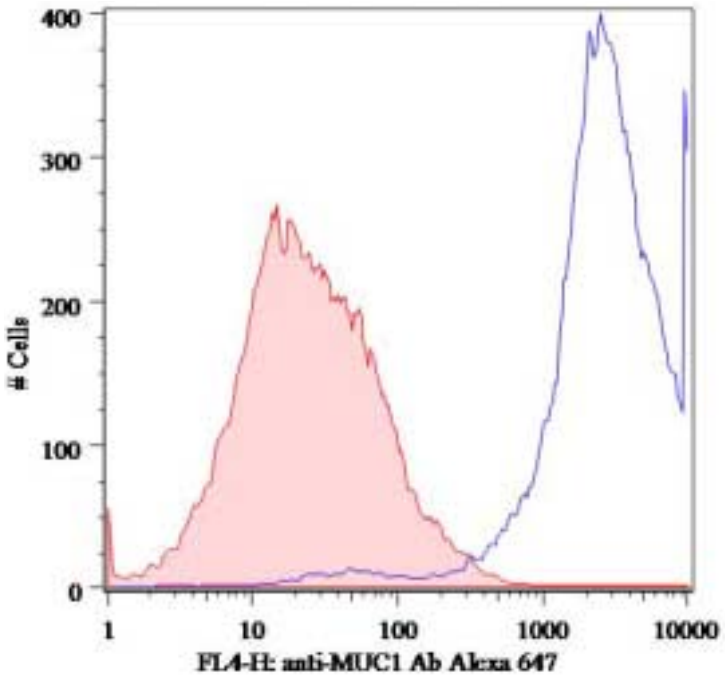

Figure 2.0-10 Surface expression of MUC1 on MUC1-EGFP transduced Jurkat cells. After transduction and positive selection, MUC1-EGFP Jurkat cells were stained with isotype control or anti-MUC1 antibody VU-3-C6 followed by anti-mouse Alexa647, whose emission is distinct from EGFP emission, then analyzed by flow cytometry. Shaded histogram is the fluorescence of isotype control staining. Open histogram is the fluorescence of anti-MUC1 staining.

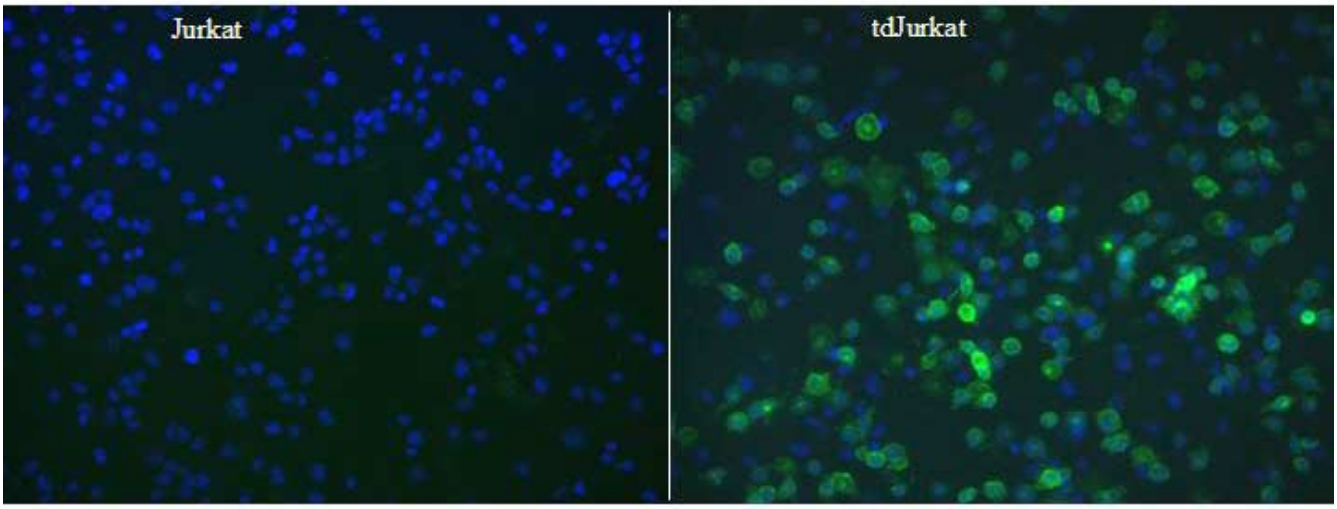

Figure 2.0-11 Fluorescent microscopy of untransduced and MUC1-EGFP transduced Jurkat cells. After transduction and positive selection of transduced cells, fluorescent microscopic pictures were taken of untransduced Jurkat cells (Jurkat) or MUC1-EGFP transduced Jurkat cells (tdJurkat). Cells were activated overnight to enhance expression of MUC1-EGFP then placed on fibronectin coated slides and stained with Hoescht to dye the nuclei (blue); MUC1-EGFP appears green.

These cells were stimulated with the chemokine SDF1α and examined for polarization and MUC1 localization by fluorescent microscopy, confocal microscopy and live cell microscopy. Slides were coated with fibronectin to both aid in cell attachment, since Jurkat cells are non-adherent, and to aid in presenting chemokine to the cells (118). With fluorescent microscopy there were indications of polarized cell morphology in some cells and bright spots on the cells where MUC1 was focused (Figure 2.0-12).

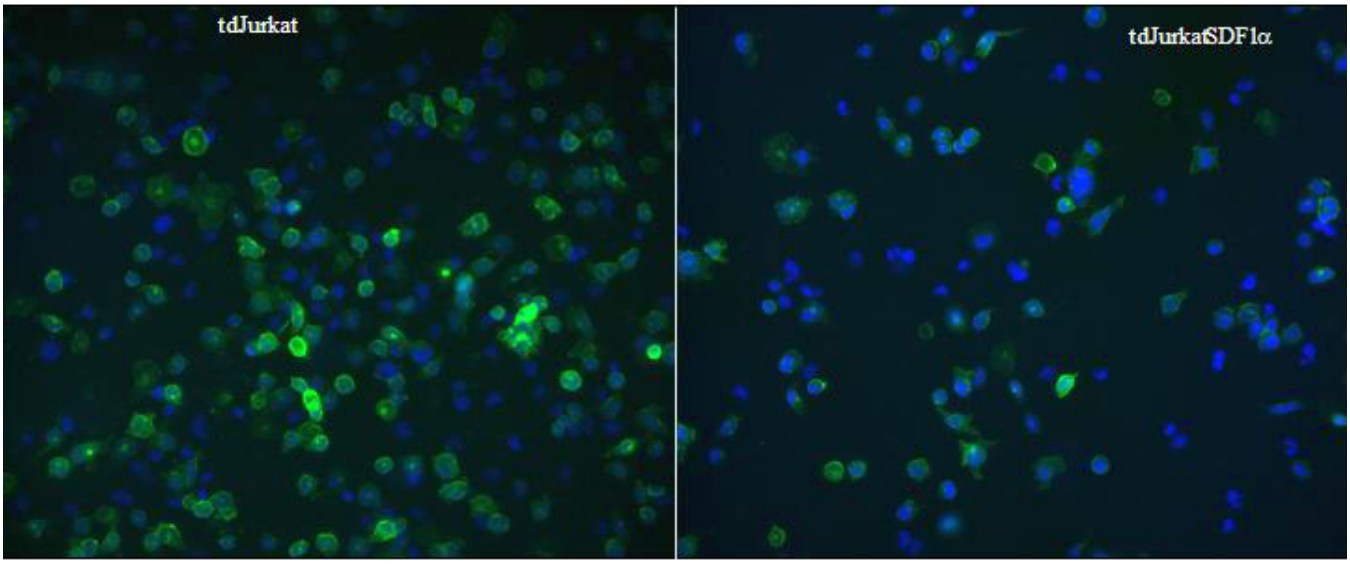

Figure 2.0-12 Fluorescent microscopy of MUC1-EGFP transduced Jurkat cells in the absence or presence of polarizing chemokine. Cells were first activated overnight to enhance expression of MUC1-EGFP and then placed on fibronectin coated slides without (A. TdJurkat) or with (B. tdJurkatSDF1α) SDF1α. After a 30 minute incubation, slides were washed and stained with Hoescht to dye the nuclei (blue); MUC1-EGFP appears green.

However, it could not be conclusively determined that MUC1 was being localized to the leading edge as seen with primary cultures of activated human T cells since we did not have a similar phenotype. The polarized MUC1-EGFP Jurkat cell population does appear to be dimmer but MUC1–EGFP expression is unaffected by a wide range of SDF1α concentrations. SDF1α concentrations ranging from 0 to 300 ng/ml did not affect the fluorescence of MUC1-EGFP transduced Jurkat cells, as seen by flow cytometry analysis (Figure 2.0-13).

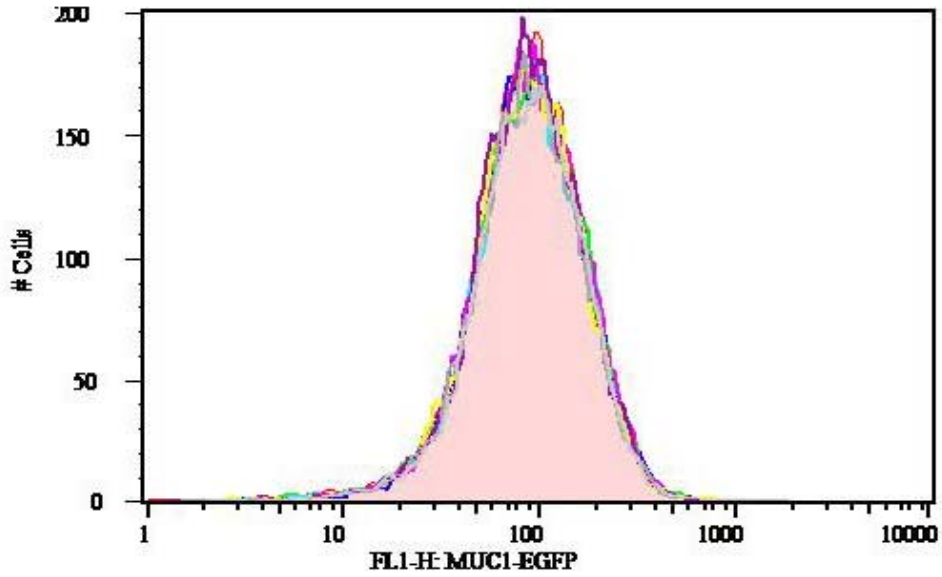

Figure 2.0-13 MUC1-EGFP expression on MUC1-EGFP transduced Jurkat cells following incubation with SDF1α. Cells were placed in fibronectin-coated wells containing 0 to 300 ng/ml of SDF1α for 30 minutes then analyzed for EGFP fluorescence by flow cytometry. Differently colored histograms from cells incubated at each concentration were overlaid. The shaded histogram represents cells incubated with no chemokine.

In agreement with recent characterization of chemokine receptors on Jurkat cells (153), our MUC1-EGFP Jurkat cells do express the receptor for SDF1α, CXCR4, and can respond to SDF1α by down-regulating receptor expression with increasing doses of chemokine (Figure 2.0-14).

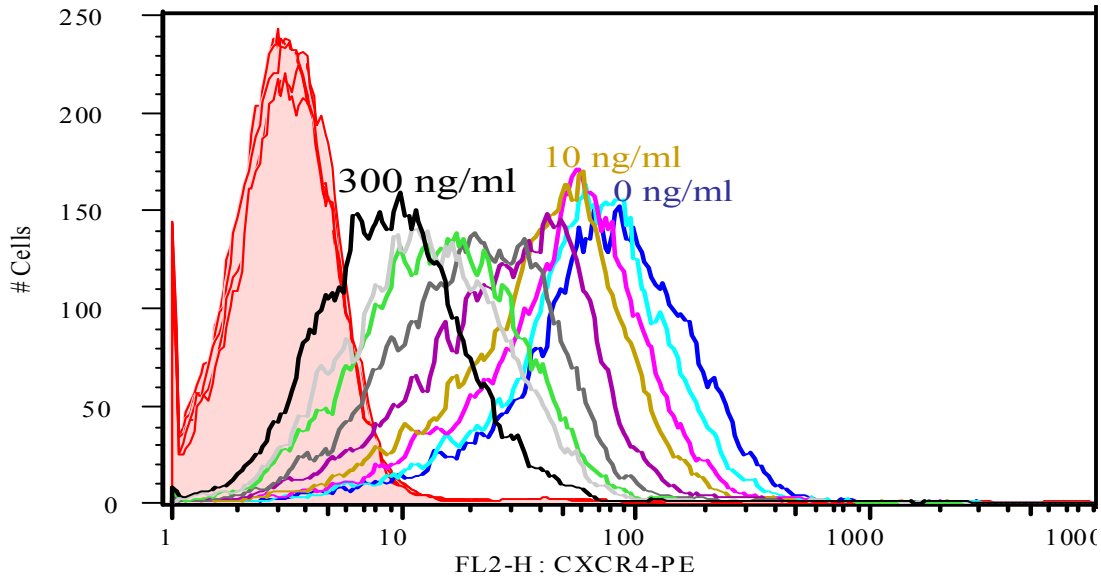

Figure 2.0-14 CXCR4 expression on MUC1-EGFP transduced Jurkat cells following incubation with SDF1α. MUC1-EGFP Jurkat cells were placed in fibronectin-coated wells containing 0 to 300 ng/ml SDF1α for 30 minutes. Cells were then stained with anti-CXCR4-PE and analyzed by flow cytometry. Shaded histograms are the fluorescence of isotype control staining. Open histograms are the fluorescence of anti-CXCR4-PE staining on cells incubated with different SDF1α concentrations (ng/ml).

It is possible that the dimness observed by fluorescent microscopy may be due to movement of leading edge localized MUC1-EGFP underneath the cell. Pelletier et al reported that SDF1α is presented by matrix and causes the receptor for SDF1α, CXCR4, to polarize to the leading edge of migrating cells, particularly to the basal surface touching the matrix (118). Similar localization has been reported for other chemokine receptors (119). Del Pozo et al likewise reported that leading edge localized LFA-1 was distributed along the contact area between T cells and endothelium (121). Perhaps the dimness of MUC1-EGFP on the transduced Jurkat cells following polarization is due to the intervening cell body. To see whether MUC1-EGFP was moving to the leading edge opposite of the uropod, confocal microscopy was done to polarized cells. Following incubation with SDF1α, cells were stained for intracellular spectrin, a marker for uropods (Figure 2.0-15).

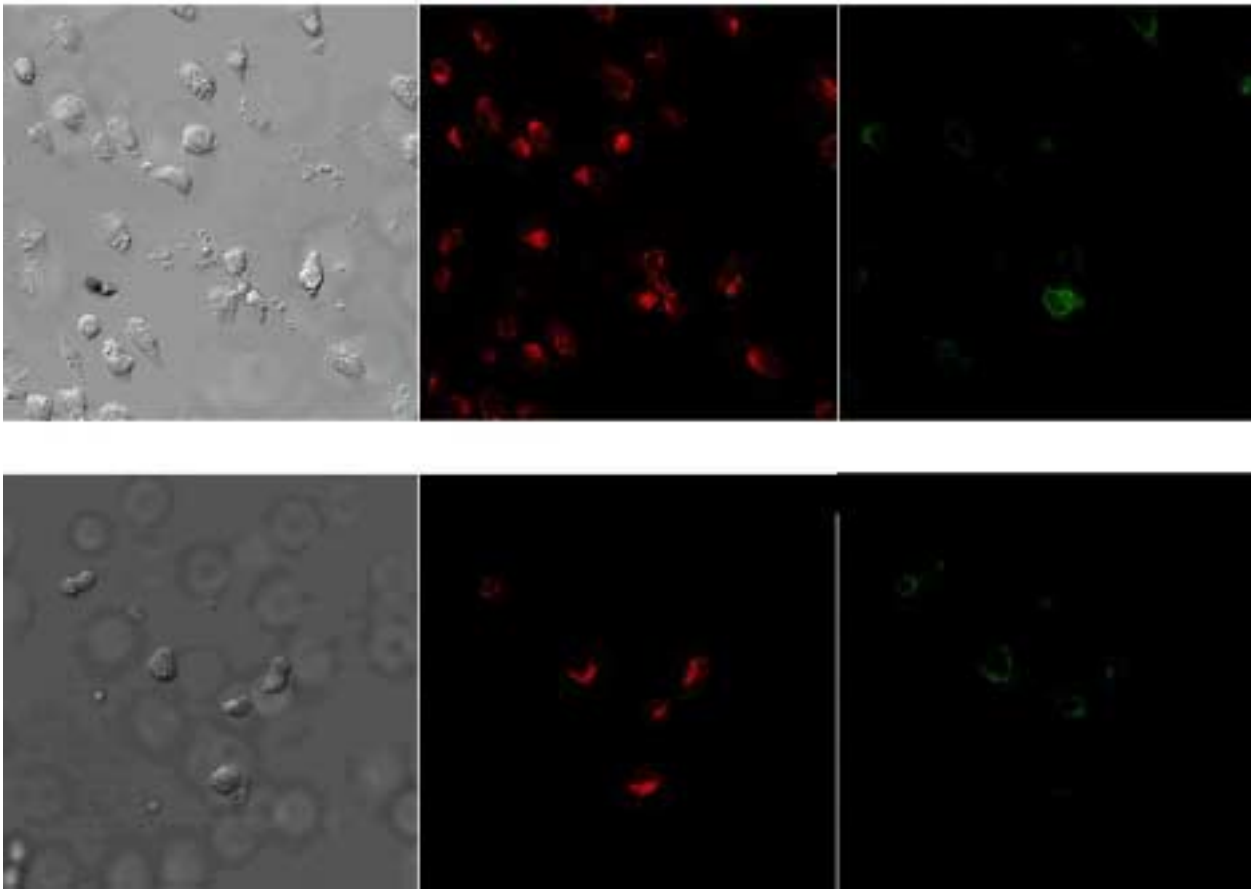

Figure 2.0-15 Analysis by confocal microscopy of MUC1-EGFP on MUC1-EGFP transduced Jurkat cells in the absence or presence of SDF1α. Cells were incubated in the absence (top row) or presence (bottom row) of SDF1α in fibronectin coated 4-well chamber slides and stained for intracellular spectrin (red); MUC1-EGFP appears green. Light images shown on left to visualize cell shape.

It is difficult to draw conclusions because some of the cells appear to have MUC1 and spectrin in distinct areas but in other cells they appear to overlap. This is probably due to partial polarization of the cell population during the exposure to SDF1α. When the MUC1-EGFP transduced Jurkat cells were allowed to simply interact with endothelium during live cell microscopy we can watch definite changes in cell morphology and distribution of fluorescent MUC1 on the cell surface on some cells (Figure 2.0-16). Though our live cell microscopy cannot pinpoint the focal plane to conclusively demonstrate MUC1 has localized to only the

leading edge, as shown by confocal microscopy of normal human T cells, these data indicate that MUC1 is moved on the cell surface when MUC1-expressing cells interact with endothelium.

Figure 2.0-16 Live cell microscopy of MUC1-EGFP Jurkat cells interacting with endothelium. HMVEC monolayers were grown on 4-chambered coverglasses. MUC1-EGFP Jurkat cells were added to chambers and images collected over 15 minutes as the cells began to interact. The same field of view is shown in both microscopic images, DIC (left) and fluorescent (right).

2.3.4 Expression of MUC1 mRNA in activated T cells.

The results from the antibody staining suggested that MUC1 was expressed in activated, and not resting, human T cells. We confirmed this observation at the level of MUC1 RNA by RT-PCR from T cells at different times after activation. Figure 2.0-17A shows the presence of the predicted 446bp RT-PCR fragment using primers 3' to TR domain of MUC1 on T cells activated with anti-CD3 antibody. No RNA was detectable on day 0 but the level of expression appears to increase with time after activation (Figure 2.0-17A). Extraction of the bands and DNA sequencing confirmed these to be the expected fragment of MUC1 mRNA. Similar results were obtained using primers yielding a 331bp fragment from the region 5' to the TR domain (data not shown) and for T cells activated with phytohemagglutinin. Sequencing of this fragment also showed it to correspond to the expected MUC1 nucleotide sequence. Using semi-quantitative RT-PCR, a comparison was made of levels of MUC1 mRNA in activated T cells and breast cancer cells from the same individual. Figure 2.0-17B shows that using cDNA from the breast

cancer cells, strong bands were produced up to dilutions of 1/100, whereas a weak band was obtained from equivalent amounts of undiluted cDNA from activated T cells, which was lost rapidly on dilution. The data suggest that the level of expression of the glycoprotein in activated T cells was at least 50 times lower than in the breast cancer cells.

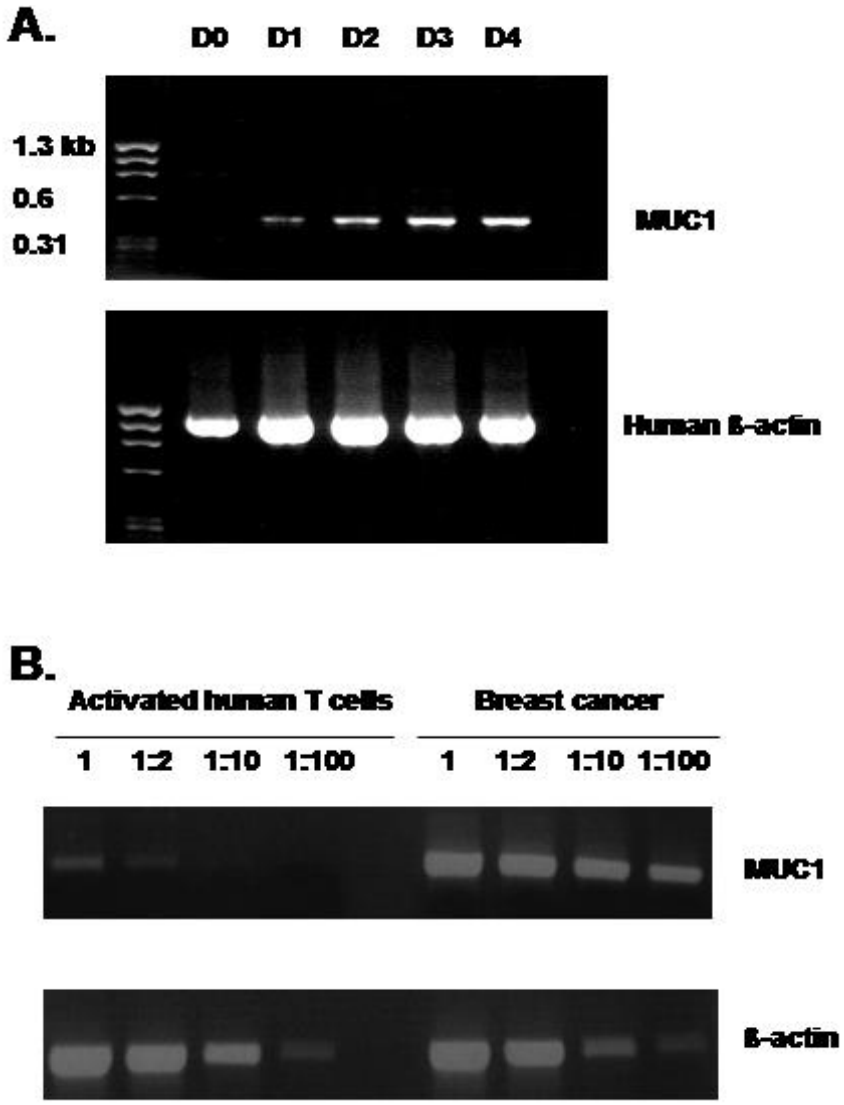

Figure 2.0-17 Detection by reverse transcription-polymerase chain reaction (RT-PCR) of MUC1 transcript in activated T cells. (A) Human T cells were activated *in vitro* by anti-CD3 antibody. Total RNA was extracted and RT-PCR performed on the indicated days (D0, day 0; D1, day 1; D2, day 2; D3, day 3; D4, day4). MUC1 transcript (446 bp) was identified after at least 24 hr. Human β–actin was included as a positive control, and a molecular weight marker is present in lane 1. (B) Semiquantitative RT-PCR for MUC1 in activated T cells and autologous breast cancer. Total RNA was extracted from autologous breast cancer cells and from purified human T cells following 4 days of *in vitro* activation using anti-CD3 antibody. cDNA was synthesized and then used as the template for RT-PCR at the dilutions shown. Human β–actin was included as a positive control.

Northern blot analysis of MUC1 RNA expression after stimulation of T cells with PHA or CD3 antibody also showed expression, but at very low levels, beginning to appear after 1 day. Figure 2.0-18A shows that with a level of sensitivity sufficient to detect a strong signal for MUC1 RNA expressed by a breast cancer cell line, T47D, no transcript was detected in activated T cells. A much higher level of sensitivity was necessary to detect MUC1 RNA in the activated T cells. In the Northern blots the probe used was from the TR domain, and the size of the transcripts was as expected for full length MUC1. We conclude that activation of T cells is accompanied by low level expression of the full length MUC1 RNA.

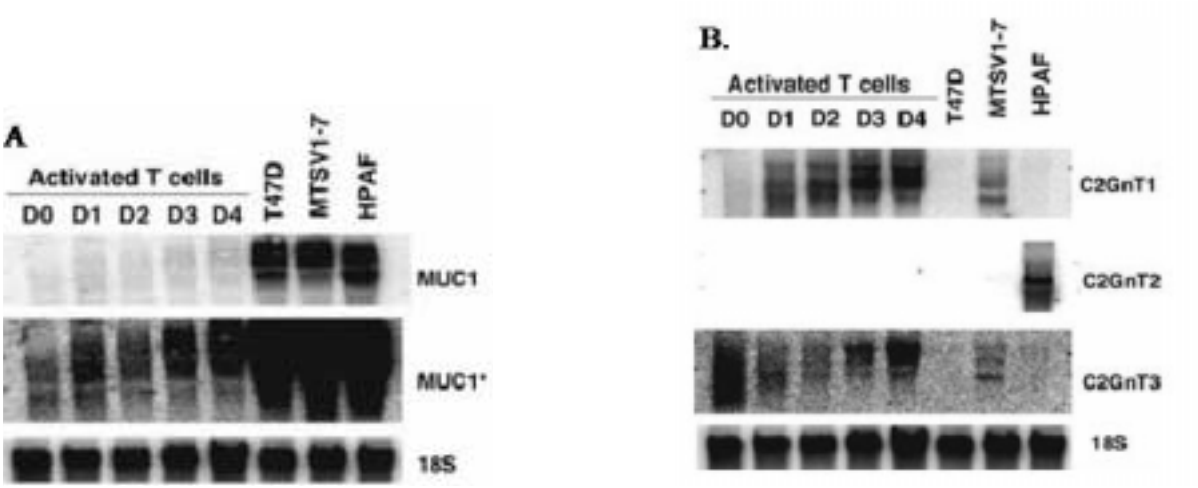

Figure 2.0-18 Northern blot analysis of resting and activated human T cells. (A) Resting T cells (D0) or T cells activated by anti-CD3 antibody for the indicated periods of time (D0, day 0; D1, day 1; D2, day 2; D3, day 3; D4, day4) were analyzed by Northern blot analysis for expression of MUC1. MUC1* represents the same blot with increased sensitivity. The cell lines T47D, MTSV1-7 and HPAF were included as positive controls for MUC1. (B) The O-glycosylation enzymes C2GnT1, C2GnT2 and C2GnT3 from resting T cells (D0) or T cells activated by anti-CD3 antibody for the indicated time periods were analyzed for expression by Northern blot analysis and compared to MUC1 expressing tumor cell lines.

2.3.5 Expression of glycosyl transferases synthesizing core 2 structures in activated T cells.

The lack of reactivity of the SM3 and HMFG2 antibodies with MUC1 expressed on activated T cells suggested that the O-glycans on the MUC1 expressed by these cells were core 2 -based (150, 154). Indeed the first cDNA coding for a core 2 synthesizing enzyme, β6GlcNAc-transferase 1 (C2GnT1), was isolated by expression cloning from activated T cells (155). Two additional β6GlcNAc transferase enzymes, C2GnT2, and C2GnT3 have now been isolated (156, 157) and we examined the expression of transcripts coding for each of the three enzymes by Northern blot analysis in resting and in activated T cells (Figure 2.0-18B). An increase in the expression of C2GnT1 mRNA was seen upon T cell activation, C2GnT2 transcripts were not detected, whereas the level of expression of C2GnT3 appeared to fluctuate, both in size and level of expression. We conclude from this data that the increased activity responsible for synthesizing core 2 structures in activated T cells is likely to be due to increased expression of the C2GnT 1 enzyme as had been previously assumed (96).

2.3.6 Expression of MUC1 mRNA in normal adult tissues.

Expression of MUC1 in normal adult tissues has been documented by immunohistochemical staining using antibodies to epitopes in the TR domain. These studies have suggested that MUC1 expression is largely seen in epithelial cells, particularly those of the lung, stomach, pancreas, kidney lactating mammary gland and salivary gland (158-160). While mRNA levels do not necessarily predict the levels of expressed glycoprotein, detection of the transcript avoids the problem of different glycoforms being differentially recognized by antibodies to the TR domain. To define the profile of expression of MUC1 mRNA in normal

adult tissues, a dot blot of polyA$^+$ RNA was subjected to Northern analysis using a probe to the TR domain of MUC1. Figure 2.0-19 shows that, as expected, high expression of MUC1 is seen in the epithelial tissues. However the levels of transcript detected in the intestinal tract and in trachea were much higher than those seen with antibody staining (161), presumably because of the extensive glycosylation, which blocks access of antibody to TR epitopes. Foetal lung and kidney also showed high expression levels. Significantly, MUC1 transcripts were not detected in thymus, spleen and PBL, confirming our observation that MUC1 is not expressed in resting T cells and only at low levels in activated T cells.

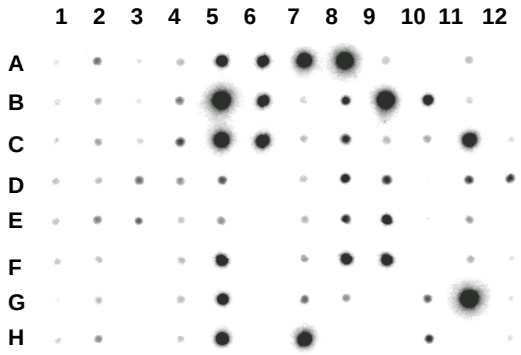

	1	2	3	4	5	6	7	8	9	10	11	12
A	whole brain	cerebellum	substantia nigra	heart	esophagus	transverse colon	kidney	lung	liver	HL-60	fetal brain	yeast total RNA
B	cerebral cortex	cerebellum	accumbens nucleus	aorta	stomach	descending colon	skeletal muscle	placenta	pancreas	HeLa	fetal heart	yeast tRNA
C	frontal lobe	corpus callosum	thalamus	atrium	duodenum	rectum	spleen	bladder	adrenal	K562	fetal kidney	E. coli rRNA
D	parietal	amygdalla	pituitary	atrium	jejenum		thymus	uterus	thyroid	MOLT-4	fetal liver	E. coli DNA
E	occipital	caudate nucleus	spinal cord	ventricle	ileum		PBLs	prostate	salivary gland	Raji	fetal spleen	Poly r(A)
F	temporal lobe	hippocampus		ventricle	iliocecum		lymph node	testis	breast	Daudi	fetal thymus	human Cot-1 DNA
G		medulla oblongata		septum	appendix		bone marrow	ovary		SW 480	fetal lung	human DNA 100 ng
H	pons	putamen		apex	ascending colon		trachea			A549		human DNA 500 ng

Figure 2.0-19 The presence of MUC1 mRNA transcript in fetal and adult human tissues. A commercial multiple tissue expression array was assayed for MUC1 transcript using a probe to the tandem repeat (TR) region.

More detailed analysis by flow cytometry of some other hemopoietic lineages using the same antibodies indicated that MUC1 is not expressed on monocytes or monocyte-derived dendritic

cells, and only very low levels could be detected on B cells (data not shown). Finally, T cells in lymph nodes removed at surgery for breast cancer did not stain with the antibodies in immunohistochemistry, whereas metastatic breast cancer cells in the lymph nodes did stain strongly with all the antibodies.

2.4 Discussion

In this study, we have analyzed in detail the expression of MUC1 in human T cells. Following activation *in vivo* and by different stimuli *in vitro*, human T cells expressed MUC1 at the cell surface, although the level of expression was much lower than that seen in breast cancer cells. Our findings demonstrated that resting T cells do not bind anti-MUC1 mAbs, nor is MUC1 mRNA detectable by RT-PCR or Northern blot analysis in these cells. As the activated T cells progress to the memory state they maintain MUC1 on the cell surface. Confocal microscopy revealed that MUC1 was uniformly expressed at the cell surface until a migratory chemokine was present; following such a stimulus, the cells focused MUC1 to the leading edge. The Jurkat cell line transduced with MUC1-EGFP showed a similar tendency to localize MUC1 when exposed to chemokines or an endothelial monolayer. The profile of reactivity with different antibodies suggests that the glycoform of MUC1 expressed by the activated T cells carries core 2-based O-glycans as opposed to the core 1 structures that dominate in the cancer-associated mucin.

It is well established that the glycosylation pattern of MUC1 can vary with the cell type expressing the glycoprotein (126, 162, 163). The binding of antibodies to epitopes in the TR domain of MUC1 is strongly influenced by the composition and density of the O-glycans attached to serines and threonines in this domain. The preferential reactivity of the HMFG1 mAb

with activated T cells probably reflected the fact that it can recognize MUC1 carrying core 2-based structures (as well as the cancer-associated glycoforms; see refs (150, 154)). The same must be true for mAbs HMPV and MF06. As activated T cells are known to synthesize core 2 O-glycans (155), MUC1 will probably carry core 2-based structures. In contrast, the mAbs SM3 and HMFG2, which react better with MUC1 glycoforms carrying core 1-dominated structures (150), bound activated T cells poorly. This preferential reactivity of T cells with antibodies recognizing the normal form of MUC1 holds true for a variety of antibodies with different epitopes. Northern analysis of the transcripts for the three enzymes able to synthesize core 2 O-glycans in the activated cells, suggested that the increase in C2GnT1 was responsible for the increased capacity to synthesize core 2 structures in activated T cells, although a role for C2GnT3 cannot be excluded. C2GnT1 expression in lymphocytes is also involved in the optimal expression of selectin ligands for adhesion and lymphocyte homing properties, and it has been reported that its expression is regulated by the cytokine milieu subsequent to T cell activation (96, 97).

The mAbs 232A1 and 12C10, reactive with single epitopes outside of the tandem repeat region and therefore unaffected by glycosylation patterns, did show positive staining of a fraction of activated T cells, but the percentage of cells staining was less than that seen with HMFG1. This is probably a result of the fact that lower levels of expression of MUC1 could be detected using an antibody recognizing an epitope repeated 25-100 times (depending on the allele), such as HMFG1, as compared to the level which can be detected by an antibody binding to a single epitope. The mAb B27.29, used in the previous study where expression of MUC1 in activated T cells was described (141), also recognizes an epitope in the TR region, overlapping with that recognized by HMFG1, HMPV and MF06 mAb (149).

Previous reports had examined MUC1 expression by human T cells. One of these studies used the mAb DF3-P and suggested that MUC1 was present in resting human T cells and the leukemia cell line Jurkat (142). This antibody, like mAb SM3, has been reported to bind to cancer-associated glycoforms of MUC1, where core 1 structures predominate. However, in our study, the antibody SM3 did not bind to resting T cells, neither could MUC1 mRNA be detected. The HMFG1 antibody, which can recognize MUC1 carrying extended core 2-based O-glycans, as well as cancer associated glycoforms, also did not bind to resting T cells. Our findings are substantiated by other studies that demonstrated minimal staining of Jurkat cells using DF3-P and no staining of resting T cells with MUC1-specific mAbs VU-4H5 and VU-3C6 (143), and no staining of resting T cells with MUC1-specific mAb B27.29 (141). Therefore, the majority of published reports support our observation that MUC1 is not expressed by resting human T cells.

The different reactivities of antibodies, which are affected by the glycosylation pattern of the cell producing the glycoprotein, emphasize the importance of documenting expression of MUC1 mRNA transcripts. The expression of full length MUC1 was confirmed by sequencing the products of RT-PCR and by Northern blot analysis. Very low levels of transcripts were detected by Northern blot analysis as compared to levels in breast cancer cells, and in semi-quantitative RT-PCR, the level of MUC1 transcript in activated human T cells was found to be at least 50-fold lower than that seen in human breast cancer. It is also important to note that using immunohistochemistry, there was no significant staining of T cells within activated lymph nodes. In contrast, micrometastases from breast cancer were readily identifiable within these same lymph nodes using HMFG1 or the other MUC1-specific mAbs used in the study. Therefore, the data presented here demonstrate that although MUC1 is expressed by activated human T cells, the level of expression is very low and certainly much lower than seen in breast cancer and

normal epithelial tissues. The relative levels of target antigens are important in determining whether a cellular immune response is activated or is effective. The low level of expression in T cells probably precludes induction of autoimmunity as a result of MUC1 immunization strategies. In addition when immune responses elicited by vaccines are focused on tumor-specific forms of MUC1 these immunogens generate immune cells specific for epitopes present only on tumor cells. Activated T cells express the glucosyltransferase enzymes that lead to long, highly branched polysaccharides on MUC1 (164) and do not present the same MUC1 epitopes found on tumor cells. Thus it is highly unlikely that an immune response elicited by MUC1 cancer vaccines would target activated T cells.

This information is of interest as MUC1-based immunotherapy is under investigation in the clinic, and the induction of autoimmunity or the lack of response, due to immunological tolerance must be considered. In the trials carried out with radiolabelled HMFG1 mAb, no side effects suggestive of toxicity to lymphocytes have been noted (165). On the other hand, the expression of MUC1 by cells of the immune system could result in higher-than-expected levels of immunological tolerance. Also, the high expression of MUC1 mRNA in the gastrointestinal tract (Figure 2.0-19), if translated into protein, could also lead to high levels of immunological tolerance, as described for ovalbumin when expressed by intestinal cells (166).

The function of MUC1 in activated T cells is uncertain. It has been proposed that MUC1 has a role in immune response regulation (141), but the evidence is controversial. Inhibition of T cell proliferation by synthetic MUC1 peptides (covering the TR sequence) (167), or MUC1 from tumor cell supernatants (168), has been reported. In another report, the T cell-inhibitory factor in tumor-cell supernatants could be separated from MUC1 (169). We have found no effect of MUC1 TR peptides on the activation or function of T cells, and the level of MUC1 in the

supernatants from activated T cells is barely detectable (T. Plunkett, J. Taylor-Papadimitriou, unpublished). In addition T cells, stimulated with MUC1-peptide-pulsed dendritic cells, express MUC1 on the T cell surface while the culture proliferates without evidence of T cell-T cell killing (J. Kettel, unpublished). It seems more likely that it is the expression of MUC1 on the surface of T cells which plays some role, as yet undefined, in T cell function. Previous reports using tumor cells over-expressing MUC1 have indicated a role for MUC1 molecules in inhibition of intercellular adhesion (170-172). However, a certain density of surface expression may be required for blocking such cell-cell interactions. The distribution of MUC1 over the cell surface is also a factor, as it was shown that MUC1 capped by anti-MUC1 antibodies no longer inhibited cell adhesion to extracellular matrix components (173).

The confocal microscopic analysis of activated T cells showed two distinct patterns of MUC1 expression. The molecule is uniformly expressed over the entire cell surface in non-polarized T lymphocytes but, interestingly, it forms polar aggregates in T cells undergoing cytoskeletal rearrangements in response to a chemokine. It is known that to initiate migration, T lymphocytes switch from a spherical to a polarized shape and that actin is enriched in the cytosol of the leading edge of polarized T cells (114). We have correlated the spatial distribution of MUC1 with that of other molecules associated with cytoskeletal rearrangement (151, 152). Following RANTES-induced cell polarization we found MUC1 at the leading edge of the polarized T cell. To visualize MUC1 movement we generated a cell line expressing fluorescent MUC1 using a MUC1-EGFP fusion construct. The Jurkat cell line has been shown to respond to CD3 engagement by moving its microtubule-orienting center, localizing polymerized actin (174), and undergoing similar shape changes in response to CD3 engagement (175) just as normal T cells do. In addition, Jurkat cells have been used in studies examining T cell polarization (115,

118, 153, 176, 177). It has also specifically been shown that Jurkat cells polarize in response to the chemokine SDF1α: the SDF1α receptor CXCR4 is moved to the leading edge (115, 118) and basal surface (118), migration and actin polymerization are induced (178). Because of its similarity to activated human T cells we chose this as our cell model. The MUC1-EGFP transduced Jurkat cells strongly express the fusion construct, as seen by EGFP fluorescence and antibody staining for MUC1. Polarization of these cells did not produce the same static elongated phenotype seen in polarized activated human T cells but MUC1 was focused opposite of spectrin on some cells. Interestingly, when MUC1-EGFP Jurkat cells were allowed to interact with endothelium in the absence of exogenous chemokine there was active shape change accompanied by altered brightness of MUC1-EGFP, possibly due to asymmetrical movement of MUC1-EGFP on the cell surface. This is consistent with reports of Jurkat and T cell shape change in response to integrin engagement (110, 175) and work showing the gradual spontaneous polarization of resting PBL co-cultured with endothelium in the absence of exogenous stimuli (179, 180). The latter observations were not pursued using activated T cells or Jurkat cells but our results indicate that Jurkat cells may replicate their findings in a much shorter time span.

The movement of MUC1 on the cell surface suggests that activated T cells may use MUC1 on their leading edge to affect interactions with endothelial cells as they travel to inflammatory sites and/or MUC1 plays a role in events that occur after the lymphocytes have passed through the endothelium into the underlying tissues (e.g. migration through tissue or interactions with target cells). It is possible that the large size of MUC1 molecules promotes interactions at a long distance and mediates the initial contact between the T cell and endothelium or other cells. Which molecules on endothelial or other cells might be responsible

for the interaction with MUC1, and the nature of this interaction, are yet to be defined. The E- and P-selectins are well-studied surface molecules on endothelial cells known to bind to carbohydrate ligands such as Lewis x (Le^x) and the sialylated form of Lewis x (sLe^x). Although MUC1 may carry specific O-glycans (e.g. sLe^x) that are recognized by selectins, it is unlikely that MUC1 is interacting with selectins on endothelial cells because the functionality of selectin ligands appears to depend on modifications of the core protein as well as the specific O-glycans (181). It needs to be said that by virtue of the extended structure of the MUC1 molecules, they can inhibit cell interactions such as those mediated by integrins and E-cadherin (173, 182), as well as participate in cell adhesion through interaction with lectins such as sialoadhesin (183). Which of these effects predominate in the polarized T cell could depend on the immediate environment.

The function of MUC1 on activated T cells has not been clearly defined but indications of its role *in vivo* may come from determining where MUC1 expressing T cells are found. Rheumatoid arthritic joints are sites of chronic inflammatory disease, and activated effector/memory T cells are the dominant cell type present in synovial tissue (184). $CD45RO^+$ T cells from these inflammatory infiltrates display a polarized morphology (120). In addition, there is increased expression of adhesion molecules on inflamed endothelium in arthritic joints (185). As MUC1 is expressed on the surface of activated memory T cells, it has the potential to play a role in T-cell migration into inflamed arthritic joints and/or events inside the joints. Finding MUC1 expressing T cells in synovial fluid from a person with rheumatoid arthritis supports this idea.

3.0 CONSEQUENCES OF MUC1 EXPRESSION ON T CELLS

Hypothesis 2:

MUC1 on T cells interacts with one or more molecules on the surface of blood vessels as a means to initiate adhesion. Upon interaction with a ligand MUC1 signals to the T cell via phosphorylation of its cytosolic tail and association with intracellular signaling proteins.

Specific Aim 2:

Determine if MUC1 on T cells affects their interactions with endothelial adhesion molecules and if there are changes in protein phosphorylation occurring within the T cell, to the MUC1 cytosolic tail and/or other proteins, during interaction with endothelium.

Rationale:

Cell surface molecules enable the T cell to interact with and adhere to endothelium in the context of appropriate ligands. Most T cell adhesion molecules project only a small distance above the cell. MUC1, with its elongated rod-like structure, stretches above the cell surface and would be the first molecule of the T cell to make contact. The results of this contact would likely play an initial role in the homing of a T cell to an immunologically active site. Furthermore, phosphorylation and association with intracellular proteins, observed in MUC1 expressing tumor cells, may also be occurring in activated MUC1 expressing T cells in response to interaction with endothelium. The role of MUC1 in adhesion and signaling would be important not only to understanding T cell biology but also in the hopes of manipulating T cell trafficking.

3.1 INTRODUCTION

3.1.1 MUC1 in adhesion

The possible function of MUC1 on T cells can be hypothesized by looking at the work done studying the function of MUC1 on other MUC1 expressing cells. Such functions may also be carried out in the T cell. Studies have looked at MUC1 as having a potential role in cell adhesion. This topic has been nicely reviewed by Hilkens et al (186). Because of its rigidity, size and high negative charge due to sialic acid groups, MUC1 would likely be an anti-adhesive molecule. Studies by Ligtenberg et al (187) using MUC1 transfected cell lines showed that MUC1 expression inhibits cell aggregation. Removing the sialic acids only partially decreased the anti-aggregation effect of MUC1. Wesseling et al (173) looked at the effect of MUC1 expression all over the surface of transfected cells and observed inhibition of integrin mediated binding to extracellular matrix components. Activating β1 integrins or using anti-MUC1 antibodies to cap MUC1 on the cell surface prevented the MUC1-mediated inhibition of binding. Contributions of MUC1 cytosolic portion were ruled out by using a tailless form of MUC1. Consistent with this, MUC1 was shown to decrease binding to type I collagen, with increasing size of extracellular MUC1 having a greater effect, though much less of a decrease in binding to fibronectin was observed (188).

Kondo et al (171) examined how sodium butyrate caused breast cancer cell lines' increased adherence to each other as well as to tissue culture surfaces. By antibody blocking experiments the adherence was shown to be E-cadherin mediated. By Northern and by FACS staining they showed that MUC1 expression decreased in response to sodium butyrate. The association between decreased MUC1 expression and increased adherence following sodium butyrate treatment was confirmed by introducing MUC1 anti-sense DNA into the cells. Another

group looking at E-cadherin mediated cell adhesion found that steric hindrance was the primary mechanism for MUC1 inhibition of adhesion. They compared aggregation of fibroblasts before and after transfection with MUC1 of different lengths. While both sizes of MUC1 inhibited aggregation, the smaller MUC1 had much less of an effect. Removing sialic acids did not affect the inhibition of large MUC1 molecules (36 repeats in the VNTR region), though smaller MUC1 molecules (eight repeats in the VNTR region) did show less inhibition without sialic acids. Using anti-MUC1 antibodies on cells expressing the large MUC1 removed anti-aggregation effects (182). They concluded that the extracellular portion of MUC1 mediated the inhibitory effect with steric hindrance being the main mechanism, though charge repulsion could play a role depending on the size of MUC1 and its density on the cell surface. These and other studies (172) have established that MUC1 can act as an anti-adhesive molecule. However, the story of MUC1 in cell adhesion may not be limited to anti-adhesive effects. Recent works have also shown that MUC1 can bind to lectin-like receptors (183) and to ICAM-1 (189, 190) Taken together, all of this information indicates that MUC1 on the surface of T cells may help prevent or facilitate cell-cell interaction.

3.1.2 Signaling by MUC1

The cytosolic tail of MUC1 is well conserved among many species (7). Seven tyrosines are present in that region (13) and available for phosphorylation. According to work done with tumor cells, MUC1 transfected cells, or CD8/MUC1 chimeric fusion protein expressing cells, these tyrosines can be phosphorylated (191-194). Since the MUC1 tail has no apparent intrinsic enzyme activity (16), the phosphorylation must be done by an associated kinase. In a variety of cells and conditions MUC1 co-immunoprecipitates several intracellular protein(s) (16, 191, 192, 195, 196). Pandey et al (191) showed that tyrosine phosphorylated MUC1 associates with Grb2,

an adapter protein involved in signaling pathways. Grb2 complexed with MUC1 connects with the guanine exchange protein Sos, which can activate Ras. Though not able to replicate the Grb2 association, Quin et al (192) did however co-immunoprecipitate with MUC1 a 60 kDa phosphorylated molecule as yet unidentified. Associations between MUC1 and the c-Src tyrosine kinase have been reported (197-199) as well as activation of ERK1/2 *in vivo* (196) and indirect activation of ERK2 via Ras and MEK *in vitro* (200). MUC1 also interacts with the catenin, p120, increasing the nuclear localization of p120 (201). Association of MUC1 with transmembrane tyrosine kinases, erbB1 (epidermal growth factor receptor), erbB2, erbB3 and erbB4 has been shown *in vivo* (196). The combination of available phosphorylation sites and association with kinases makes it highly likely that MUC1 plays an active role in cell signaling, perhaps as a transmembrane receptor. This has yet to be shown for full-length MUC1 expressed on the cell surface though MUC1/Y has been proposed to act in a analogous manner to cytokine receptors (193).

MUC1 in tumor cells has been associated with β-catenin (195, 197, 202-206), a protein involved in cadherin-mediated cell adhesion. Binding to β-catenin is affected by phosphorylation of the MUC1 tail. There is increased binding following MUC1 threonine phosphorylation by protein kinase C δ (PKCδ) (204) or tyrosine phosphorylation by c-Src (197) or Lyn (205), but decreased binding to β-catenin following serine phosphorylation by glycogen synthase kinase 3β (GSK-3β) (203). The interaction between MUC1 and β-catenin has been proposed to explain the inhibitory effect of MUC1 expression on cadherin mediated adhesion (207). However, though the biochemical studies indicated competition for β–catenin between MUC1 and E-cadherin (203), MUC1 inhibition of E-cadherin binding still occurs with tail-less mutants of MUC1 (173). Though signaling may play a role, E-cadherin inhibition is probably

due to the high degree of steric hindrance that MUC1 provides on the cell surface (187), illustrated by experiments using MUC1 with varying numbers of repeats (182, 188). Whether competition for β–catenin enhances MUC1-mediated inhibition of E-cadherin expressing cells remains to be determined. Much further work is needed to illuminate these interesting associations between MUC phosphorylation, interactions with other proteins inside the cell and the effect on adhesion.

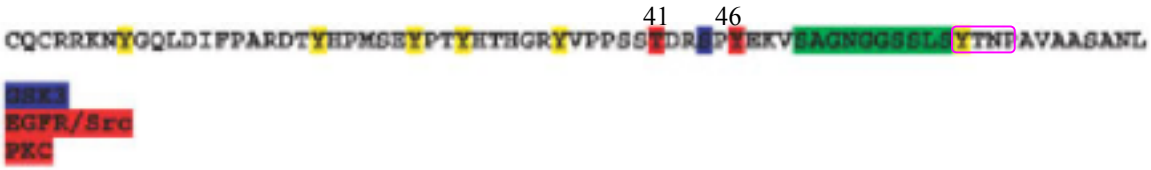

Figure 3.0-1 Role of MUC1 cytoplasmic domain in β-catenin binding. Sequence of cytoplasmic domain of MUC1, showing binding sequence for β-catenin (green) and phosphorylation sites for its regulation. Threonine 41 is phosphorylated by PKCδ to increase β-catenin binding to MUC1. The serine highlighted in blue is phosphorylated by GSK-3β to decrease binding of β-catenin. Tyrosine 46 is phosphorylated by c-Src to increase β-catenin binding and decrease GSK-3β binding. The binding sequence for Grb2 is shown in lavender. Modified from (207).

3.2 MATERIALS AND METHODS

3.2.1 Cells and antibodies

Jurkat cells were grown in RPMI supplemented with 10% fetal bovine serum (FBS), 1% L-glutamine and 1% penicillin/streptomycin. Jurkat cells were transfected with a MUC1 22 tandem repeat expression vector (pRc/CMV-MUC1). MUC1 expression is under the control of the CMV promoter and the vector contains a neomycin resistance gene. Twenty micrograms of pRc/CMV-MUC1 DNA were linearized with the Xba1 restriction enzyme and electroporated into 5 x 106 Jurkat cells. Electroporation was done in 0.4 cm electroporation cuvettes using BioRad (BioRad Laboratories, Hercules CA) Gene Pulser at 800 volts and 3 μF settings. Cells were kept on ice for an additional 10 minutes and then transferred into culture flasks. After 48

hours, selection began by growing the cells in normal growth medium supplemented with 1 mg/ml G418.

Human microvascular endothelial cells (HMVEC) were purchased from Cambrex and grown according to manufacturer's instructions. HMVEC were used in experiments at the end of passage 2 or 3. All Chinese hamster ovary (CHO) cells were grown in RPMI supplemented with 10% fetal bovine serum, 1% L-glutamine and 1% penicillin/streptomycin. 3T3 cells were grown in DMEM supplemented with 10% FBS. 3T3-PECAM-1 cells were grown in DMEM supplemented with 10% FBS and 0.3 mg/ml G418. ICAM-1, VCAM-1 and E-selectin transfected CHO cells were by provided Dr. Timothy Carlos (University of Pittsburgh, PA). P-selectin transfected CHO cells were provided by Dr. Geoffrey Kansas (Northwestern University Medical School, IL). 3T3 and PECAM-1 transfected 3T3 cells were provided by Dr. Steven Albelda (University of Pennsylvania, PA).

Unlabeled antibodies against L-seletin, PSGL-1, CD11a, P-selectin, PECAM-1, PE-labeled antibodies against CD38, VLA-4, ICAM-1, and FITC-labeled antibodies against CD43, MUC1 (clone HMPV), and their isotype controls were purchased from BD Pharmingen (San Jose, CA). Goat anti-mouse Alexa488 secondary antibody was purchased from Molecular Probes (Eugene, OR). Antibody against ICAM-2 and MUC1 (clone BC2) were purchased from Chemicon (Temecula CA). Antibodies against VCAM-1 (clone 5E1) and E-selectin (clone 7G8) were provided by Dr. Timothy Carlos. Anti-phosphotyrosine antibody (clone 4G10) was purchased from Upstate Biotechnology, Lake Placid NY.

3.2.2 Flow cytometric analysis

Jurkat cells were stained with directly conjugated antibodies to CD43, CD38, and VLA-4. Staining of other adhesion molecules, CD11a (LFA-1), PECAM-1, PSGL-1 and L-selectin

was followed by a secondary antibody, goat anti-mouse Alexa488. For experiments involving resting and activated HMVEC, half of the cells were incubated in 10ng/ml IL-1β (R&D Systems, Minneapolis MN) in fresh medium, while the other half received unsupplemented fresh medium, for 5-7 hours at 37^{o}C. HMVEC cells were stained with directly conjugated antibody against CD54 while staining for other adhesion molecules, ICAM-2, PECAM-1, E-selectin, VCAM-1 and P-selectin was followed by a secondary antibody, goat anti-mouse Alexa488.

3.2.3 Cell-cell adhesion assay

HMVEC or cell lines expressing individual adhesion molecules were grown as a monolayer in flat-bottomed 96-well plates. Upon reaching confluency the plates were used in the adhesion assay. For experiments involving resting and activated HMVEC, half of the wells on each plate received 10 ng/ml IL-1β (R&D Systems, Minneapolis MN) in fresh medium while the other half received unsupplemented medium. HMVEC were incubated 5-7 hours at 37^{o}C and then washed three times with PBS before use to eliminate residual IL-1β.

Jurkat and MUC1-Jurkat cells, suspended at 5 x 10^{6} cells/ml, were labeled for 30 minutes with 5 μl/ml calceinAM (Molecular Probes, Eugene OR), a lipophilic ester that is cleaved intracellularly to yield fluorescent calcein. After washing off unincorporated calceinAM, PBS or 2-2.5 x 10^{5} Jurkat or MUC1-Jurkat cells were added to each well containing the adherent cell line, either HMVEC or the cell lines expressing individual adhesion molecules. Each cell-cell combination was tested in either triplicate or quintuplicate. Plates were incubated at 37^{o}C for the indicated times and then, using a multichannel pipettor, the wells were washed to remove non-adherent Jurkat or MUC1-Jurkat cells. The monolayer was inspected after the final wash to be sure it had remained intact. A replica control plate with wells containing the adherent monolayer

and the maximum amount of labeled cells was not washed so that the maximum fluorescence could be measured.

Fluorescence of labeled cells (excitation 485 nm/emission 530 nm) was measured on a SPECTRAmax GeminiXS fluorimeter using the accompanying SOFTmax Pro software program (Molecular Devices, Sunnyvale CA). Percent of maximum adhesion was calculated by subtracting the fluorescence of wells containing only PBS from the fluorescence of each well containing cells. The resulting fluorescence value of each experimental well was then divided by the average maximum amount of fluorescence from wells containing the whole volume of labeled cells to indirectly measure the percentage of cells still adherent to the monolayer. Statistical analysis was performed by Dr. Doug Potter (Biostatistics Facility, University of Pittsburgh Cancer Institute, PA) using the stratified Wilcoxon test with ranks computed independently within each stratum. The statistical package used was StatXact-5.

3.2.4 T cell - Endothelial Interaction Assay

HMVEC cells were grown to confluency in 6 well plates and then half were activated with 10 ng/ml IL-1β for 5-7 hours on the day of the assay. Equal numbers of Jurkat or MUC1-Jurkat cells were added to endothelium containing wells or left in the tube to represent no endothelial interaction. Plates were then incubated at 37^{o}C for 15 minutes to allow interaction to occur and then placed on ice while the Jurkat and MUC1-Jurkat cells were collected from the wells using ice cold PBS containing phosphatase inhibitors (1 mM activated sodium fluoride, 1 mM sodium orthovanadate). Microscopic examination showed that the monolayers remained intact and that all Jurkat and MUC1-Jurkat cells had been collected from each well. Cells were pelleted by centrifugation at 4^{o}C and then lysed in modified RIPA buffer (50 mM Tris-HCl, pH 7.4; 1% NP-40, 0.25% sodium deoxycholate; 150 mM sodium chloride; 1 mM EDTA; 1 mM

PMSF; 1 μg/ml leupeptin; 1 μg/ml aprotinin; 1 μg/ml pepstatin A; 1 mM activated sodium orthovanadate; 1 mM sodium fluoride) for 40 minutes on ice, vortexing every 10 minutes. Lysates were centrifuged in a cold room at 13,000 x g for 15 minutes. Supernatants were collected to new tubes, aliquoting equal cell equivalents (4 x 10^6 cells) to each tube, and frozen until use.

3.2.5 Immunoprecipitation and immunoblotting for phosphorylated MUC1

Aliquots of supernatants from MUC1-Jurkat cell lysates were thawed on ice, diluted up to 0.5 ml with modified RIPA lysis buffer and then pre-cleared by rotating with 25 μl of protein G bead slurry for 1 hour at 4°C (Amersham Biosciences, England). Five micrograms of 4G10 antibody was loaded onto protein G slurry by rotating for 2 hours at 4°C followed by removal of unbound antibody. Pre-cleared lysates were then rotated overnight at 4°C with 4G10 (Upstate Biotechnology, Lake Placid NY) coated beads. After washing, the beads were suspended in NuPage LDS Sample buffer (Invitrogen, Carlsbad CA), and dithiothreitol (DTT) to yield a final concentration of 0.05 M DTT. Samples were heated for 3 minutes at 95°C and the supernatants electrophoresed on a 1.5 mm 4-12% Bis-Tris polyacrylamide gel (Invitrogen, Carlsbad CA) alongside SeeBlue Plus1 molecular weight markers in MOPS (3-(N-morpholino) propane sulfonic acid) SDS running buffer at 200 volts. Proteins were transferred onto nitrocellulose membranes (BioRad Laboratories, Hercules CA) in 10% Towbin buffer using 30 volts overnight at 4°C.

The membrane was blocked with 10% dry milk in PBS by rocking for 45 minutes at room temperature then immunoblotted with 0.5 μg/ml mouse anti-MUC1 antibody (clone BC2; Chemicon, Temecula CA). Bound primary antibody was detected with a 1:2000 dilution of sheep anti-mouse horseradish peroxidase conjugated secondary antibody (Amersham

Biosciences, England). ECL detection reagents (Amersham Biosciences, England) were added to the membrane as directed by the manufacturer and proteins were visualized using X-Omat film (Kodak, Rochester NY). Quantitation of BC2 signal was obtained with Versadoc imaging system model 3000 using the Quantity One software (BioRad Laboratories, Hercules CA). Calculation of MUC1 signal intensity in Versadoc intensity units was determined by subtracting background signal from raw MUC1 signal in each lane. A431 cell lysate (human epidermoid carcinoma line; Upstate Biotechnology, Lake Placid NY) was used as a negative control for MUC1 expression.

3.2.6 Immunoblotting for phosphorylated tyrosines and for β–catenin

Aliquots of supernatants from indicated cell lysates were thawed on ice, mixed with NuPage LDS Sample buffer (Invitrogen, Carlsbad CA), and dithiothreitol (DTT) added to yield a final concentration of 0.05 M DTT. A431 cell lysate (Upstate Biotechnology, Lake Placid NY) was used as a positive control for immunoblotting phosphotyrosine and β–catenin. Samples were heated for 10 minutes at 70^{o}C then electrophoresed on 1.0 mm 10% Bis-Tris polyacrylamide gels (Invitrogen, Carlsbad CA) alongside SeeBlue Plus1 molecular weight markers in MOPS (3-(N-morpholino) propane sulfonic acid) SDS running buffer at 200 volts. Proteins were transferred onto nitrocellulose membranes (BioRad Laboratories, Hercules CA) in 10% Towbin buffer using 30 volts overnight at 4^{o}C.

Membranes were blocked by rocking for 20 minutes in 3% dry milk in PBS and then immunoblotted with 1 μg/ml mouse anti-phosphotyrosine antibody 4G10 (Upstate Biotechnology, Lake Placid NY) followed by 1:2000 dilution of sheep anti-mouse horseradish peroxidase conjugated secondary antibody (Amersham Biosciences, England). ECL detection reagents (Amersham Biosciences, England) were added to the membrane and proteins were

visualized using X-Omat film (Kodak, Rochester NY). Membranes were reblotted for β–catenin using 1:1000 dilution of polyclonal rabbit anti-β–catenin (Sigma, St. Louis MO), using a new species as the primary antibody to prevent cross-reactivity of the secondary, followed by 1:2500 dilution of donkey anti-rabbit horseradish peroxidase conjugated secondary antibody (Amersham Biosciences, England).

3.3 RESULTS

3.3.1 Expression of adhesion molecules on Jurkat, HMVEC and transfected cell lines

The extended structure of MUC1 leads us to believe that the presence of MUC1 on the T cell surface would impact T cell adhesion to other molecules. To investigate this aspect we wanted to compare adhesion by T cells with and without MUC1. However the activation state of T cells greatly alters their adhesive state as well as inducing MUC1 expression. Since this precludes comparing MUC1 negative cells, which are resting, to MUC1 positive cells, which are activated, we needed to generate a T cell model with and without MUC1 expression. Jurkat cells are a well established model to study resting T cells and these cells do not have endogenous MUC1 expression (Figure 3.0-2B). A 22 tandem repeat MUC1 construct was successfully expressed on the surface of Jurkat cells (Figure 3.0-2A). These cells express MUC1 at a higher level than seen on normal activated human T cells and we hoped this would highlight the effect of MUC1 as compared other molecules on the Jurkat cell surface. Jurkat cells also express adhesion molecules seen on T cells (Figure 3.0-3).

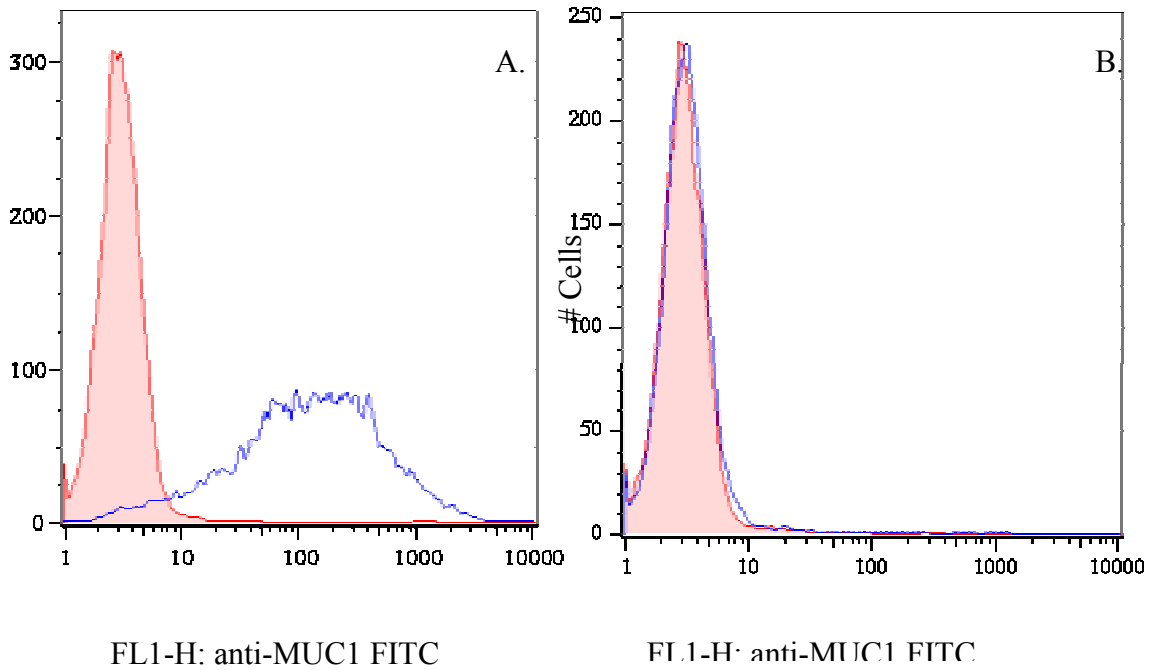

Figure 3.0-2 Expression of MUC on the surface of transfected Jurkat cells. (A) After transfection and positive selection, MUC1-Jurkat cells were stained with FITC labeled isotype control or FITC labeled anti-MUC1 antibody (clone HMPV). (B) Untransfected Jurkat cells were similarly stained for comparison. Shaded histograms are the fluorescence of isotype control staining. Open histograms are the fluorescence of anti-MUC1 staining.

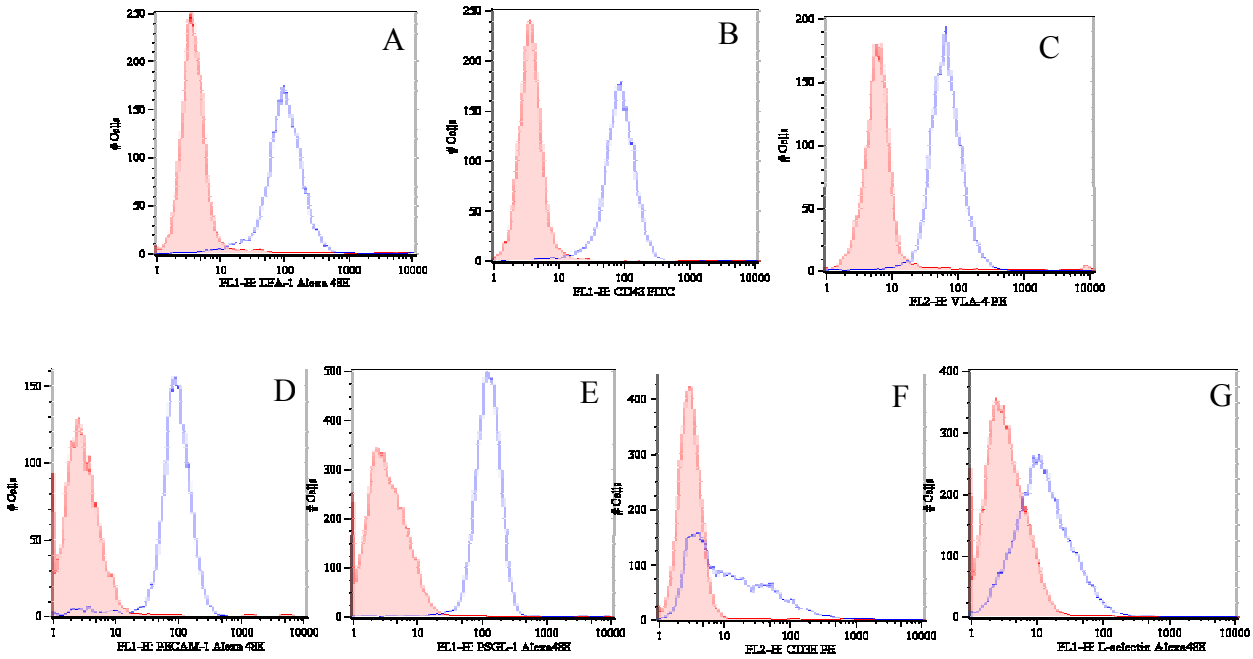

Figure 3.0-3 Expression of adhesion molecules on Jurkat cells. Jurkat cells were stained with antibodies against (A) LFA-1, (B) CD43, (C) VLA-4, (D) PECAM-1, (E) PSGL-1 (F) CD38 (G) L-selectin and with the isotype control antibodies. Shaded histograms are the fluorescence of isotype control staining. Open histograms are the fluorescence of adhesion molecule staining.

First we wanted to see the effect of MUC1 in adhering to endothelium, with all the molecules and complex interactions involved. Endothelium in the region of an immune response is much altered to attract and allow passage of effector cells, as compared to resting endothelium. We decided to look for a MUC1 effect in both situations to see if there was a different impact depending on the state of the endothelium. The human microvascular endothelial cell line (HMVEC), a model cell line recommended to study adhesion (Dr. Joost Oppenheim, personal communication) was examined to document its expression profile in the resting (Figure 3.0-4, top) and activated (Figure 3.0-4, bottom) state. As expected, ICAM-2 and PECAM-1 were constitutively expressed on both resting and activated HMVEC. Also as expected, ICAM-1 expression on resting endothelium was enhanced while E-selectin and VCAM-1 were induced in response to activation. Only P-selectin was not seen on the surface of HMVEC cells.

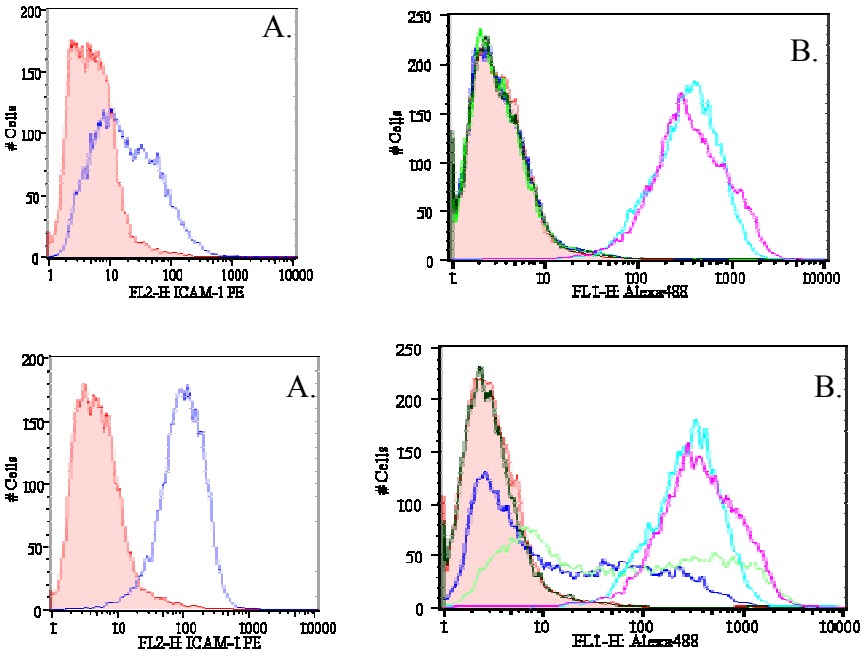

Figure 3.0-4 Adhesion molecules expressed on resting and activated endothelium. Resting HMVEC (top) and IL-1β activated HMVEC (bottom) were stained for adhesion molecules: (A.) PE-labeled antibody against ICAM-1. (B) Unlabeled antibodies against ICAM-2 (light blue), PECAM-1 (pink), E-selectin (light green), P-selectin (dark green) and VCAM-1 (dark blue) followed by goat anti-mouse Alexa488. Shaded histograms represent staining with isotype control antibodies.

We examined earlier time points during activation (Figure 3.0-5), since P-selectin is stored pre-formed in endothelium and could be expressed much sooner than other induced molecules; however we still could not detect P-selectin, though it may have been present at an even earlier time than we examined. This appeared to be the only inconsistency of the HMVEC line from expectations but is consistent with findings using the human umbilical vein endothelial cell line (208).

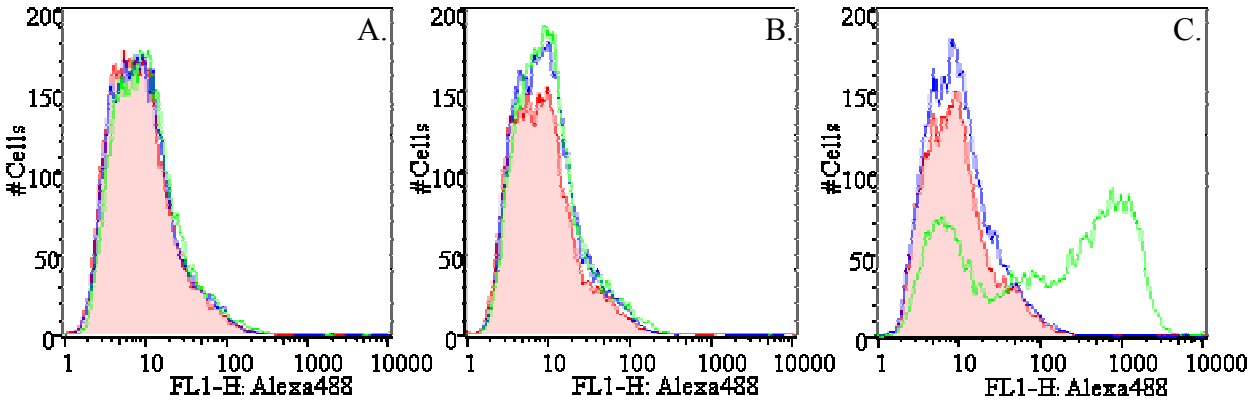

Figure 3.0-5 P-selectin and E-selectin on the surface of HMVEC. HMVEC in the (A) resting state, (B) after 30 minutes of activation, and (C) after 2.5 hours of activation were stained with unlabeled antibodies against P-selectin (blue) or E-selectin (light green). Shaded histograms represent staining with isotype control antibodies.

Adhesion to endothelium is a complex cascade of interactions with many molecules involved. In addition to looking at the impact of MUC1 on the overall process we wanted to look for interactions with specific molecules. To do this we obtained cell lines transfected with individual adhesion molecules and documented their expression profile (Figure 3.0-6 and data not shown).

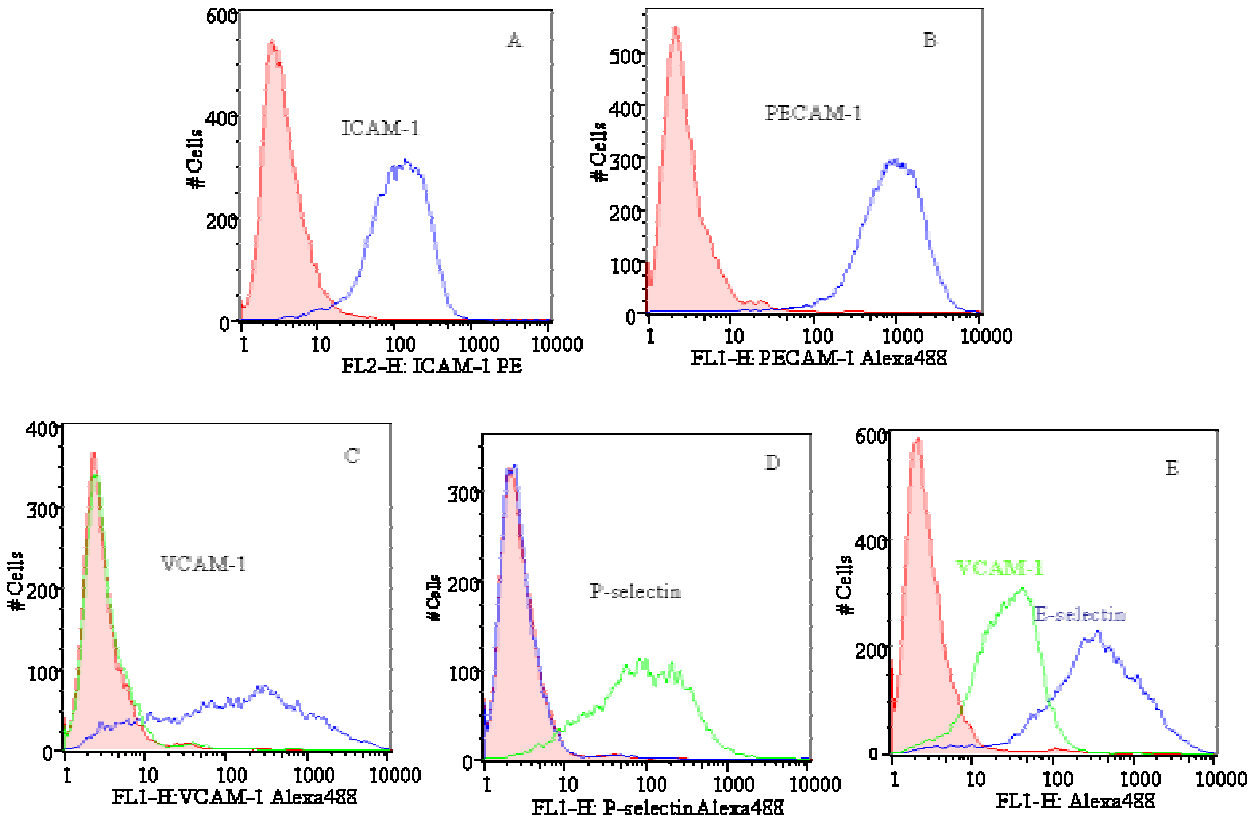

Figure 3.0-6 Expression of individual adhesion molecules on cell lines. (A) CHO-ICAM-1 cells, (B) 3T3 – PECAM-1 cells, (C) CHO-VCAM-1 cells, (D) CHO-P-selectin cells, and (E) CHO-E-selectin cells were stained with antibodies against the indicated adhesion molecules. Unlabeled primary antibodies were followed by Alexa488 labeled goat anti-mouse antibody. Shaded histograms represent staining with isotype control antibodies.

The parental cell lines CHO and 3T3 do not express any adhesion molecules (data not shown). Each of the transfected cell lines expressed the expected molecule with one exception. CHO-E-selectin cells are also positive for VCAM-1 expression (named E-selectin/VCAM-1 cells) (Figure 3.0-6 E). The expression level of VCAM-1 is much higher on the CHO-VCAM-1 cells than on the CHO-E-selectin/VCAM-1 cells so any effect VCAM-1 has will be more apparent on the single transfectants. Since we can examine VCAM-1 by itself (Figure 3.0-6 C), we will infer the interaction of MUC1 with E-selectin through comparisons between CHO-VCAM-1 and CHO-E-selectin/VCAM-1 cells.

3.3.2 Cell-cell adhesion assays

Because MUC1 is so much longer than other molecules on the T cell surface we expected that its effect would be seen earlier rather than later, when the MUC1-expressing cells first begin to interact with endothelium. To test this we looked at adhesion after short periods of incubation (5-20 minutes) versus long periods of incubation (45-60 minutes) with resting or activated endothelium. The baseline binding of both Jurkat cells and MUC1-Jurkat cells to activated endothelium is greater, as expected due to the additional adhesion molecules expressed. At the early timepoints (Figure 3.0-7) we see that MUC1 enhances the binding to endothelium. This is true regardless of whether the endothelium is resting or activated.

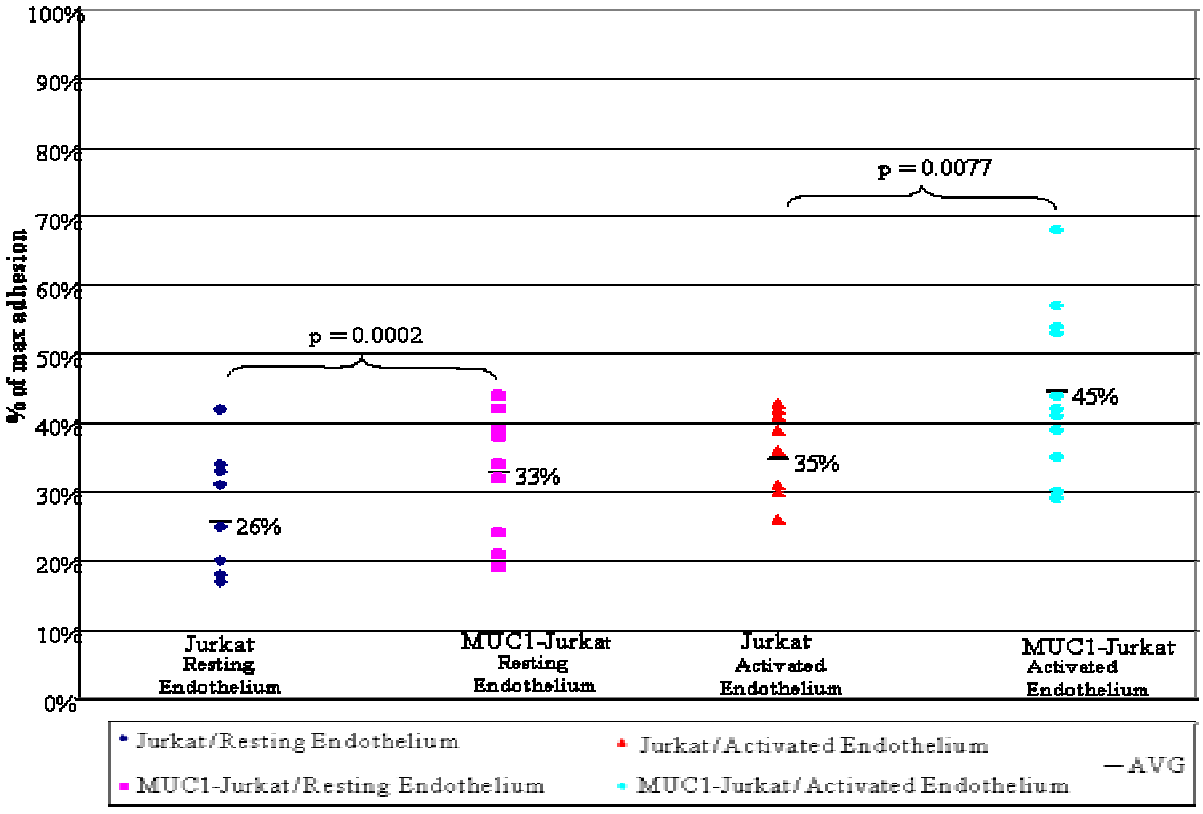

Figure 3.0-7 Adhesion of Jurkat and MUC1-Jurkat cells to resting and activated endothelium after a short incubation. HMVEC monolayers were grown to confluency and half activated with IL-1β. Fluorescently labeled Jurkat or MUC1-Jurkat cells were allowed to adhere prior to washing. Adhesion was calculated by subtracting background fluorescence and dividing by the maximum possible fluorescence. Each point represents a single well of adherent cells. Experiment was performed three times and data analyzed together.

When incubated for longer times the enhancing effect of MUC1 expression is eliminated (Figure 3.0-8). It is likely that after 45 – 60 minutes the other molecules on the Jurkat cell surface have taken over and their interactions dominate over the effect MUC1 exerts.

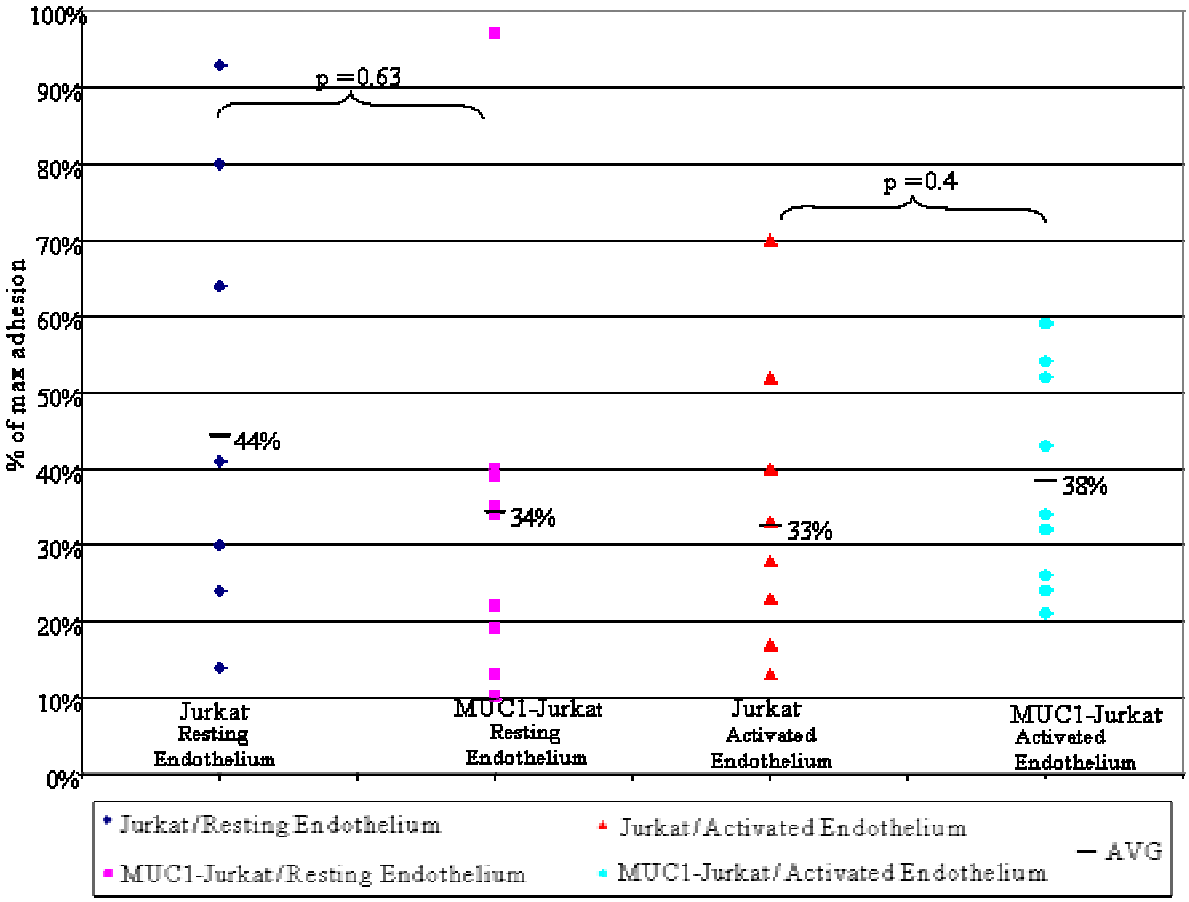

Figure 3.0-8 Adhesion of Jurkat and MUC1-Jurkat cells to resting and activated endothelium after longer incubation. HMVEC monolayers were grown to confluency and then half activated with IL-1β. Fluorescently labeled Jurkat or MUC1-Jurkat cells were allowed to adhere prior to washing. Adhesion was calculated by subtracting background fluorescence and then dividing by the maximum possible fluorescence. Each point represents a single well of adherent cells. Experiment was performed three times and data analyzed together.

Because the effect of MUC1 was seen only during early interaction with endothelium, we looked at individual adhesion molecules at either 5 or 20 minutes of incubation to more closely gauge when MUC1 has an effect on adhesion. At 5 minutes there is no statistically significant effect of

MUC1 expression on the adhesion of Jurkat to ICAM-1 or to E-selectin/VCAM-1 expressing cells (Figure 3.0-9). There is a slight indication that adhesion to E-selectin/VCAM-1 cells is diminished when MUC1 is present.

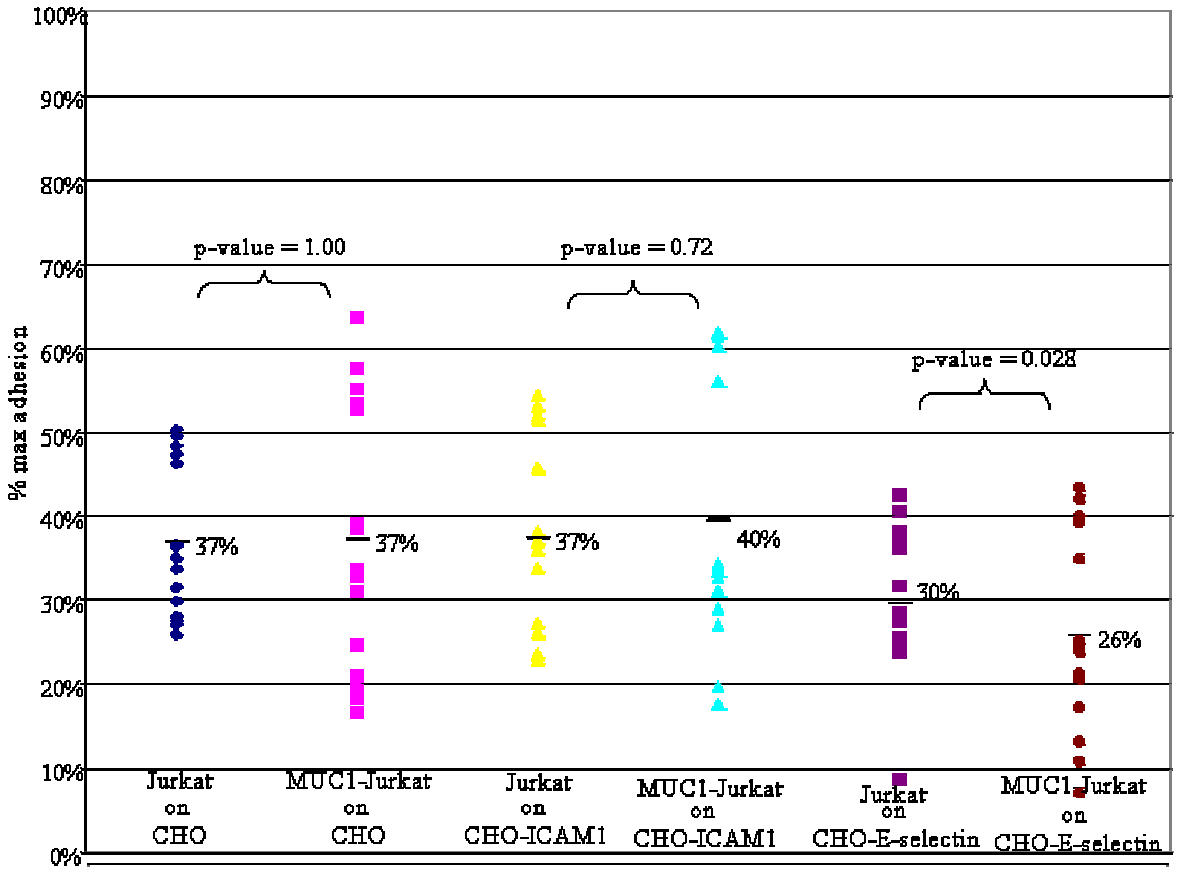

Figure 3.0-9 Adhesion of Jurkat and MUC1-Jurkat cells to CHO, CHO-ICAM-1 or CHO-E-selectin/VCAM-1 cells after a 5 minute incubation. Monolayers were grown to confluency and fluorescently labeled Jurkat or MUC1-Jurkat cells were allowed to adhere prior to washing. Adhesion was calculated by subtracting background fluorescence and then dividing by the maximum possible fluorescence. Each point represents a single well of adherent cells. Experiment was performed three times and data analyzed together.

At the 20 minute timepoint the effect of MUC1 is significant (Figure 3.0-10). Adhesion to ICAM-1 is enhanced by MUC1 while adhesion to E-selectin/VCAM-1 is diminished.

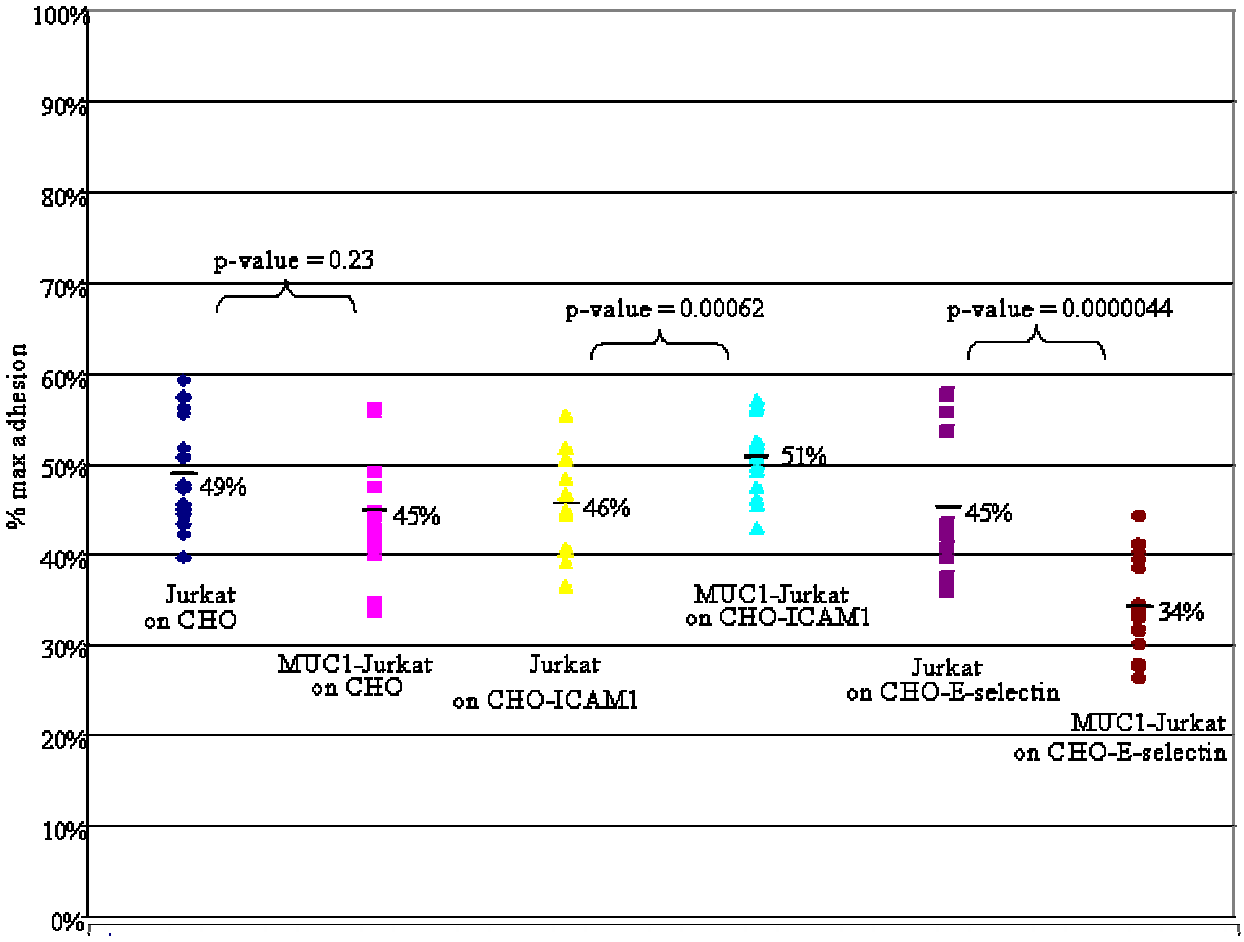

Figure 3.0-10 Adhesion of Jurkat and MUC1-Jurkat cells to CHO, CHO-ICAM-1 or CHO-E-selectin/VCAM-1 cells after a 20 minute incubation. Monolayers were grown to confluency and fluorescently labeled Jurkat or MUC1-Jurkat cells were allowed to adhere prior to washing. Adhesion was calculated by subtracting background fluorescence and then dividing by the maximum possible fluorescence. Each point represents a single well of adherent cells. Experiment was performed three times and data analyzed together.

When we examined VCAM-1 and P-selectin expressing cells there were no significant differences seen at 5 minutes (Figure 3.0-11).

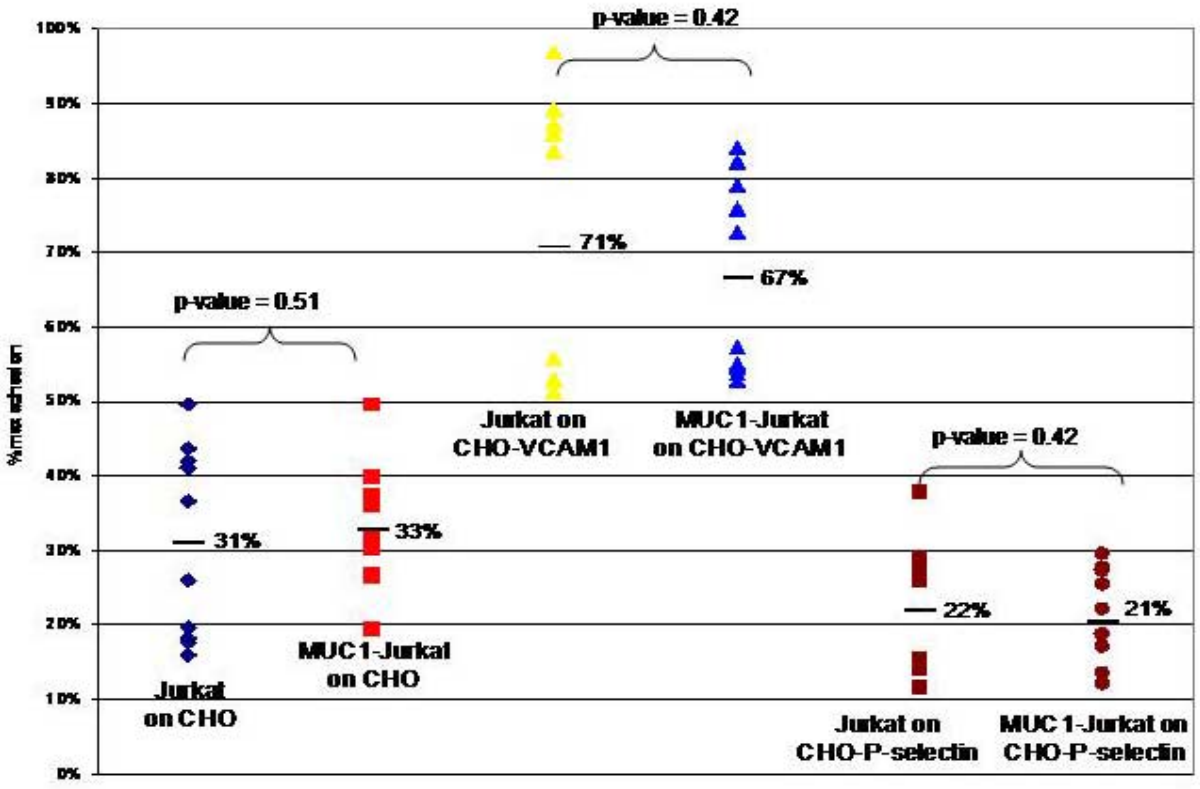

Figure 3.0-11 Adhesion of Jurkat and MUC1-Jurkat cells to CHO, CHO-VCAM-1 or CHO-P-selectin cells after a 5 minute incubation. Monolayers were grown to confluency and fluorescently labeled Jurkat or MUC1-Jurkat cells were allowed to adhere prior to washing. Adhesion was calculated by subtracting background fluorescence and then dividing by the maximum possible fluorescence. Each point represents a single well of adherent cells. Experiment was performed three times and data analyzed together.

Later, at 20 minutes, differences in adhesion due to MUC1 start to emerge but do not reach statistical significance. MUC1 tends to diminish binding to both VCAM-1 and P-selectin expressing cells (Figure 3.0-12).

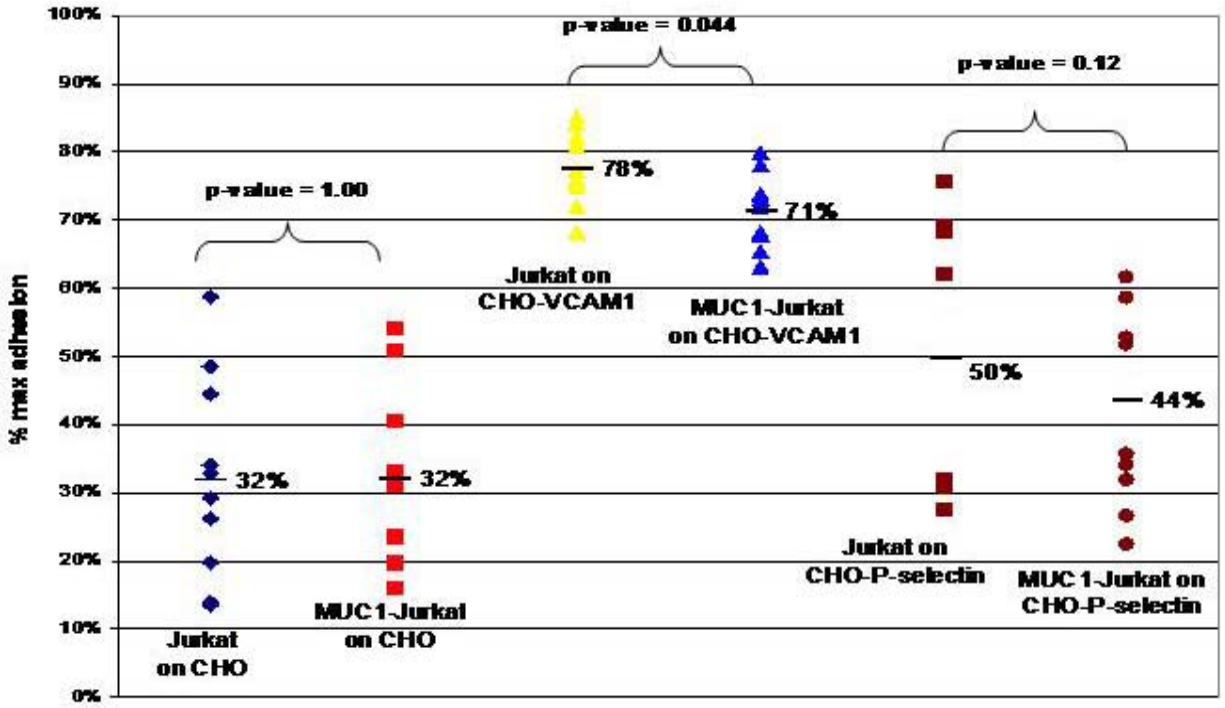

Figure 3.0-12 Adhesion of Jurkat and MUC1-Jurkat cells to CHO, CHO-VCAM-1 or CHO-P-selectin cells after a 20 minute incubation. Monolayers were grown to confluency and fluorescently labeled Jurkat or MUC1-Jurkat cells were allowed to adhere prior to washing. Adhesion was calculated by subtracting background fluorescence and then dividing by the maximum possible fluorescence. Each point represents a single well of adherent cells. Experiment was performed three times and data analyzed together.

VCAM-1 levels are different on CHO-VCAM-1 cells (broad range of expression, predominantly higher) as compared to the CHO-E-selectin/VCAM-1 cells, (tighter range of expression, predominantly lower) (see Figure 3.0-6). Keeping this in mind, since cells expressing VCAM-1 alone do not show significant effect of MUC1 on adhesion, despite their higher level of VCAM-1, it seems that the MUC1-mediated decreased adhesion to E-selectin/VCAM-1 cells is due to E-selectin expression, (compare Figure 3.0-12 to Figure 3.0-10). This observation bears further analysis using singly transfected cells. We were unable to obtain ICAM-2 transfected cells. The final endothelial adhesion molecule we examined was PECAM-1. As seen with the other adhesion molecules, at 5 minutes MUC1 does not make a statistical difference in the adhesion of Jurkat cells (Figure 3.0-13).

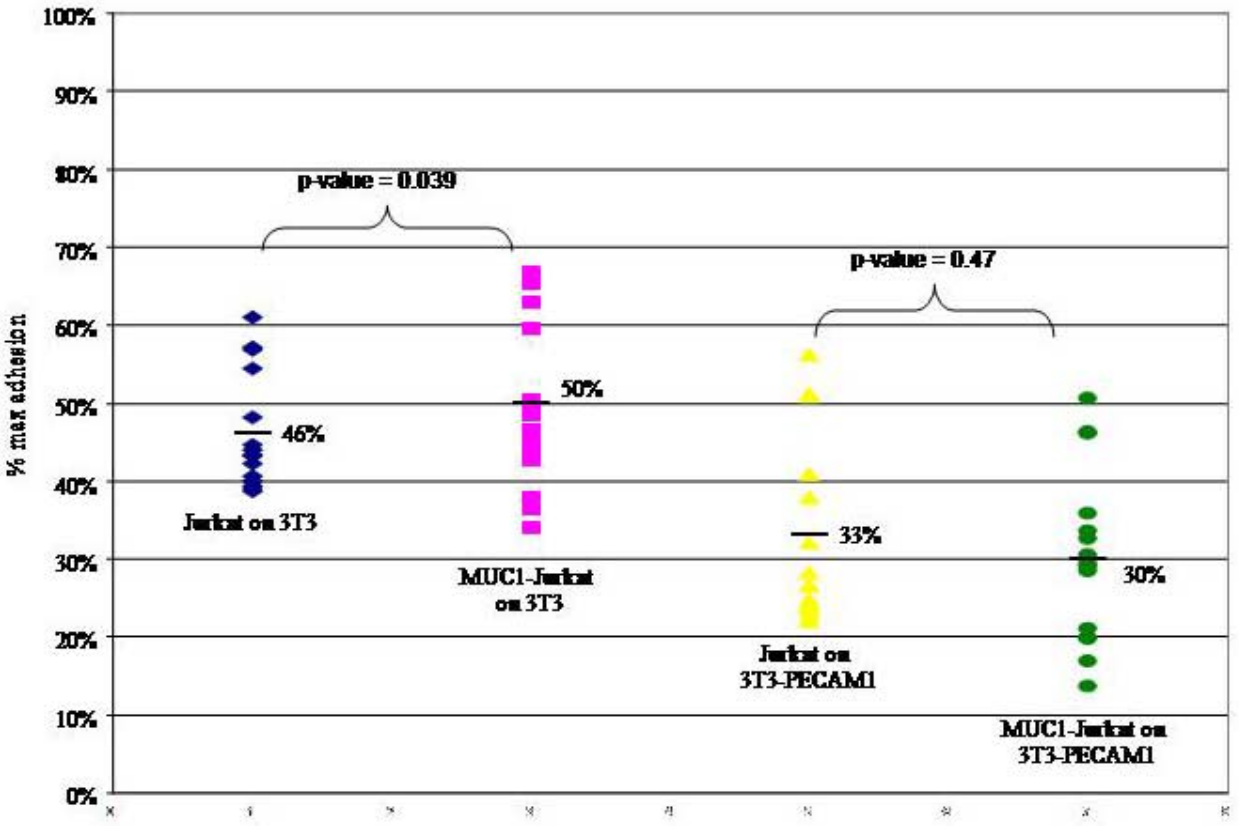

Figure 3.0-13 Adhesion of Jurkat and MUC1-Jurkat cells to 3T3 or 3T3-PECAM-1 cells after a 5 minute incubation. Monolayers were grown to confluency and fluorescently labeled Jurkat or MUC1-Jurkat cells were allowed to adhere prior to washing. Adhesion was calculated by subtracting background fluorescence and then dividing by the maximum possible fluorescence. Each point represents a single well of adherent cells. Experiment was performed three times and data analyzed together.

Given more time, there is a strongly significant MUC1 enhancement in adhesion to untransfected 3T3 cells but this is not seen with the PECAM-1 expressing cells (Figure 3.0-14) This may indicate that PECAM-1 prevents MUC1-mediated adhesion to 3T3 cells.

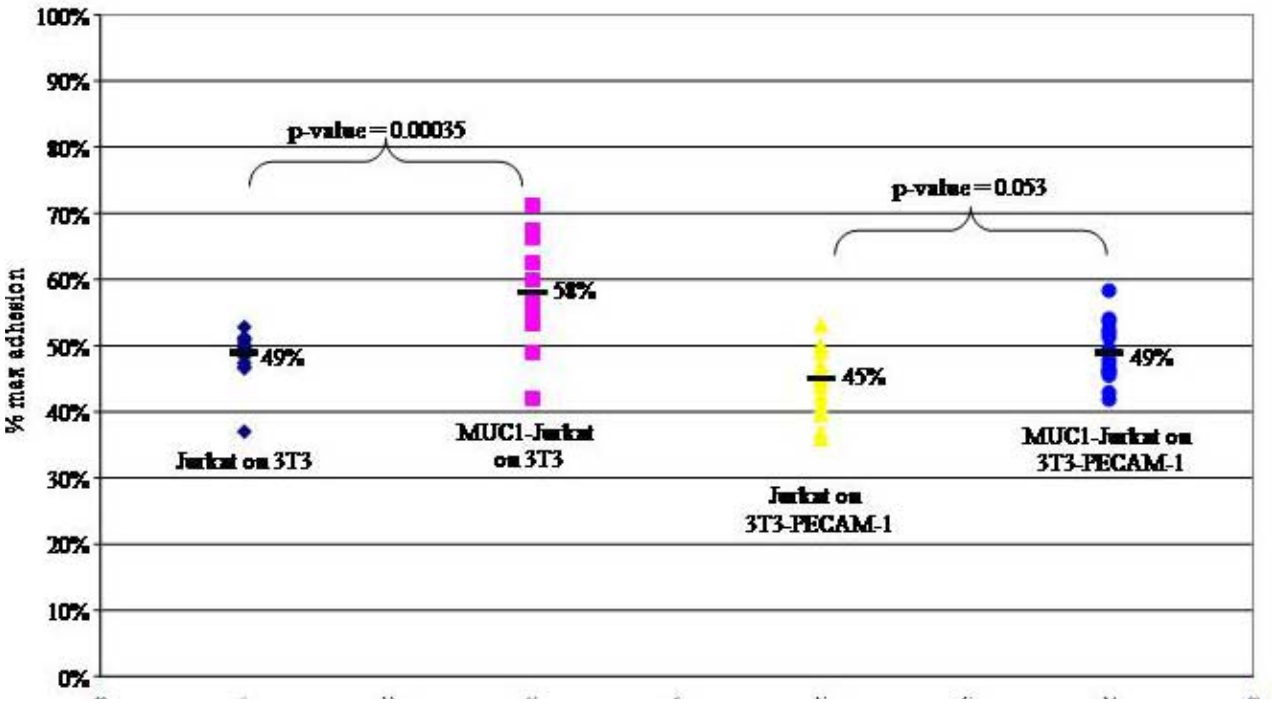

Figure 3.0-14 Adhesion of Jurkat and MUC1-Jurkat cells to 3T3 or 3T3-PECAM-1 cells after a 20 minute incubation. Monolayers were grown to confluency and fluorescently labeled Jurkat or MUC1-Jurkat cells were allowed to adhere prior to washing. Adhesion was calculated by subtracting background fluorescence and then dividing by the maximum possible fluorescence. Each point represents a single well of adherent cells. Experiment was performed three times and data analyzed together.

Within the first 20 minutes of interaction, MUC1 enhanced Jurkat cell adhesion to both resting and activated endothelium. Looking at individual adhesion molecules, ICAM-1 showed MUC1-mediated enhancement of binding while adhesion to E-selectin seemed to decrease. These effects are seen by 20 minutes of cell-cell interaction. Other adhesion molecules show an increased effect of MUC1 over time, greater difference at 20 minutes compared to 5 minutes, but do not reach as significant levels as ICAM-1 and E-selectin. Though it is possible that given more time we might see an effect of MUC1 on the other individual adhesion molecules, this would probably be irrelevant to endothelial adhesion since MUC1 had no effect on binding to resting or activated endothelium over longer time periods.

3.3.3 Phosphorylation of MUC1

The amino acid sequence of the MUC1 cytosolic tail is well-conserved among species. It is believed that the tail may play an important role in the function of MUC1, a belief bolstered by the presence of seven tyrosines in the fairly short tail. These tyrosines can be phosphorylated and this has been extensively studied in tumor and transfected cells. Interestingly, the phosphorylation of MUC1 by tumor cells has been shown to correlate with their adhesion (192). To see whether T cells might exhibit similar behavior in modifying MUC1 phosphorylation in response to adhesive interactions, we examined MUC1 phosphorylation in MUC1 transfected Jurkat cells in the absence or presence of endothelium.

We indirectly detected MUC1 tail phosphorylation by first immunoprecipitating with antibody against phosphorylated tyrosines and then immunoblotting with an antibody against the extracellular region. As shown in Figure 3.0-15, whole cell lysates of MUC1-Jurkat cells either left alone (lane 1) or placed on resting (lane 2) or activated (lane 3) endothelium all have MUC1. When those same cells are immunoprecipitated with antibody against phosphorylated tyrosine (lanes 4, 5, 6) MUC1 can still be detected, indicating phosphorylation of the MUC1 tail has occurred.

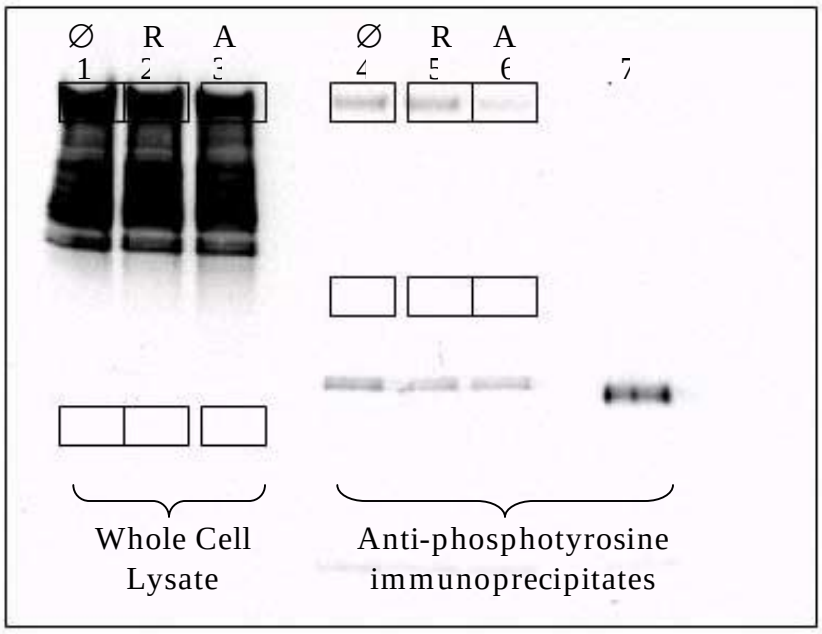

Figure 3.0-15 Phosphorylation of MUC1 in MUC1 transfected Jurkat cells. MUC1-Jurkat cells were incubated with nothing (∅) or resting (R) or activated (A) endothelium and then lysed in the presence of phosphatase inhibitors. Whole cell lysates of MUC1-Jurkat cells from each condition (lanes 1, 2, 3) were electrophoresed alongside of anti-phosphotyrosine immunoprecipitates from MUC1-Jurkat lysates (lanes 4, 5, 6) and a MUC1 negative cell lysate (lane 7). After transfer, the membrane was immunoblotted with antibody against the extracellular region of MUC1. The boxes indicate the regions used for quantitation by Versadoc camera imaging in Figure 3.0-16 and Figure 3.0-17.

The previous data indicated that phosphorylation of MUC1 tail was occurring regardless of interacting with endothelium. However, there appeared to be quantitative differences in the amount of phosphorylated MUC1. To detect this, the MUC1 signal was quantitated by Versadoc camera imaging immediately after immunoblotting with anti-MUC1 antibody reactive to the extracellular VNTR region. Figure 3.0-16 shows the quantitation of MUC1 in whole cell lysates. MUC1-Jurkat cells either left alone or placed on resting endothelium have approximately the same amount of MUC1 detected. MUC1-Jurkat cells incubated with activated endothelium have about 25% less signal. In contrast, Figure 3.0-17 shows that while phosphotyrosine immunoprecipitates from MUC1-Jurkat cells left alone or placed on resting endothelium still have approximately equal amounts of MUC1 detected, the phosphotyrosine immunoprecipitate

from MUC1-Jurkat cells incubated on activated endothelium have much less MUC1 signal, roughly 80% less signal. This decrease in MUC1 signal is much greater than when looking at the whole cell lysates, indicating that phosphorylation of MUC1 is decreased by interacting with activated endothelium.

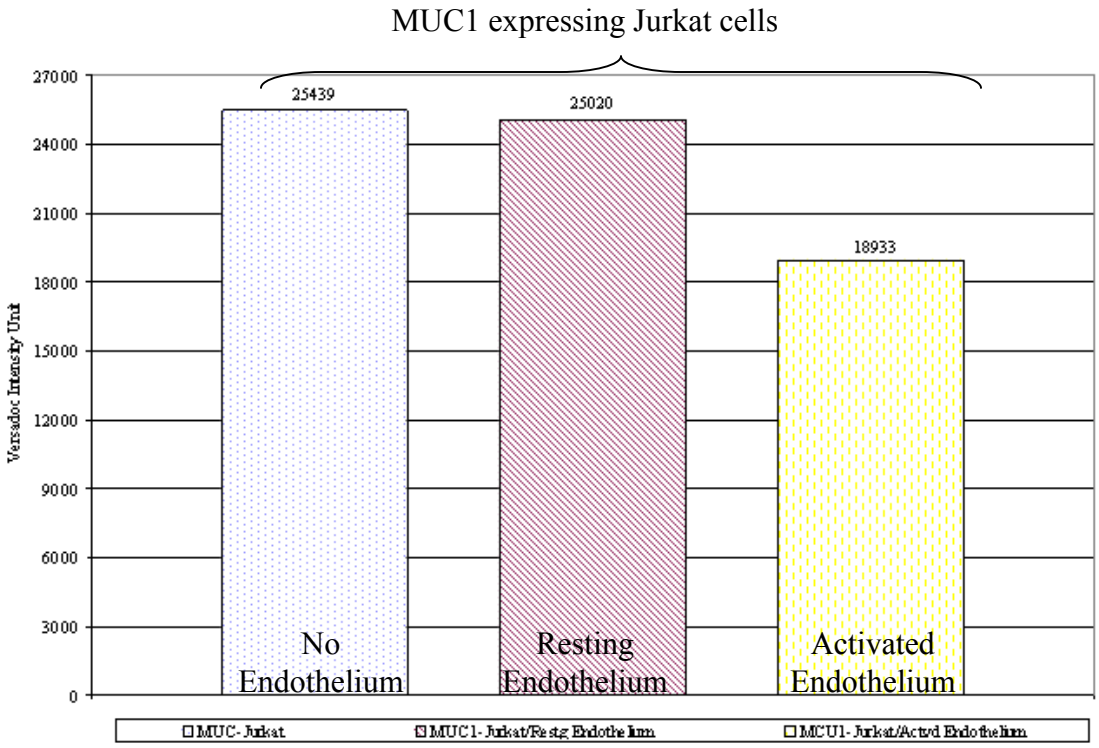

Figure 3.0-16 Quantitation of MUC1 signal from the immunoblot of MUC1-Jurkat whole cell lysate exposed to no endothelium, resting endothelium or activated endothelium. The initial MUC1 signal from the immunoblot in Figure 3.0-15 lanes 1, 2, and 3 was quantitated with a Versadoc camera image collecting system. The bottom box in each lane was subtracted as background signal from the top box in each lane containing the MUC1 signal.

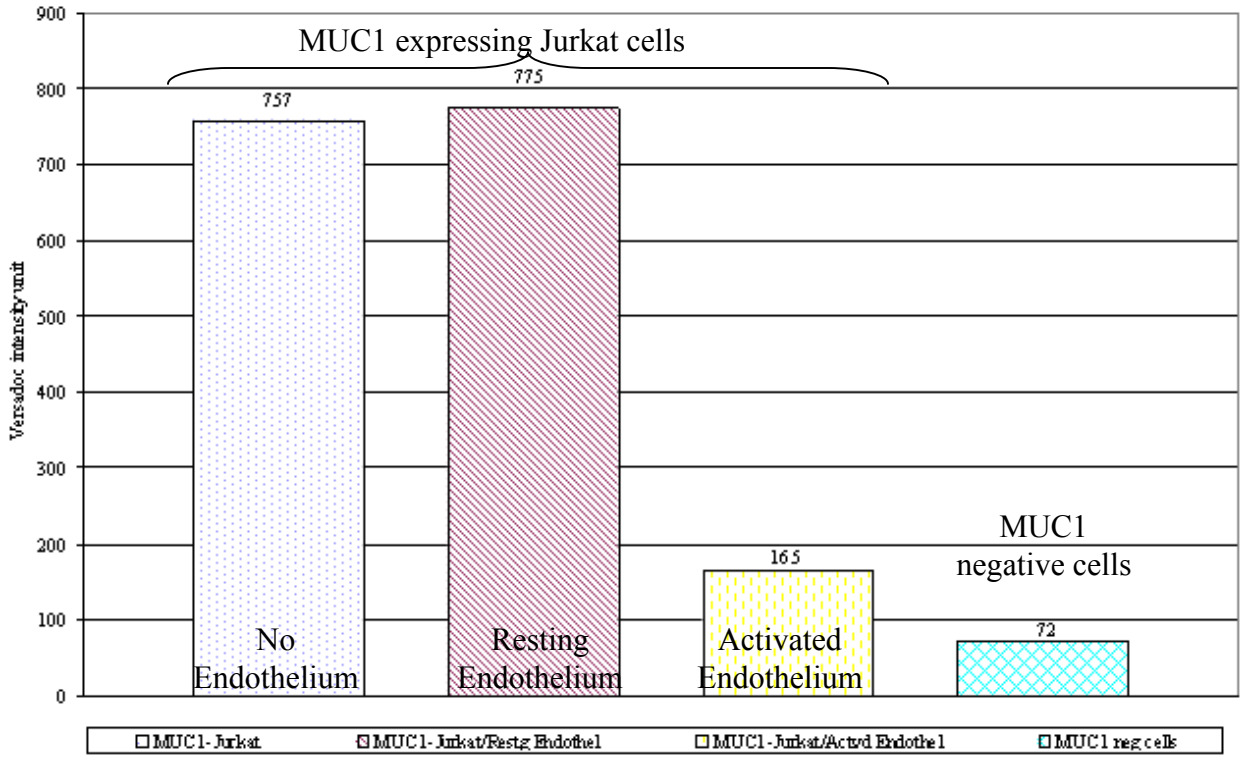

Figure 3.0-17 Quantitation of MUC1 signal from the immunoblot of MUC1-Jurkat cell lysates immunoprecipitated with anti-phosphotyrosine antibody following exposure to no endothelium, resting endothelium or activated endothelium. The initial MUC1 signal from the immunoblot in Figure 3.0-15 lanes 4, 5, 6, 7 was quantitated with a Versadoc camera image collecting system. The bottom box in each lane was subtracted as background signal from the top box in each lane containing the MUC1 signal.

3.3.4 Differences in phosphorylated protein pattern within Jurkat cells

Given the indication for differential phosphorylation of MUC1, we were interested in seeing if there were other differences in intracellular protein phosphorylation. We looked at tyrosine phosphorylated proteins in Jurkat and MUC1 Jurkat cells either left alone or incubated with an endothelial monolayer. Figure 3.0-18 shows the results of immunoblotting for phosphorylated tyrosines in lysates of Jurkat (J) or MUC1-Jurkat cells (M). Lanes 5 and 6 are lysates from cells that were not put into contact with endothelium. There are 3 bands that are different between Jurkat and MUC1-Jurkat cells, in the roughly approximate 39 kDa, 64-97 kDa and 190 kDa regions. As we looked at Jurkat and MUC1-Jurkat interacting with endothelium,

these 3 bands were consistently the distinguishing bands, though their pattern of appearance is not always the same, likely due to experimental variation. In Figure 3.0-18 the pattern seen in lanes 5 and 6 is the repeated in cells interacting with resting endothelium, lanes 3 and 4. In contrast, when Jurkat and MUC1-Jurkat cells were placed on a monolayer of activated endothelium, lanes 1 and 2, there was no difference in the phosphorylated protein pattern (Figure 3.0-18). Rather, it appears that MUC1 no longer makes a difference in phosphorylation of those 3 bands.

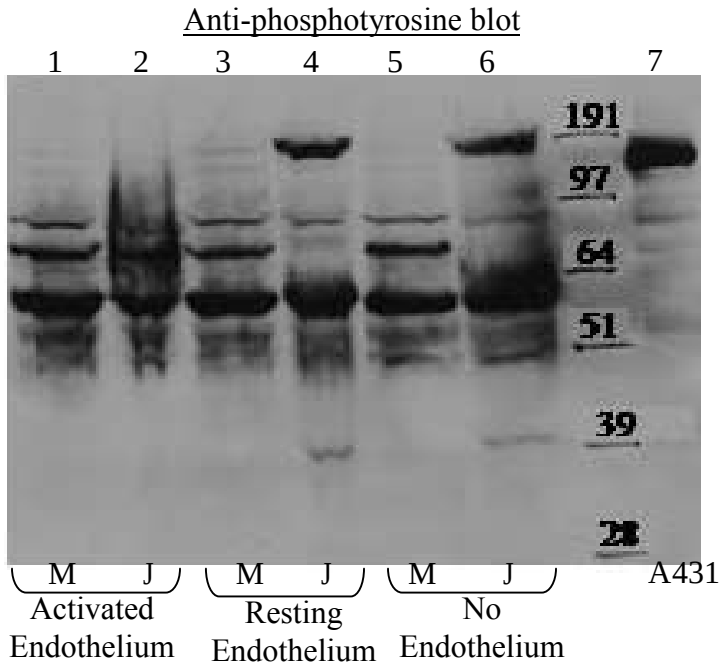

Figure 3.0-18 Phosphorylated proteins from Jurkat (J) and MUC1-Jurkat (M) cells after interacting with activated endothelium (lanes 1 and 2), resting endothelium (lanes 3 and 4) or no endothelium (lanes 5 and 6). Jurkat and MUC1-Jurkat cells were incubated with the indicated cell type and then lysed in the presence of phosphatase inhibitors. Whole cell lysates of Jurkat and MUC1 Jurkat cells were electrophoresed and then immunoblotted with antibody against phosphotyrosine. A431 cell lysate containing tyrosine phosphorylated proteins was used as a positive control (lane 7).

We were interested in the identity of these bands. Reprobing a previously anti-phosphotyrosine probed membrane (Figure 3.0-19A) with antibody against β-catenin (Figure 3.0-19B) shows that the 64-97 kDa band is likely to be β–catenin, which is regulated through

tyrosine phosphorylation (209-211). This warrants further investigation to look for phosphorylated β-catenin in MUC1 expressing T cells.

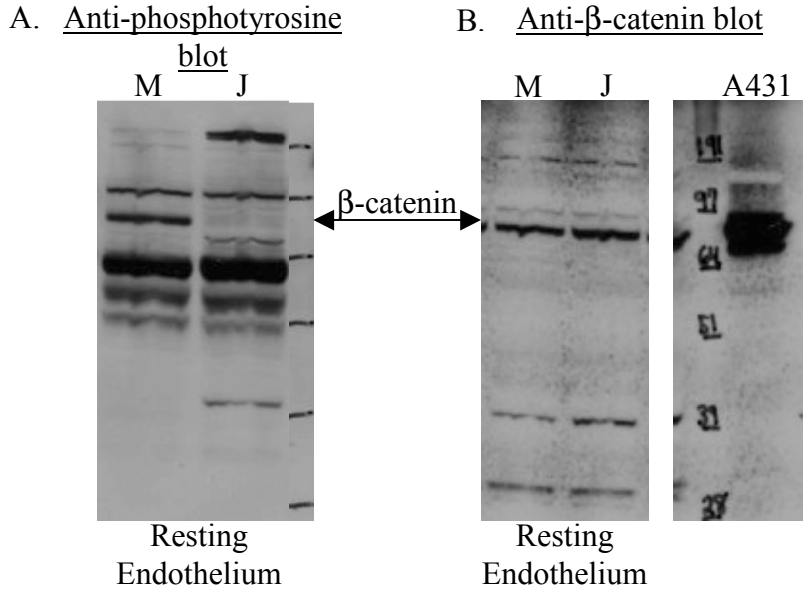

Figure 3.0-19 Immunoblotting for β–catenin. A membrane blotted for anti-phosphotyrosine (A) in Jurkat (J) and MUC1-Jurkat (M) cells following exposure to resting endothelium was reblotted with rabbit anti-β–catenin (B) primary antibody followed by horseradish peroxidase conjugated donkey anti-rabbit secondary antibody. Because the same membrane was used for each blot the molecular weight markers are identical; sizes indicated in (B). A431 cell lysate containing β-catenin was used as a positive control (lane 7).

3.4 Discussion

Anti-adhesive effects of MUC1 have been well-studied on tumor cells, where it is thought that expression over the cell surface aids in detachment of cells from the tumor mass. Some pro-adhesive effects of MUC1 have also been reported, adding to the belief that MUC1 plays a role in metastasis by causing tumor cells to leave the primary site and attach at secondary sites. We show here that MUC1 expressed in a model T cell line can also be anti-adhesive and pro-adhesive. When Jurkat cells were placed on endothelium, the expression of MUC1 enhanced their adhesion. This effect was only seen during short incubation times, within the first

20 minutes of interaction (Figure 3.0-7). After that MUC1 expression made no difference in cell adhesion (Figure 3.0-8). This is probably due to increased involvement of other adhesion molecules on the Jurkat surface dominating over the effect of MUC1. As expected, the increase in adhesion molecule expression following activation of endothelium (Figure 3.0-4) caused greater Jurkat and MUC1-Jurkat cell adhesion. MUC1 enhanced adhesion to both resting and activated endothelium, indicating that MUC1 can interact with molecule(s) expressed in both conditions.

Looking at individual adhesion molecules, ICAM-1 expressing cells showed MUC1-mediated enhancement of binding (Figure 3.0-10). This result with our MUC1 transfected Jurkat cells is consistent with other work examining MUC1 interactions with ICAM-1. Regimbald et al (189) showed that MUC1 expressed on tumor and transfected cells could bind to ICAM-1. They tested both plate-bound ICAM-1 and ICAM-1-expressing cells. Binding specificity between MUC1 and ICAM-1 was confirmed by blocking assays, using soluble MUC1 peptide and an anti-MUC1 antibody against a peptide epitope in the tandem repeat region. They later showed that at least six tandem repeats were required in a MUC1 peptide for binding with ICAM-1 to take place (190). Another group looked at cell-cell aggregation assays with ICAM-1 expressing cells and showed that MUC1 binds ICAM-1 in a tandem repeat dependent manner. This binding was enhanced by decreased glycosylation of MUC1, not affected by antibodies against sLe^x or sLe^a, but was inhibited by antibodies against ICAM-1 or against the tandem repeat of MUC1 (172). These results looking at ICAM-1 binding were virtually repeated in a separate report that also indicated that domain 1 of ICAM-1 is responsible for MUC1 binding (212), the same domain LFA-1 utilizes. ICAM-1 is constitutively expressed by most endothelial cells and we also saw it expressed on our resting HMVEC line, followed by upregulation after HMVEC

activation (Figure 3.0-4). Since MUC1 enhanced Jurkat cell binding to endothelium in both the resting and activated states (Figure 3.0-7), the MUC1 mediated attachment of Jurkat cells to ICAM-1 expressing cells is consistent with ICAM-1 being a ligand for MUC1 in our T cell model as well. Using MUC1 peptides to specifically block ICAM-1 binding to MUC1-Jurkat cells would substantiate this. MUC1 binding to ICAM-1 *in vivo* could take place not only to endothelium, as we have examined here, but could also play a role in bystander leukocyte recruitment. This process uses the T cell uropod, expressing ICAM-1 and -3, and extending above a polarized, adherent T cell to seize other passing T lymphocytes. Antibodies against ICAM-1, -3 and LFA-1 can decrease T cell recruitment but do not eliminate it (120). Binding between MUC1 and ICAM-1 could augment uropod mediated recruitment.

Adhesion of Jurkat cells to E-selectin decreased when MUC1 was expressed by the Jurkat cells (Figure 3.0-10). E-selectin is known to bind to carbohydrate ligands. Although MUC1 may carry specific O-glycans (e.g. sLe^x) that are recognized by selectins, it is unlikely that MUC1 can bind to selectins because the functionality of selectin ligands appears to depend on modifications of the core protein as well as the specific O-glycans (148), as discussed in chapter 2. Using soluble MUC1 secreted from a colon cancer line there have been reports of binding to E-selectin (213-215). This may not hold true when examining membrane bound MUC1 on the surface of cells. Recent work looking at specific molecular interactions between MUC1 and adhesion molecules showed that while tumor cells could bind E- and P-selectin, MUC1 expressed on their cell surface could not. Additionally, tumor cell binding of E-selectin was blocked by MUC1 expression on the tumor cell when the tandem repeat was of sufficient size. In agreement with our data (Figure 3.0-11, Figure 3.0-12), binding to P-selectin was not affected, indicating a specific inhibition to E-selectin (172). It is likely that the different results

concerning E-selectin binding are due to looking at secreted MUC1 versus cell bound MUC1. Consistent with reports looking at tumor MUC1, we also observed an E- selectin inhibitory effect when MUC1 was expressed by Jurkat cells (Figure 3.0-10). This is despite the expression of E-selectin ligand PSGL-1 on Jurkat cells (Figure 3.0-3).

The overall enhanced adhesion between MUC1 expressing Jurkat cells and activated endothelium suggests that MUC1 – ICAM-1 binding overrides the repulsion between MUC1 and E-selectin in our *in vitro* system. Our *in vitro* data (Figure 3.0-4) showed that the inflammatory cytokine IL-1 induces expression of E-selectin and upregulates ICAM-1 on endothelial cells. *In vivo* the kinetics for expression of each molecule are different with E-selectin expression detected much sooner but with a shorter half-life than ICAM-1. Maximum E-selectin expression can be detected within two to four hours of endothelial activation but ICAM-1 peak expression does not occur until 12 hours after activation. E-selectin is generally down to basal levels 24 hours after activation while ICAM-1 persists for at least 3 days (36). This means that the effect of MUC1 may hinder T cell binding to endothelium that has just been activated, allowing strong E-selectin binding cells such as neutrophils early access to inflammatory sites. Later when the endothelium is expressing ICAM-1, MUC1 may give a binding advantage to MUC1 expressing T cells that generally reach inflammatory sites after neutrophils and monocytes.

The Jurkat T lymphoblastoid cell line is a well-established model to study mature T cells. It has been used extensively to examine T cell signaling (216) and adhesion via selectins (92, 99, 153, 217, 218), integrins (175, 177, 179, 219-224) and endothelium (153, 219, 225, 226) over the years. Glycosylation by Jurkat cells was studied by in depth analysis of leukosialin (CD43), a sialoglycoprotein found on normal leukocytes. Piller et al unexpectedly found that 83% of the O-linked saccharides on leukosialin were composed of only N-acetylgalactosamine (227). This

was attributable to very low levels of the enzyme core 1 GalNAc;β1,3Galactosyltransferase, the enzyme responsible for adding an additional galactose N-acetylgalactosamine to form the core 1 structure, so that more complex oligosaccharide structures can be synthesized. Only 17% of the O-linked saccharides on leukosialin from Jurkat cells had more complex structures than the N-acetylgalactosamine (227). The lack of core 1 GalNAc;β1,3Galactosyltransferase activity was not due to a defect in the core 1 GalNAc;β1,3Galactosyltransferase protein but rather due to a mutation in a chaperone protein, Cosmc (*co*re 1 β3-Gal-T-specific *m*olecular *c*haperone) (228). A single nucleotide mutation in the gene for Cosmc was found in Jurkat cells which resulted in lack of most of the cytosolic tail of Cosmc. When wild type Cosmc was expressed in Jurkat cells, the activity of intrinsic core 1 GalNAc;β1,3Galactosyltransferase was restored (228). Additionally, it was very recently shown that Jurkat cells show much lower levels of mRNA for the enzyme FucT-VII unless constitutively active Ras was present (99) although earlier work reported that PMA activation of Jurkat cells increased the steady-state level of FucT-VII mRNA (92). The physiological significance of these findings is confusing since Jurkat adhesion to endothelium has been shown to be inhibited by anti-E-selectin antibodies (226). Though we need to fully characterize the O-glycosylation occurring to MUC1 in our MUC1 transfected Jurkat cell line, it is possible that the MUC1 is lacking complex O-linked saccharides. This could be a reason why our results are so similar to work looking at the adhesion of tumor MUC1.

Most work examining MUC1 adhesion has involved peptides or tumor MUC1. It is not known what normal MUC1 binds to, or even if it does bind differently than the commonly studied tumor form of MUC1. Enhanced glycosylation of MUC1 by normal cells makes a different binding profile likely, but this remains to be proven. We have developed a model that shows the impact of MUC1 on T cell binding; the next step is to demonstrate the impact of

normally glycosylated MUC1. It would be fruitful to characterize the MUC1 expressed on our model, to verify that it is underglycosylated, and then add wild type Cosmc to the MUC1 transfected Jurkat cells. If we could verify that MUC1 glycosylation was changed, it would be interesting to then repeat our assays to see if MUC1 still enhances Jurkat cell binding to endothelium and ICAM-1 but decrease binding of Jurkat cells to E-selectin. Comparing the results would give insight into adhesion differences between the normal and tumor forms of MUC1.

Glycosylation deficiency in Jurkat cells does not seem to have come up in other work looking at adhesion of Jurkat cells. However, there is a much higher degree of glycosylation that occurs on MUC1 as compared to other smaller molecules. Even though our MUC1 construct has only 22 repeats, smaller than the number commonly seen in human cells (41-85 (1, 2)), there are still a great deal more glycosylation sites than on other cell surface proteins. As a result a glycosylation deficiency may be more conspicuous on MUC1.

In our model, MUC1 transfected Jurkat cells are expressing a much higher level of MUC1 than is seen on activated T cells, so that we could highlight MUC1 mediated interactions. However, it may be more difficult to distinguish an effect due to MUC1 when examining normal activated human T cells since a certain density of surface expression may be required. On the other hand, MUC1 on normal T cells would likely have more repeats than the 22 in our construct. Depending on whether the MUC1 VNTR region is responsible for MUC1 mediated cell adhesion, as seems likely, the avidity of interaction may be greater for activated normal human T cells. It would be interesting to repeat the adhesion assays with Jurkat cells expressing a much lower level of MUC1 and with a larger MUC1 construct, to better mimic the activated human T cells and to compare with our observations.

The adhesion of T cells to the blood vessel wall is only the beginning of what happens to a T cell as it interacts with endothelium. There are signaling pathways initiated that prepare it to tightly bind the vessel wall and then move through the wall and into the tissue. Adhesion between cells and signaling within cells are inextricably linked. Adhesion molecules that are binding to the endothelium can initiate their own signaling pathways. Similar to MUC1, integrins such as LFA-1, which can also bind to ICAM-1, do not have their own ability to catalyze signaling events but they do associate with intracellular proteins that can mediate signaling. Intracellular molecules involved in integrin outside-in signaling include c-Src which has also been associated with MUC1 (197-199). Bianchi et al (109) showed that the LFA-1 integrin can mediate signals affecting gene expression. Other groups have demonstrated LFA-1 signaling to modify the cytoskeleton, enhance binding to ICAM-1, and regulate the adhesiveness of β1 integrins (106, 110, 113). Our data showing changes in the phosphorylation of MUC1 and other proteins indicate that MUC1 is also likely to be involved in signaling to the T cell that extracellular interaction has occurred.

Phosphorylation of the MUC1 cytosolic tail has been shown to occur in tumor cells and transfected cells (191-193). We show here that MUC1 expressed in Jurkat cells is phosphorylated. However, during interaction of MUC1 expressing Jurkat cells with activated endothelium this phosphorylation decreases (Figure 3.0-17). Adhesion-dependent alteration in MUC1 phosphorylation has been observed by others (192). In MUC1-expressing tumor cells, the adhesive state was associated with the extent of MUC1 phosphorylation. As tumor cells adhered, their MUC1 phosphorylation decreased over time. When a series of decreasing amounts of cells were seeded in separate tissue culture flasks, those at higher density that became confluent sooner had less tyrosine phosphorylation. Cells seeded at a lower concentration, and

therefore not confluent at the same timepoint, had more tyrosine phosphorylation. This same phenomenon seems to be occurring when MUC1 expressing Jurkat cells adhere to activated endothelium. The tighter interaction is associated with a decrease in the phosphorylation of MUC1. This work should be repeated using human T cells activated to express MUC1, though it is likely the results would be same as Jurkat cells since they are a well known model for signaling in T cells.

Tyrosine phosphorylation of the MUC1 tail is decreased in the context of interacting with activated endothelium, likely as part of a mechanism regulating adhesion. Phosphorylated MUC1 was reported to bind the SH2 domain of Grb2 whose SH3 domain then associated with the guanine nucleotide exchange protein Sos (191). Grb2 is involved in integrin mediated signaling (229). Competition for Grb2 binding may be regulated by dephosphorylating MUC1 to decrease Grb2 association so that it would be available for use by integrins. However these results bear further exploration as Quin et al (192) were unable to detect Grb2 in association with MUC1. MUC1 in tumor cells has been shown to co-immunoprecipitate β–catenin, a protein involved in cadherin-mediated cell adhesion. Yamamoto et al (195) found that MUC1 in human tumor cells co-immunoprecipitated with β-catenin only when the cells were adherent. Cells in suspension showed no association of MUC1 with β-catenin. The phosphorylation of MUC1 in this tumor cell model was not examined. Whether MUC1 in Jurkat cells also has an association with β–catenin may indicate adhesion signaling pathways involved in T cell binding to endothelium.

Regulation of the association of MUC1 with β-catenin has been explored (195, 197, 198, 203, 204). The β–catenin binding motif in the MUC1 cytosolic tail is affected by surrounding phosphorylation sites. The tyrosine kinase c-Src binds adjacent to the β–catenin motif. C-Src

phosphorylation in the YEKV c-Src binding site enhances β–catenin binding (197). In multiple myeloma cells it has been shown that Lyn can bind to and phosphorylate MUC1 at the same site as c-Src to similarly increase β–catenin binding (205). Adjacent to the β–catenin motif is a binding site for glycogen synthase kinase 3β (GSK3β) and phosphorylation of a serine in this site by GSK3β decreases β–catenin binding to MUC1 (203). This same group found that the presence of MUC1 decreases E-cadherin –β–catenin interaction, but this effect could be reversed by GSK3β (203). It would be important to also look at serine/threonine phosphorylation in our MUC1 expressing Jurkat cells to see if there are changes associated with binding to endothelium.

Decreased cytosolic tail tyrosine phosphorylation in MUC1 expressing Jurkat cell would inhibit binding of MUC1 and β–catenin, thus freeing it to bind other molecules. The effects of this on cell adhesion may be mediated through a cadherin expressed on Jurkat and T cells (230). It is also possible that cell adhesion may not be the primary target, as β–catenin is also involved in gene regulation. It was recently shown that the association between MUC1 and β–catenin plays a role in nuclear β–catenin localization in tumor cells (206) and in multiple myeloma cells (205).

When we examined the impact of MUC1 on the tyrosine phosphorylation of proteins in Jurkat cells we observed three sizes of proteins that were differentially phosphorylated. There were alterations in the phosphorylation of these proteins in the absence and presence of endothelium (resting and activated). Evidently phosphorylation of MUC1 is not the only change occurring inside Jurkat cells following endothelial interaction. Identifying these differentially phosphorylated proteins and the kinase(s) responsible would indicate which signaling pathways, are affected by 1) MUC1 expression and 2) by adhesion of MUC1 expressing cells to endothelium. Adhesion dependent phosphorylation and activation of FAK and PYK-2 tyrosine

kinases has been demonstrated in T lymphoblasts adhering via LFA-1 to ICAM-1 (111). Phosphotyrosine immunoprecipitates showed that these proteins fall within the 110-180 kD region. Though there have been no reports of MUC1 association with FAK or PYK-2, they would be candidate to look at since their phosphorylation was mediated by ICAM-1 binding which MUC1 can also do. This would be especially interesting as activation of FAK and PYK-2 was associated with converting cell morphology from spherical to elongated (111).

Blotting for β–catenin indicated it was one of the differentially phosphorylated proteins, depending on whether MUC1 was expressed and whether cells were incubated with endothelium. β–catenin is in PHA activated peripheral blood T cells (230), in Jurkat cells, but not resting lymphocytes, and was shown to regulate PHA stimulated cell aggregation (231). The tyrosine kinase c-Src can phosphorylate tyrosines in β–catenin and this modification has been shown to decrease its affinity for E-cadherin (211). In MUC1 expressing cells binding of c-Src occurs close to the β–catenin binding site so c-Src would have access to phosphorylate β–catenin bound to MUC1. Once phosphorylated, β–catenin may be released into the cytosolic pool, as has been shown in epithelial cells (210), and free to engage in nuclear translocation, perhaps bringing along the cytosolic tail of MUC1 (206).

In our endothelial assays there actually are two types of cell-cell interactions occurring: Jurkat cells with Jurkat cells as well as Jurkat cells with endothelium. Though we did not directly examine a MUC1 effect on Jurkat cell-Jurkat cell interaction, MUC1 would likely have an effect. It has been shown that the mucin-like molecule, CD43, increases homotypic aggregation of Jurkat cells and T cells in a β2 integrin dependent manner (232). CD43 intracellular signaling, via phosphorylation and association with cytosolic proteins (233, 234) likely mediated the enhanced adhesion. Similarly MUC1 in our system may be influenced by

and/or influencing Jurkat cell aggregation, as well as binding to endothelium. It has also been shown that blocking protein tyrosine kinases can inhibit homotypic aggregation of Jurkat cells (235), implying that Jurkat adhesion depends on phosphorylation of tyrosines. It would be interesting to see whether blocking tyrosine kinases would alter our adhesion assay results linking MUC1 to enhanced adhesion to endothelium and ICAM-1 expressing cells. Further work is needed to illuminate these interesting associations between MUC adhesion, phosphorylation, and interactions with other proteins inside the cell.

4.0 MUC1 EXPRESSION ON MOUSE T CELLS

Hypothesis 3:

In vivo manipulation of T cell MUC1 would affect the ability of T cells to reach inflammatory sites. As observed in humans, T cells from MUC1 transgenic mice should express MUC1 on their cell surface following activation and thus be susceptible to blocking MUC1 with antibodies. Failure to express MUC1 would indicate either inability of mouse T cells to express the human transgenic MUC1 or an intrinsic difference between mouse and human T cells.

Specific Aim 3:

Determine expression of human MUC1 on the surface of MUC1 transgenic mouse T cells following activation and document any differences in the mouse model from human T cell expression of MUC1.

Rationale:

An *in vivo* model is necessary to best study the effect of MUC1 on T cell migration. Mouse Muc-1 and human MUC1 have a homologous structure but differ in size, sequence, and the number of repeats in the extracellular region. The mouse system cannot be used however

because there are no reliable reagents such as anti-Muc-1 antibodies commercially available to study mouse Muc-1. In order to take advantage of the numerous reliable well-characterized human MUC1 reagents, the human MUC1 transgenic mouse model (124) could be used. It has been documented to express human MUC1 on the same epithelial surfaces where MUC1 is seen in humans. Due to its fidelity in reproducing human MUC1 expression on epithelium, this model should be ideal to study the role of MUC1 on T cells via *in vivo* manipulation of the T cell MUC1. Additionally, this transgenic mouse is used in many cancer vaccine studies. Any differences seen between the mouse and human T cell would be relevant to comparisons made between humans and mice in numerous immune research studies.

4.1 INTRODUCTION

To explore the effect of MUC1 on T cell migration *in vivo*, a mouse model would be valuable. Mouse Muc-1 and human MUC1 have a homologous structure but differ in size, sequence, and the number of repeats in the extracellular region. These differences may not give a true picture of human MUC1 on human T cells. In addition, there is a dearth of reliable reagents commercially available to study mouse Muc-1. In order to take advantage of the numerous reliable human MUC1 reagents, the human MUC1 transgenic mouse model could be used. It has been documented to express human MUC1 on the same epithelial surfaces where MUC1 is seen in humans (124). Due to its fidelity in reproducing human MUC1 expression on epithelium, we decided to use this model to study the role of MUC1 on T cells.

4.1.1 Human MUC1 transgenic mouse model

MUC1 transgenic mice have been developed in an effort to create a better model for MUC1 immunotherapy of human cancers. Rowse et al have generated mice that contain the

entire gene sequence for the human form of MUC1 (124). These mice express MUC1 under the control of its endogenous promoter and immunohistochemical staining has shown that it is expressed in a similar tissue pattern and level as in humans. This modeling of MUC1 expression has also been demonstrated in a spontaneous tumor model in which MUC1 transgenic mice have been crossed with mice that develop pancreatic cancer. The pancreatic disease that develops in these double transgenic mice is analogous to human pancreatic cancer in the overexpression and underglycosylation of MUC1 (236). Significantly, the spleen from MUC1 transgenic mice shows no MUC1 expression (124), consistent with our data showing that the human spleen does not contain MUC1 transcripts (Figure 2.0-19). All indications point to a fully suitable mouse model in which to study human MUC1 expression on T cells.

4.1.2 Mouse Muc-1

The mouse homolog of human MUC1, referred to as Muc-1, was cloned in 1991 (237, 238) and subsequently mapped to mouse chromosome 3 (239). The genomic structure between the human MUC1 and mouse Muc-1 are similar, both contain six introns and seven exons with conserved boundaries and similar sizes. Unlike human MUC1 (11, 13-18), there is no suggestion of alternative splicing of murine Muc-1. The promoter regions of both are highly homologous, 74%, as are the transmembrane and cytosolic regions, 87% at the protein level (237). Both MUC1 and Muc-1 have the two cysteines at the junction of the transmembrane domain and cytosolic tail that are partially responsible for MUC1 trafficking (7), agreeing with observed apical expression of Muc-1 (240). Underscoring the signaling function of MUC1/Muc-1 in cells, the seven tyrosines in the cytoplasmic tail are conserved (237, 238).

In the extracellular portion there is less homology (237, 238). Though the region of proteolytic cleavage responsible for human MUC1 being expressed as a heterodimer is fairly

well conserved in the mouse, this has not yet been documented to occur in Muc-1. In contrast to human MUC1, the repeat region in rodent Muc-1 is not polymorphic (237). There are always 16 repeats of either 20 or 21 amino acids each. At the nucleotide level the repeats share only 75% homology with each other, as compared to MUC1 in which the repeats are nearly identical. Within each repeat of murine Muc-1 is an average of 9 sites for O-linked glycosylation, nearly double the number in MUC1. As a result Muc-1 may be even more glycosylated than MUC1 which is consistent with the longer transit time from the Golgi to the cell surface for mouse Muc-1 as compared to human MUC1 on tumor cells (241). Despite the expected 65kDa mass of the Muc-1 core protein (237), Muc-1 is larger than 200 kDa when run on a protein gel, indicating that extensive glycosylation does occur. Greater glycosylation in combination with the lower proline content may make the structure of Muc-1 more extended than MUC1 (238). The extracellular domain of Muc-1 would be predicted to be 70 nm (242) so like MUC1 would still stretch far above the cell surface. The immunodominant sequence in human MUC1, PDTRP, is not conserved in the mouse Muc-1, rather uncharged residues are in the place of the charged amino acids aspartic acid (D) and arginine (R). Comparisons following MUC1 vaccination of wild type mice and MUC1 transgenic mice have shown significantly different responses (124, 140, 243) highlighting *in vivo* the differences between murine Muc-1 and human MUC1.

4.2 MATERIALS AND METHODS

4.2.1 Cells, mice and antibodies

BT-20 tumor cells were grown in RPMI supplemented with 10% fetal bovine serum, 1% L-glutamine and 1% penicillin/streptomycin. HBL/Y2 cells, a human mammary epithelial cell line immortalized by SV40 T antigen, were grown in DMEM supplemented with 10% fetal

bovine serum, 1% L-glutamine and 1% penicillin/streptomycin. These cells had been transfected with an expression vector containing MUC1/Y (Dr. Daniel Wreschner). Peripheral blood was obtained as a leukopheresis research product from the Central Blood Bank (Pittsburgh, PA). Peripheral blood mononuclear cells (PBMC) were isolated from whole blood by Ficoll/Paque (Amersham Pharmacia Biotech, Uppsala, Sweden) density gradient centrifugation. MUC1 transgenic mice, inbred on a C57BL/6 background, were purchased from the Mayo Clinic (Scottsdale, AZ). Wild type C57BL/6 mice were purchased from The Jackson Laboratory (Bar Harbor, ME). Mice were housed at the University of Pittsburgh Cancer Institute animal facility under standard pathogen-free conditions.

FITC labeled mouse isotype control mouse IgG1, FITC labeled mouse anti-human MUC1 (clone HMPV), PE-labeled isotype control rat IgG2b, PE-labeled rat anti-mouse CD25, PerCP labeled isotype control hamster IgG group 1 and PerCP hamster anti mouse CD3, PE-labeled isotype control mouse IgG1, PE labeled mouse anti-human CD25, PerCP-labeled isotype control mouse IgG1, and PerCP-labeled mouse anti-human CD3 were purchased from BD Pharmingen. Anti-human MUC1 monoclonal antibody VU-3-C6 was provided by Dr. J. Hilgers (Department of Obstetrics and Gynecology, Academisch Ziekenhuis, Vrije Universiteit, Amsterdam, The Netherlands). Anti-human MUC1 monoclonal antibody BC3 was provided by Dr. I. McKenzie (The Austin Research Institute , Heidelberg, Vic., Australia).

4.2.2 Activation of human PBMC and mouse splenocytes

PBMC were cultured in RPMI-1640 supplemented with 10% human serum (Cellgro, Herndon, VA), 1% L-glutamine, 1% penicillin/streptomycin, and activated with PHA **(**5 μg/ml; Sigma, St. Louis, MO) and 20 U/ml interleukin-2 (IL-2) (Dupont, Wilmington, DE). Mouse splenocytes were cultured in RPMI-1640 supplemented with 10% fetal calf serum, 1% L-

glutamine, 1% penicillin/streptomycin, 1% non-essential amino acids, 1% sodium pyruvate, 0.1% β-mercaptoethanol and activated with ConA (10 μg/ml; Amersham Biosciences, England) and 20 U/ml interleukin-2 (IL-2) (Dupont, Wilmington, DE). Activation of T cells was verified by flow cytometry staining for CD3 and CD25 prior to using cells in experiments.

4.2.2. Extracellular flow cytometry

Activated PBMC and mouse cells were stained with directly conjugated antibodies against MUC1 (clone HMPV), CD25 and CD3. Samples were analyzed by first gating out dead cells on the basis of forward and side light scatter. Then the CD3 positive population was examined for CD25 expression and MUC1 expression. Resting cells were stained with directly conjugated antibodies against MUC1 (clone HMPV) and CD3. Live cells were examined for CD3 expression and CD3 positive cells were assessed for MUC1 expression. Samples were analyzed using a FACSCalibur flow cytometer (Becton Dickinson, San Jose, CA) and FlowJo 3.2 software (Tree Star, Inc., San Carlos, CA).

4.2.3 Intracellular flow cytometry for human MUC1

Human PBMC, MUC1 transgenic and wild type splenocytes were activated as described for seven days. Live PBMC were purified by Lymphocyte Separation Medium (ICN, Aurora OH) centrifugation and live splenocytes were purified by Lympholyte-M (Cedarlane Laboratories, Ontario Canada) centrifugation before staining. Live cells were then stained for extracellular MUC1 and for intracellular MUC1, no additional markers were examined. Intracellular staining was done by first fixing the cells in 4% formaldehyde for 20 minutes at room temperature. This was followed by washing in FACS medium (5% FBS, 0.1% sodium azide in PBS) and permeabilization with 0.5% saponin in FACS medium (permeabilization

FACS medium) for 10 minutes at room temperature. Keeping the cells in permeabilization FACS medium, FITC labeled anti-MUC1 or FITC labeled isotype control antibody was added to cells for 45 minutes at 4^{o}C. Cells were then washed in permeabilization FACS medium followed by normal FACS medium and analyzed alongside cells stained for extracellular MUC1. Samples were analyzed using a FACSCalibur flow cytometer (Becton Dickinson, San Jose, CA) and FlowJo 3.2 software (Tree Star, Inc., San Carlos, CA).

4.2.4 RT-PCR for human MUC1 and MUC1/Y

Total RNA was isolated using the RNeasy Mini Kit (Qiagen, Valencia CA) according to the manufacturer's instructions. cDNA was generated from total RNA using Gene Amp RNA PCR kit (Roche Molecular Systems, Branchburg NJ) according to the manufacturer's instructions, using random hexamer or oligo $d(T)_{16}$ primers as indicated. In all experiments, 1 μg of total RNA was used to generate cDNA. The cDNA was amplified using one of three sets of primers. Primers to amplify GAPDH (glyceraldehydes 3 phosphate dehydrogenase), a housekeeping gene, were used as a control. These forward, 5'-GGG GAG CCA AAA GGG TCA TCA TCT 3' and reverse 5'-GCC ATC ACG CCA CAG TTT C-3', primers amplify a 257bp fragment. MUC1 forward 5'-CTT GCC AGC CAT AGC ACC AAG-3' and reverse 5'-CTC CAC GTC GTG GAC ATT GAT G-3' primers, used in screening to identify MUC1 transgenic mice (124), bind to human MUC1 genomic sequence spanning an intron so that a 341bp product is amplified from RNA and a 600bp product is amplified from genomic DNA. MUC1/Y forward 5'-T ACT GAG AAG AAT GCT TTT AAT-3' and reverse 5'-C AGA CTG GGC AGA GAA AGG A-3' primers yield a 313bp product. The first primer sequence GCT * TTT binds over the unique joining site generated during alternative splicing so that this primer can only bind MUC1/Y (* represents the unique joining site).

4.2.5 Immunoblotting for MUC1 from resting and activated MUC1tg

Human PBMC, wild type or MUC1 transgenic splenocytes were activated as described above and then analyzed by flow cytometry verify we have live, activated ($CD25^+$) T cells ($CD3^+$). Cell pellets were made of these cells and stored at -80°C until lysed for immunoblotting. BT-20 cell pellets containing 5 x 10^5 cells each were also stored at -80°C until lysed for immunoblotting. Cell pellets (5 x 10^6 or 10 x 10^6) of resting and activated human, wild type or MUC1 transgenic T cells were thawed on ice and lysed with Lysis Buffer I (50mM Tris-HCl, 150mM NaCl, 1% TritonX, 0.1% SDS, 100 μg/ml PMSF, 5 μg/ml Leupeptin, 2 μg/ml Aprotinin) on ice for 40 minutes, vortexing every 10 minutes. Lysates were centrifuged at 4°C for 15 minutes at 13,000 x g. Supernatants were collected to new tubes, mixed with reducing loading buffer (62.5 mM Tris/HCl, 10% glycerol, 5% β–mercaptoethanol, 1.05% SDS, 0.004% bromophenol blue) and boiled for 3 minutes. Samples were electrophoresed alongside Rainbow molecular weight markers (BioRad RPN756, BioRad Laboratories, Hercules CA) through a 7% acrylamide gel in Glycine-Tris-SDS running buffer (0.192M Glycine, 0.025M Tris, 0.035M SDS) at 150 volts. Proteins were transferred onto nitrocellulose membranes (BioRad Laboratories, Hercules CA) in 10% Towbin buffer using 30 volts overnight at 4°C. Membranes were blocked by rocking in 10% dry milk in PBS and then immunoblotted with anti-MUC1 antibodies BC3 and/or VU-3-C6. Bound anti-MUC1 antibody was detected by sheep anti-mouse horseradish peroxidase secondary antibody (Amersham Biosciences, England). ECL detection reagents (Amersham Biosciences, England) were added to the membrane and proteins were visualized by X-Omat film development (Kodak, Rochester NY).

4.3 RESULTS

4.3.1 Lack of human MUC1 on MUC1 transgenic mouse T cells

To explore the effect of MUC1 on T cell migration *in vivo*, a mouse model would be informative. Mouse Muc-1 and human MUC1 have a similar structure but differ in size, sequence, and the number of repeats in the extracellular region. These differences may not give a truly analogous picture of human MUC1 on human T cells. In addition, there is a dearth of reliable reagents commercially available to study mouse Muc-1. In order to take advantage of the numerous reliable human MUC1 reagents, we decided to use the human MUC1 transgenic mouse model.

The first step was to see if the MUC1 transgenic mouse T cells express MUC1 on their surface following activation, as human T cells do. Splenocytes from the MUC1 transgenic mouse were activated for seven days alongside wild type splenocytes as a negative control and human PBMC as a positive control. All three sets of cells were stained for expression of MUC1, CD25 and CD3. Analysis was performed by gating on live CD3 expressing cells; by this point in the culture all of the live cells were $CD3^+$, indicating that non-T cells in the original pool of PBMC and splenocytes have died. All samples were activated, as indicated by strong expression of the IL-2 receptor (CD25), (top panel, Figure 4.0-1). However, MUC1 expression seen on the activated human T cells was not reproduced on the activated MUC1 transgenic mouse T cells (bottom panel, Figure 4.0-1). There was no MUC1 expression on either the activated MUC1 transgenic mouse T cells or wild type mouse T cells.

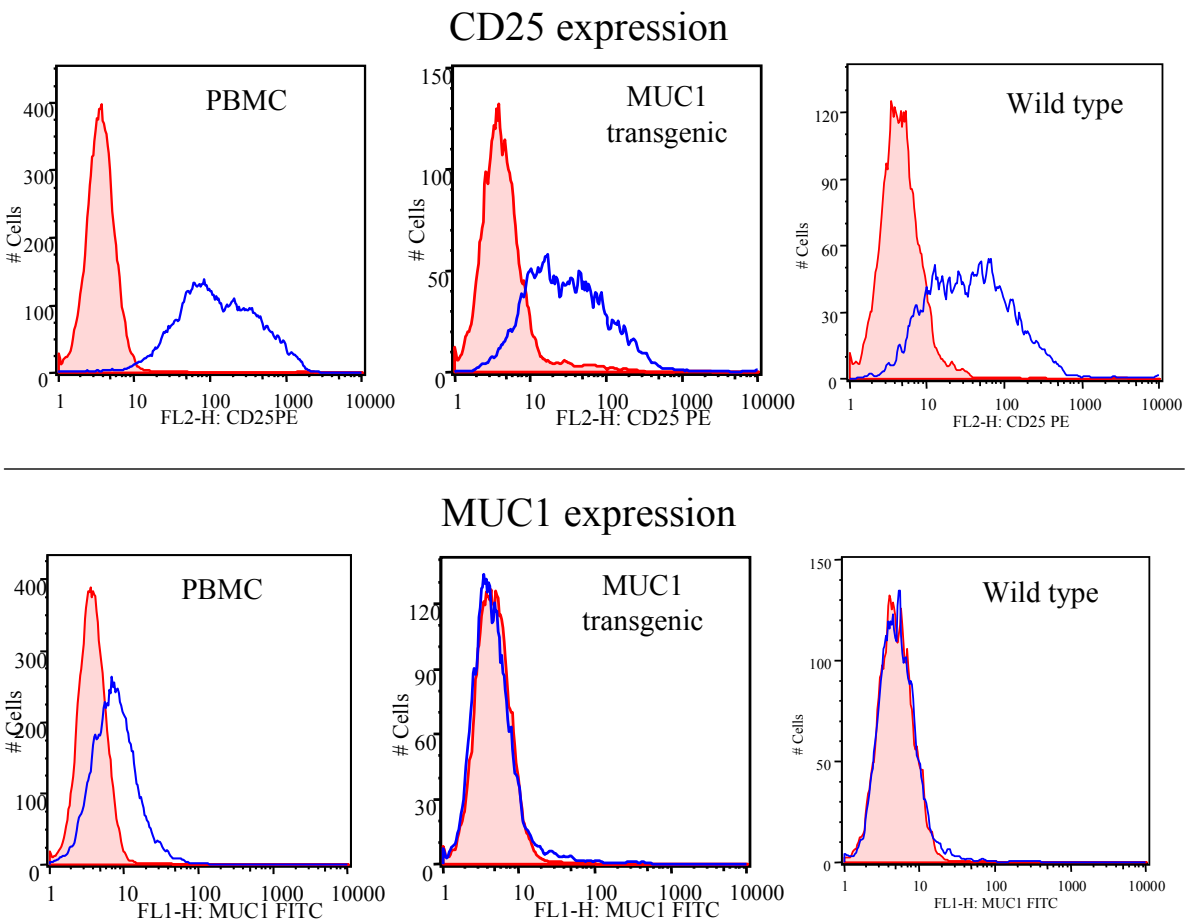

Figure 4.0-1 Activated T cells from human PBMC, MUC1 transgenic mice and wild type mice. PBMC and splenocytes were activated with PHA or ConA, respectively, and then stained for expression of CD3, CD25 and MUC1. CD3 expressing cells were examined for CD25 expression (top) and MUC1 expression (bottom). Shaded histograms are isotype control antibody fluorescence, open histograms are anti-CD25 (top panel) or anti-MUC1 (bottom panel) antibody fluorescence

Resting T cells from wild type and MUC1 transgenic mice predictably also showed no expression of MUC1 (Figure 4.0-2).

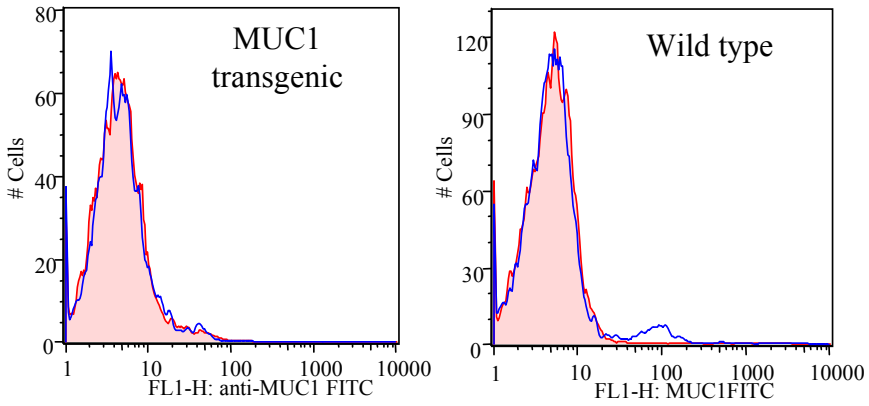

Figure 4.0-2 Resting splenocytes from MUC1 transgenic mice and wild type mice. Splenocytes were stained for expression of CD3 and MUC1. CD3 expressing cells were examined for MUC1 expression. Shaded histograms are isotype control antibody fluorescence, open histograms are anti-MUC1 antibody fluorescence

4.3.2 RT-PCR for MUC1 in mouse T cells

Since we did not see MUC1 on the surface of activated MUC1 transgenic mouse T cells, we asked whether the gene was being expressed. Primers against MUC1 were used to perform RT-PCR on resting and activated splenocytes from MUC1 transgenic mice. MUC1 RT-PCR was also done on wild type mouse cells as a negative control and the MUC1 expressing BT-20 tumor cell line as a positive control. The MUC1 primers were selected to amplify a region containing an intron so that amplification of genomic human MUC1 would produce a 600 base pair band while amplification of processed RNA would produce a 341 base pair band. In Figure 4.0-3, a 100 – 1000 base pair ladder is in lane 1 of both gels. BT-20 cells are shown in lanes 2 and 3 of both gels. The genomic MUC1 amplification product from BT-20 cells is seen in lane 2 in which no reverse transcriptase (RT) was added to the reaction. MUC1 RNA amplification product from BT-20 cells is seen in lane 3 in which RT was added to the reaction.

Splenocytes from a MUC1 transgenic mouse are shown in the top gel (Figure 4.0-3A) while splenocytes from a wild type mouse are shown in the bottom gel (Figure 4.0-3B). Lanes 4 – 7 in both gels are RT-PCR reactions on resting splenocytes, while lanes 8 - 11 in both gels are

from activated splenocytes. Resting splenocytes from MUC1 transgenic mice show the genomic MUC1 amplification product (Figure 4.0-3A, lane 5), verifying that we are looking at MUC1 transgenic mouse cells. Activated splenocytes from MUC1 transgenic mice show the processed RNA MUC1 amplification product when RT was added (Figure 4.0-3A, lane 9). In contrast, splenocytes from wild type mice show neither the MUC1 genomic nor processed RNA amplification products (Figure 4.0-3B, lanes 4, 5, 8, 9), verifying that the primers were not binding in mouse splenocytes non-specifically. Lanes 6, 7, 10, and 11 in both gels are control RT-PCR reactions with primers against a housekeeping gene. These results demonstrate that MUC1 transgenic splenoctyes do transcribe the MUC1 gene upon activation.

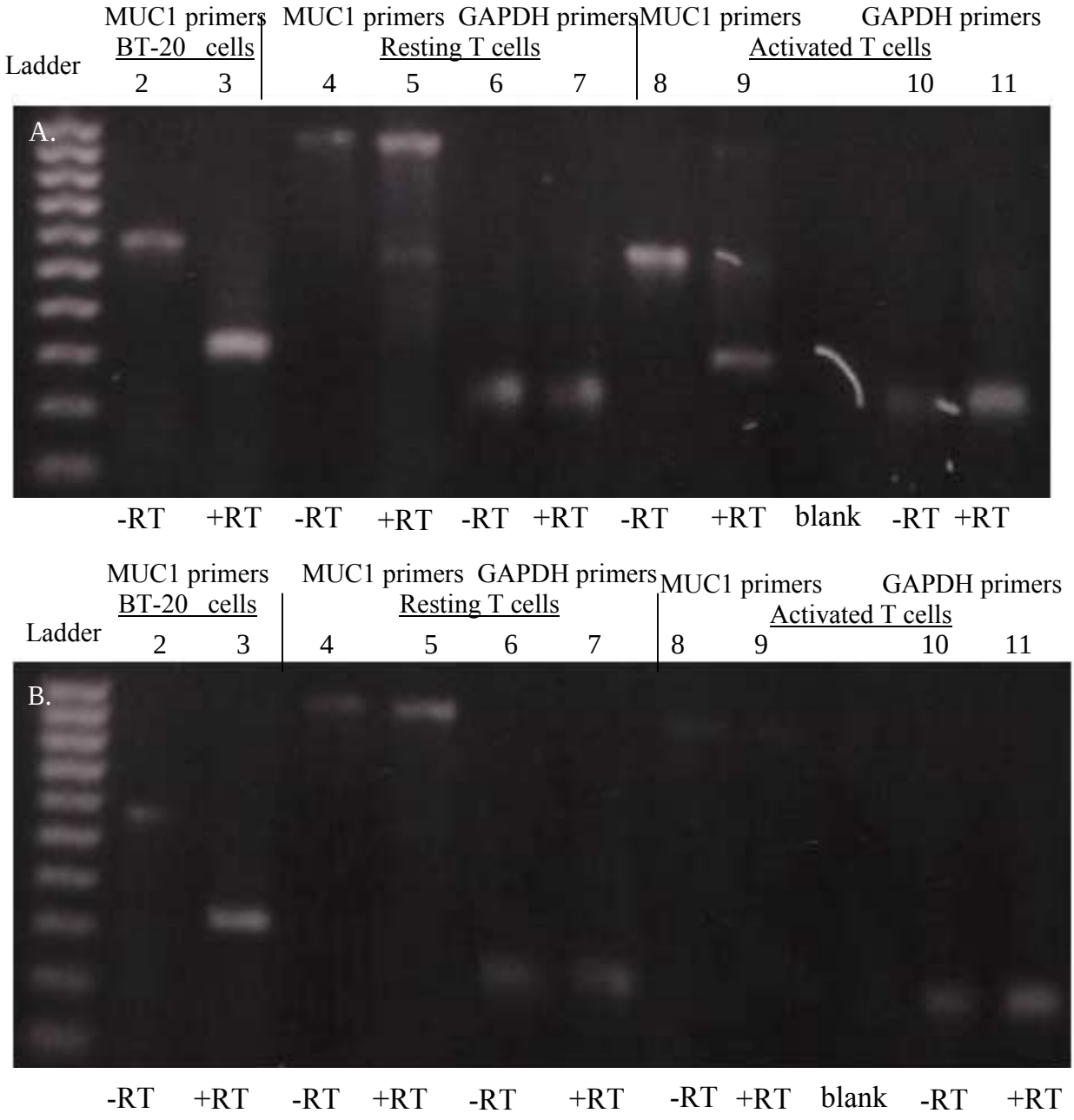

Figure 4.0-3 Detection of MUC1 transcript in resting and activated MUC1 transgenic and wild type mouse splenocytes by RT-PCR. Total RNA was collected from resting (lanes 4-7) or ConA activated (lanes 8-9, 10-11) MUC1 transgenic splenocytes (A) or wild type splenocytes (B). BT-20 cells (lanes 2 and 3) were run alongside splenocytes as a positive control. RT-PCR was performed using random hexamer primers and the cDNA was amplified with MUC1 specific primers (lanes 2-5, 8, 9) or with GAPDH specific primer (lanes 6, 7, 10, 11). The amplified MUC1 genomic fragment is 600bp, processed MUC1 RNA fragment is 341bp and the GAPDH fragment is 257bp.

As further confirmation that MUC1 messenger RNA is being made, we repeated the RT-PCR reactions on resting and activated MUC1 transgenic splenocytes using reverse transcriptase oligo(T) primers that specifically bind mRNA via the poly A tail. As before, we see MUC1 mRNA is expressed in activated MUC1 transgenic splenocytes (Figure 4.0-4).

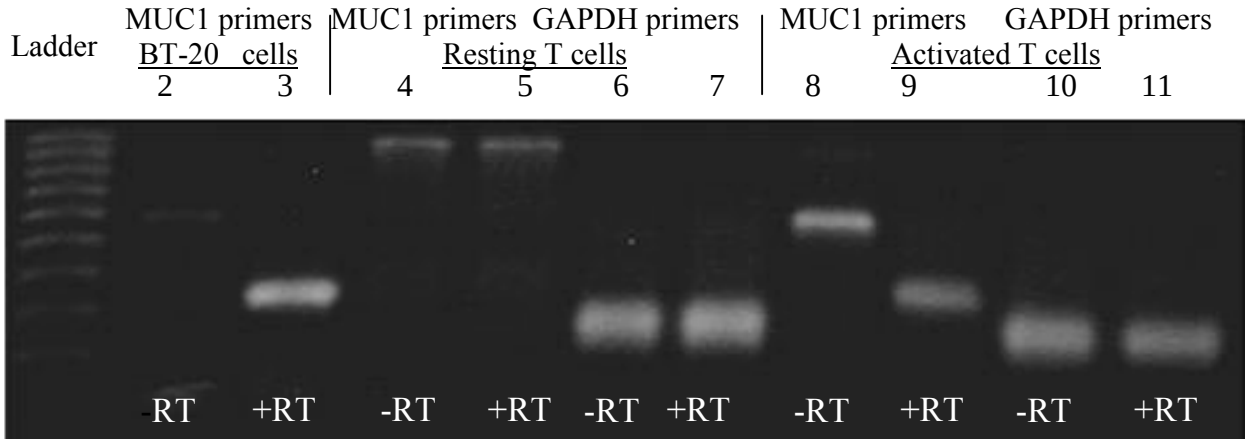

Figure 4.0-4 Detection of MUC1 messenger RNA in resting and activated MUC1 transgenic splenocytes by RT-PCR. Total RNA was collected from resting (lanes 4 – 7) or ConA activated (lanes 8 – 11) MUC1 transgenic splenocytes. BT-20 cells (lanes 2 and 3) were run alongside splenocytes as a positive control. RT-PCR was performed using oligo(T) primers and the cDNA was amplified with MUC1 specific primers (lanes 2-5, 8, 9) or with GAPDH specific primer (lanes 6, 7, 11, 12). The amplified MUC1 genomic fragment is 600bp, processed MUC1 mRNA fragment is 341bp and the GAPDH fragment is 257bp.

4.3.3 Intracellular flow cytometry for MUC1

Since we had observed that MUC1 mRNA was being made but that MUC1 protein was not expressed on the cell surface, we asked whether MUC1 protein was made but not transported to the cell surface. We first performed intracellular flow cytometry on permeabilized activated MUC1 transgenic cells, using the BT-20 tumor cell line as a positive control and wild type activated splenocytes as negative control. Resting and activated human PBMC were also analyzed for comparison. After a week of activation, dead cells were removed by gradient centrifugation and the remaining cells were analyzed for extracellular and intracellular MUC1 (Figure 4.0-5). The BT-20 cells (Figure 4.0-5A) show strong staining for both extracellular and

intracellular MUC1. There is a slight increase of intracellular staining above extracellular. Similarly, though to a much lesser extent, the activated human T cells (Figure 4.0-5B) also show definite extracellular staining with a slight increase in intracellular staining. The MUC1 transgenic (Figure 4.0-5C) and wild type (Figure 4.0-5D) T cells show no surface staining for MUC1. A slight shift is seen in intracellular staining, however this shift is seen in both transgenic and wild type mice. Since wild type mice do not contain the MUC1 gene, the observed shift in mouse T cells is likely non-specific. This data suggest that MUC1 protein is not being made in activated MUC1 transgenic mouse T cells.

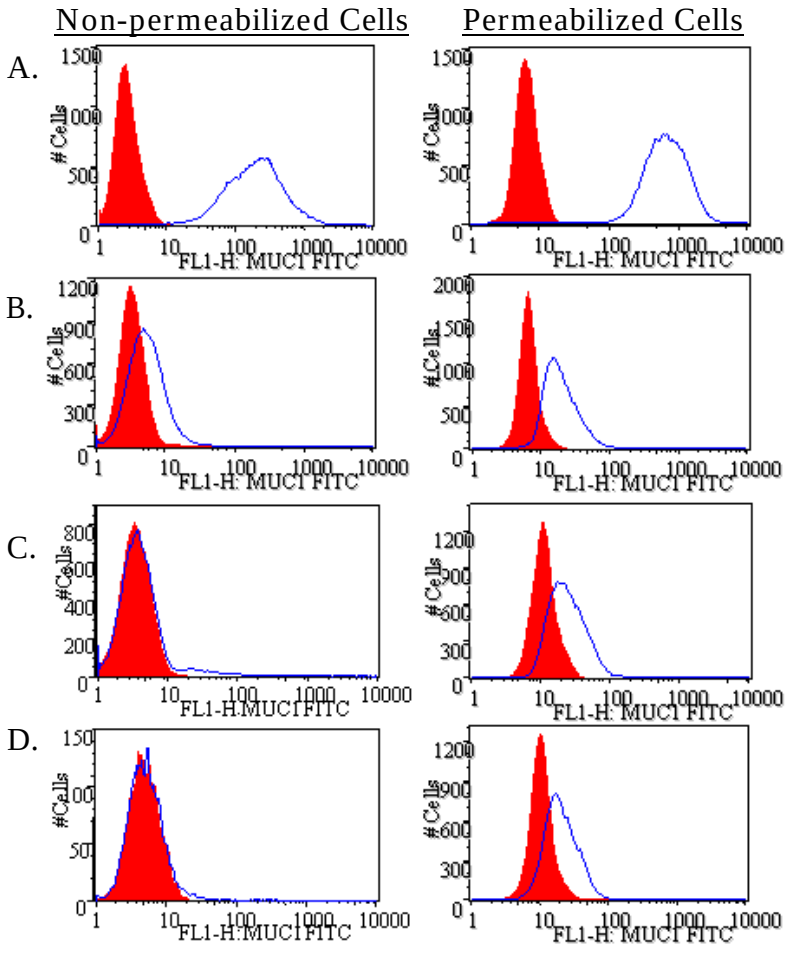

Figure 4.0-5 Extracellular and intracellular flow cytometry for MUC1 protein expression. (A) BT-20 cells are shown as a positive control for strong MUC1 expression. (B) Human PBMC, (C) MUC1 transgenic, and (D) wild type splenocytes were activated for 1 week, the live cells isolated by gradient centrifugation and stained for surface and cytosolic MUC1.

4.3.4 Immunoblotting for MUC1

In addition to intracellular flow cytometry we wanted to use another method to test for intracellular MUC1 in MUC1 transgenic splenocytes. Activated and resting wild type splenocytes, MUC1 transgenic splenocytes, human PBMC and BT-20 were immunoblotted for MUC1 (Figure 4.0-6). As expected BT-20 cells show a strong, high molecular weight MUC1 signal (lane 7); a comparable signal is not seen in any of the other lanes. There are some bands seen in the other lanes but these are all in molecular weight regions lower than expected for MUC1 (Figure 4.0-6). It is possible that MUC1 expressed by BT-20 cells is significantly bigger than that of PBMC and the MUC1 transgene. The DNA fragment used to generate these MUC1 transgenic mice (124) contains a 2.3kbp tandem repeat sequence (160), which would translate to a roughly 35 repeat VNTR region. Resting wild type (lane 4) and MUC1 transgenic (lane 5) splenocytes have virtually identical appearance. The pattern of bands in activated splenocytes from wild type (lane 1) and MUC1 transgenic (lane 2) mice are also similar but there may be an additional band in a doublet not seen in resting MUC1 transgenic splenocytes; however it was not unequivocally clear if this was MUC1.

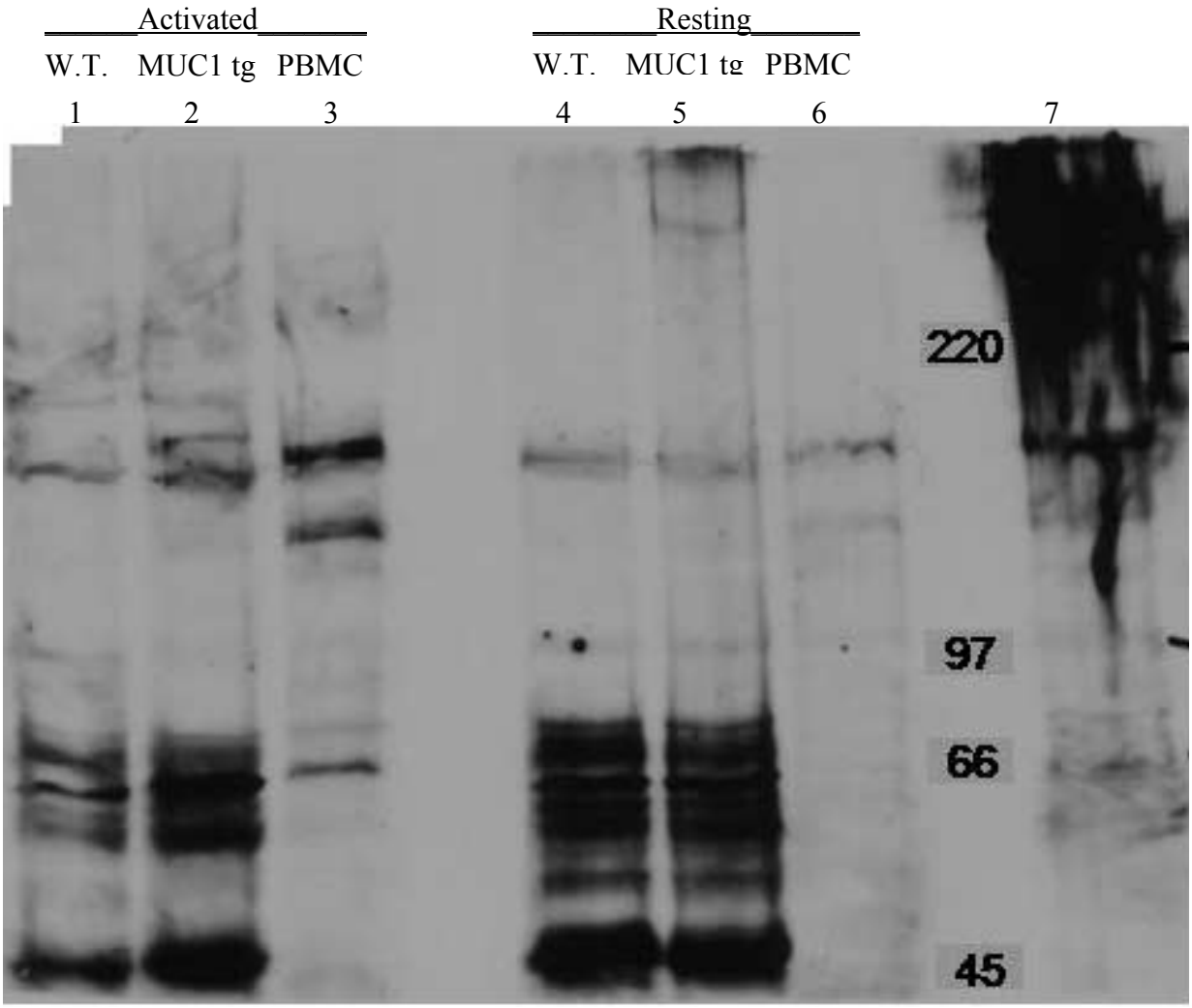

Figure 4.0-6 Immunoblotting for MUC1 in resting and activated wild type and MUC1 transgenic splenocytes, and human PBMC. Splenocytes and PBMC were activated for 6 days and each population verified to be activated T cells by flow cytometry. Activated cells were electrophoresed alongside resting cells and then immunoblotted with antibody against human MUC1 extracellular region. BT-20 cells were used as a positive control.

Since we wanted to look more convincingly for MUC1 in the transgenic splenocytes, and had expected to detect MUC1 in the activated PBMC, we repeated this experiment using twice as many resting and activated PBMC and MUC1 transgenic splenocytes per lane (Figure 4.0-7). Though MUC1 is still strongly detected from the much lower number of BT-20 cells (lane 5), we did not detect a high molecular weight band in activated PBMC (lane 2) or activated MUC1 transgenic splenocytes (lane 4). The pattern of bands is similar between resting and activated

cells, from both human PBMC (lanes 1 and 2) and MUC1 transgenic splenocytes (lanes 3 and 4) with no additional bands appearing following activation. It seems that the level of MUC1 expressed by activated human T cells as compared to tumor cells is not enough to pick up by immunoblotting, even though it is clearly seen by other means (see chapter 2.0). The possible doublet previously seen in the activated MUC1 transgenic splenocytes (Figure 4.0-6) is not evident here, despite the increased number of cells. It is likely that the possible MUC1 band seen previously in activated MUC1 transgenic splenocytes was artifactual. Combined with the intracellular flow cytometry data, we cannot show that T cells from MUC1-transgenic mice synthesize MUC1 from their transcribed mRNA.

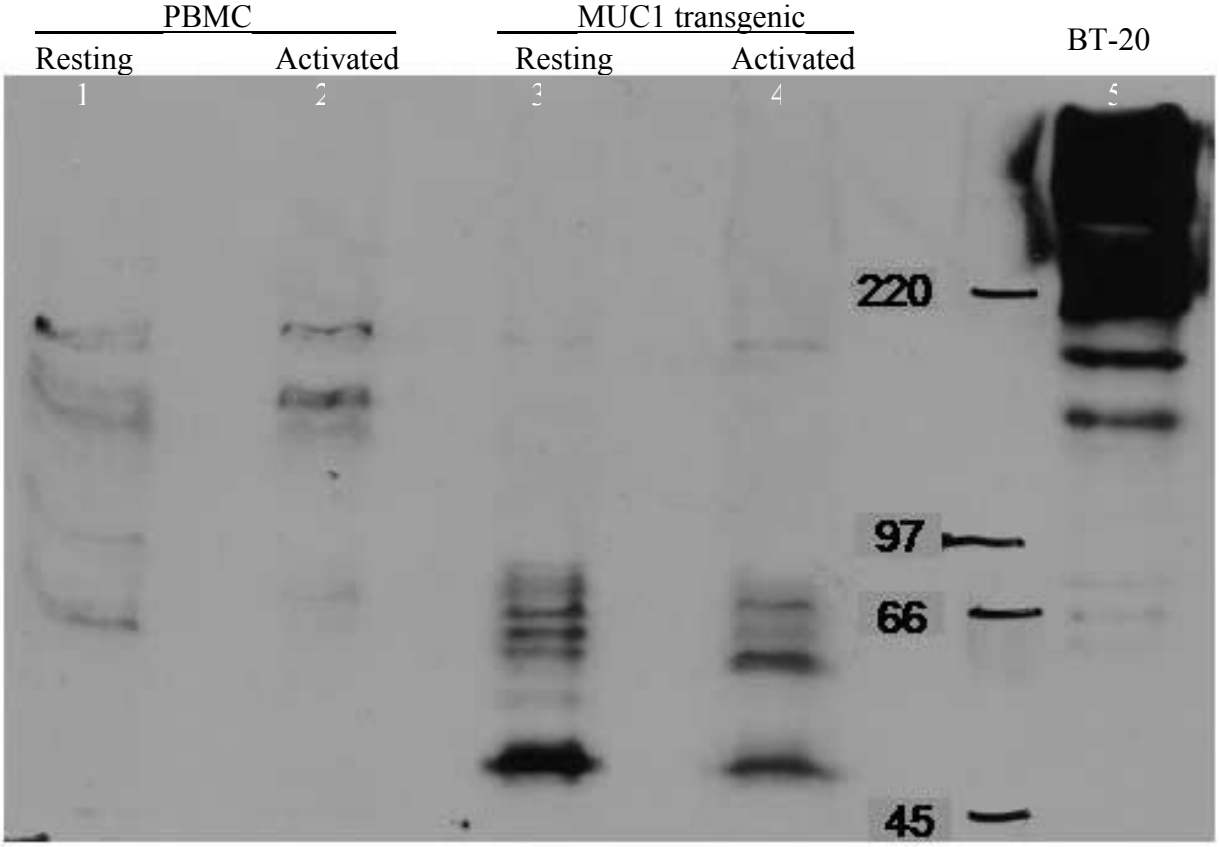

Figure 4.0-7 Immunoblotting for MUC1 in resting and activated human PBMC and MUC1 transgenic splenocytes. PBMC (lanes 1 and 2) and MUC1 transgenic splenocytes (lanes 3 and 4) were activated for 6 days and each population verified to be activated T cells by flow cytometry. Resting (lanes 1 and 3) and activated (lanes 2 and 4) cells were electrophoresed alongside BT-20 tumor cells (lane 5) as a positive control and then immunoblotted with antibody against human MUC1 extracellular region.

4.3.5 RT-PCR for MUC1/Y in mouse T cells

Since no MUC1 protein could be detected in activated MUC1 transgenic T cells, what is becoming of the MUC1 mRNA we detected? A possibility is that the transcript is being alternatively spliced to produce a different form of human MUC1, one that is not detected by antibodies against the tandem repeat region of MUC1. MUC1/Y can be expressed on the surface of human tumor cells (16). It is transcribed from the MUC1 gene but the VNTR region is spliced out before the message can be translated into protein. Since the antibodies we used to detect MUC1 are specific to peptide sequence in the VNTR region, we would not detect MUC1/Y in our flow cytometry or immunoblotting. To see if we could detect MUC1/Y message we designed primers specific to MUC1/Y and used them in RT-PCR of resting and activated MUC1 transgenic splenocytes. The HBL/Y2 cell line has been transfected with MUC1/Y and was used as our positive control. Resting and activated wild type splenocytes were used as the negative control (Figure 4.0-8).

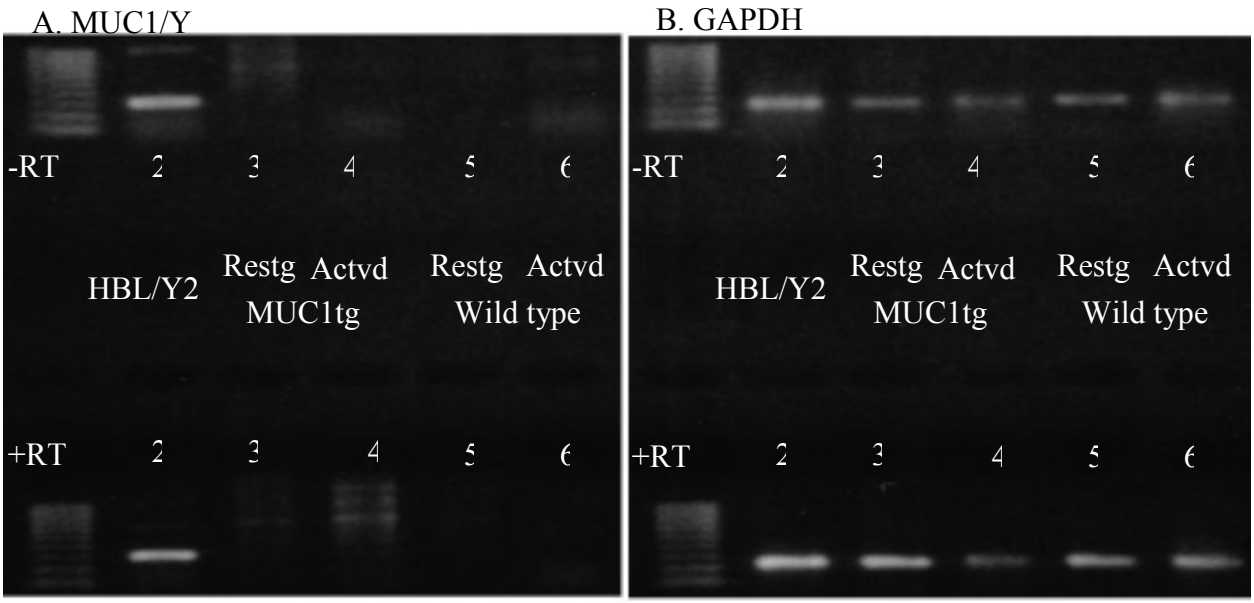

Figure 4.0-8 RT-PCR for MUC1/Y in resting and activated MUC1 transgenic and wild type splenocytes. HBL/Y2 cells (lane 2) were run alongside splenocytes as a positive control for MUC1/Y expression. Total RNA was collected from resting or ConA activated MUC1 transgenic splenocytes (lanes 3 and 4, respectively) and resting and activated wild type splenocytes (lanes 5 and 6, respectively). RT-PCR was performed using oligo(T) primers and the cDNA was amplified with (A) MUC1/Y specific primers or with (B) GAPDH specific primers. The –RT control amplification products are shown in the top row of each gel.

Figure 4.0-8A shows results from RT-PCR using the MUC1/Y primers. Control reactions without RT are shown in the top row and RT was added to reactions shown in the bottom row. Lane 1 contains a 100 - 1000 base pair ladder. Lane 2 in both rows contains RT-PCR amplification products from the HBL/Y2 cell line. The 313bp MUC1/Y amplification product is detected in the HBL/Y2 line in RT-PCR reactions done with and without the reverse transcriptase enzyme, due to the presence of the transfected construct. Lanes 3 and 4 are resting and activated MUC1 transgenic splenocytes, respectively. No MUC1/Y is detected with or without RT. This is repeated in the resting and activated wild type splenocytes, lanes 5 and 6 respectively. Figure 4.0-8B shows the same cell samples used in RT-PCR with primers against a housekeeping gene to check that the PCR reaction worked for each sample. These data demonstrate that MUC1/Y is not being produced in the activated MUC1 transgenic splenocytes

and so cannot account for the MUC1 message being detected while MUC1 protein was not found. There may be other alternatively spliced MUC1 gene products expressed in these cells but that remains to be determined.

4.4 Discussion

The need for a mouse model to study the effect of MUC1 on the migration of T cells led us to explore the MUC1 transgenic mouse. This model has been well-documented to express MUC1 in a manner similar to that seen in humans and so we expected that T cells from this model would also express MUC1. However, this turned out to not be the case. No surface MUC1 protein was observed by flow cytometry nor intracellular MUC1 protein by intracellular flow cytometry or immunoblotting. This was not due to ineffective activation or lack of transcription or processing of MUC1 mRNA. Since we could not find evidence that the full-length MUC1 protein was being translated from mRNA, we explored whether an alternatively spliced form of MUC1 was synthesized in the mouse cells. This was not the case for MUC1/Y though we did not rule out the possibility that other alternative splice variants could be made from mRNA in the transgenic mouse T cells.

Why would MUC1 be transcribed but the protein not sent to the cell surface? A likely possibility is that the mRNA is never translated to protein. This is consistent with our findings. However this would mean that the transgenic mouse T cells are uniquely unable to synthesize MUC1, as it is expressed on epithelial surfaces through out the mouse (124, 236). There have been efforts by other groups to study T cell expression by MUC1 transgenic mice. These groups have communicated either expression following stimulation (Dr. S. Gendler) or lack of expression by activated T cells (Dr. J. Taylor-Papadimitriou) using the same transgenic line. However, none of this work has yet been published. It is also possible that the transcribed

mRNA is being translated but the protein is secreted rather than put on the cell surface. However, this would be contrary to human T cell cultures in which MUC1 was reliably identified on the T cell surface while soluble MUC1 was barely detectable (Chapter 2.0).

Our findings that T cells from MUC1 transgenic mice do not express MUC1 in a manner similar to humans ruled out their use in studying the role of MUC1 in T cell migration. However it did raise a separate interesting question. Is the difference in MUC1 expression on T cells due to the model itself or is there a fundamental biological difference between mouse and human T cells? It is possible that whatever genetic elements are needed for T cell expression are simply not present in the material used to produce the transgenic mice. An alternative is that mouse T cells do not use Muc-1 protein as human T cells use MUC1. To address this possibility it is necessary to determine whether murine T cells express murine Muc-1 after activation. If they do then the failure of the transgenic mice to express MUC1 is likely simply an artifact of the model. If murine T cells do not express murine Muc-1 then this indicates that the function of MUC1 on human T cells is not needed by mouse T cells or that another molecule is used in place of Muc-1.

We began by searching for antibodies against the extracellular region of Muc-1 so that we could measure surface expression on mouse T cells. There have been studies examining Muc-1, but these have used either antibodies reactive to carbohydrate domains (244), and thus not specific to Muc-1 or reactive to the cytosolic tail so that surface expression is not explicit (240, 245). Our search yielded only one report claiming to have generated antibodies against extracellular Muc-1 (246). Attempts to verify this work using an antibody provided by Dr. Xing has thus far been inconclusive, in agreement with efforts by others (Dr. S. Gendler, personal communication). We have recently generated our own anti-Muc-1 antibodies by a novel chicken immunization strategy with Aves Labs, Inc. Work with these antibodies (data not shown) has

indicated that mouse T cells do express Muc-1 following allogeneic mixed leukocyte stimulation. Muc-1 can be detected at low levels early on and is maintained over one week, though the intensity decreases. An additional technique, perhaps biotinylation of surface proteins on activated mouse T cells followed by immunoprecipitation with the antibody reactive against MUC1/Muc-1 cytosolic tail, would be a useful confirmation of these results.

SUMMARY

The finding that MUC1 is expressed on the surface of T cells has expanded its physiological role, previously considered in the context of epithelial cells, to include playing a part in the function of T cells. We have here shown that MUC1 is expressed only on activated, and not resting T cells, following either *in vitro* or *in vivo* activation. MUC1 expression is then maintained over long time periods as the T cells acquire the memory phenotype. The glycosylation of MUC1 on T cells is similar to that on normal epithelial cells. Location of MUC1 on the T cell surface changes as cells are exposed to inflammatory conditions with MUC1 being focused to the leading edge, in contrast to other large or mucin like molecules on T cells that are moved to the trailing edge (the uropod). At the leading edge, and facilitated by its long, extended rod-like structure, MUC1 could be expected to be one of the first molecules to interact with the endothelium during T cell adhesion to blood vessels. Indeed we show in a model system with the Jurkat T cell leukemia cell line that MUC1 expression enhances binding to endothelium and the adhesion molecule ICAM-1 while inhibiting binding to E-selectin. The MUC1 cytosolic tail is constitutively phosphorylated in T cells, presumably as a result of cell-cell interactions, and this phosphorylation is maintained as T cells interact with resting endothelium. However, upon interaction with activated endothelium the phosphorylation of T

cell MUC1 drastically decreases. MUC1 expression on T cells and its interaction with endothelium also results in differential phosphorylation of at least three other proteins (39 kDa, 64-97 kDa and 191 kDa) with β-catenin tentatively identified as the 64-97 kDa protein. B-catenin is known to play a role in cell-cell adhesion and regulating gene transcription.

The expression of MUC1 by activated T cells and its influence on T cell adhesion and signaling support its role in the migration of activated T cells across the endothelium. One of the outcomes of this work is the possibility to block T cell migration by blocking the ability of MUC1 to bind to the endothelium. This would be especially of interest in alleviating the symptoms of diseases such as arthritis, diabetes, and other autoimmune disorders, as well as graft rejection, where activated T cells are the primary mediators. By preventing their adhesion to the endothelium, it may be possible to prevent their continuous migration to the diseased tissue. One approach would be to immunize the patient with MUC1 to generate a high titer of anti-MUC1 antibodies capable of blocking its function. This approach can be tried first in animal models. We have generated an antibody reactive with the mouse homologue of MUC1 (Muc-1) and used it to show that mouse cells also upregulate Muc1 expression after activation. The role of mouse Muc1 on T cells can now be examined *in vivo* in mouse models of autoimmune diseases.

BIBLIOGRAPHY

1. Carvalho, F., R. Seruca, L. David, A. Amorim, M. Seixas, E. Bennett, H. Clausen, and M. Sobrinho-Simoes. 1997. MUC1 gene polymorphism and gastric cancer--an epidemiological study. *Glycoconj J 14:107*.
2. Gendler, S. J., C. A. Lancaster, J. Taylor-Papadimitriou, T. Duhig, N. Peat, J. Burchell, L. Pemberton, E. N. Lalani, and D. Wilson. 1990. Molecular cloning and expression of human tumor-associated polymorphic epithelial mucin. *J Biol Chem 265:15286*.
3. Hilkens, J., and F. Buijs. 1988. Biosynthesis of MAM-6, an epithelial sialomucin. Evidence for involvement of a rare proteolytic cleavage step in the endoplasmic reticulum. *J Biol Chem 263:4215*.
4. Ligtenberg, M. J., L. Kruijshaar, F. Buijs, M. van Meijer, S. V. Litvinov, and J. Hilkens. 1992. Cell-associated episialin is a complex containing two proteins derived from a common precursor. *J Biol Chem 267:6171*.
5. Parry, S., H. S. Silverman, K. McDermott, A. Willis, M. A. Hollingsworth, and A. Harris. 2001. Identification of MUC1 proteolytic cleavage sites in vivo. *Biochem Biophys Res Commun 283:715*.
6. Litvinov, S. V., and J. Hilkens. 1993. The epithelial sialomucin, episialin, is sialylated during recycling. *J Biol Chem 268:21364*.
7. Pemberton, L. F., A. Rughetti, J. Taylor-Papadimitriou, and S. J. Gendler. 1996. The epithelial mucin MUC1 contains at least two discrete signals specifying membrane localization in cells. *J Biol Chem 271:2332*.
8. Fontenot, J. D., N. Tjandra, D. Bu, C. Ho, R. C. Montelaro, and O. J. Finn. 1993. Biophysical characterization of one-, two-, and three-tandem repeats of human mucin (muc-1) protein core. *Cancer Res 53:5386*.
9. Fontenot, J. D., S. V. Mariappan, P. Catasti, N. Domenech, O. J. Finn, and G. Gupta. 1995. Structure of a tumor associated antigen containing a tandemly repeated immunodominant epitope. *J Biomol Struct Dyn 13:245*.
10. Price, M. R., P. D. Rye, E. Petrakou, A. Murray, K. Brady, S. Imai, S. Haga, Y. Kiyozuka, D. Schol, M. F. Meulenbroek, F. G. Snijdewint, S. von Mensdorff-Pouilly, R. A. Verstraeten, P. Kenemans, A. Blockzjil, K. Nilsson, O. Nilsson, M. Reddish, M. R. Suresh, R. R. Koganty, S. Fortier, L. Baronic, A. Berg, M. B. Longenecker, J. Hilgers, and et al. 1998. Summary report on the ISOBM TD-4 Workshop: analysis of 56 monoclonal antibodies against the MUC1 mucin. San Diego, Calif., November 17-23, 1996. *Tumour Biol 19 Suppl 1:1*.

11. Ligtenberg, M. J., H. L. Vos, A. M. Gennissen, and J. Hilkens. 1990. Episialin, a carcinoma-associated mucin, is generated by a polymorphic gene encoding splice variants with alternative amino termini. *J Biol Chem 265:5573*.
12. Engelmann, K., S. E. Baldus, and F. G. Hanisch. 2001. Identification and topology of variant sequences within individual repeat domains of the human epithelial tumor mucin MUC1. *J Biol Chem 276:27764*.
13. Wreschner, D. H., M. Hareuveni, I. Tsarfaty, N. Smorodinsky, J. Horev, J. Zaretsky, P. Kotkes, M. Weiss, R. Lathe, A. Dion, and et al. 1990. Human epithelial tumor antigen cDNA sequences. Differential splicing may generate multiple protein forms. *Eur J Biochem 189:463*.
14. Ligtenberg, M. J., A. M. Gennissen, H. L. Vos, and J. Hilkens. 1991. A single nucleotide polymorphism in an exon dictates allele dependent differential splicing of episialin mRNA. *Nucleic Acids Res 19:297*.
15. Obermair, A., B. C. Schmid, M. Stimpfl, B. Fasching, O. Preyer, S. Leodolter, A. J. Crandon, and R. Zeillinger. 2001. Novel MUC1 splice variants are expressed in cervical carcinoma. *Gynecol Oncol 83:343*.
16. Zrihan-Licht, S., H. L. Vos, A. Baruch, O. Elroy-Stein, D. Sagiv, I. Keydar, J. Hilkens, and D. H. Wreschner. 1994. Characterization and molecular cloning of a novel MUC1 protein, devoid of tandem repeats, expressed in human breast cancer tissue. *Eur J Biochem 224:787*.
17. Baruch, A., M. Hartmann, S. Zrihan-Licht, S. Greenstein, M. Burstein, I. Keydar, M. Weiss, N. Smorodinsky, and D. H. Wreschner. 1997. Preferential expression of novel MUC1 tumor antigen isoforms in human epithelial tumors and their tumor-potentiating function. *Int J Cancer 71:741*.
18. Oosterkamp, H. M., L. Scheiner, M. C. Stefanova, K. O. Lloyd, and C. L. Finstad. 1997. Comparison of MUC-1 mucin expression in epithelial and non-epithelial cancer cell lines and demonstration of a new short variant form (MUC-1/Z). *Int J Cancer 72:87*.
19. Peterson, J. A., C. D. Scallan, R. L. Ceriani, and M. Hamosh. 2001. Structural and functional aspects of three major glycoproteins of the human milk fat globule membrane. *Adv Exp Med Biol 501:179*.
20. Patton, S. 2001. MUC1 and MUC-X, epithelial mucins of breast and milk. *Adv Exp Med Biol 501:35*.
21. McGuckin, M. A., P. L. Devine, L. E. Ramm, and B. G. Ward. 1994. Factors effecting the measurement of tumor-associated MUC1 mucins in serum. *Tumour Biol 15:33*.
22. Croce, M. V., M. T. Isla-Larrain, M. R. Price, and A. Segal-Eiras. 2001. Detection of circulating mammary mucin (Muc1) and MUC1 immune complexes (Muc1-CIC) in healthy women. *Int J Biol Markers 16:112*.
23. Smorodinsky, N., M. Weiss, M. L. Hartmann, A. Baruch, E. Harness, M. Yaakobovitz, I. Keydar, and D. H. Wreschner. 1996. Detection of a secreted MUC1/SEC protein by MUC1 isoform specific monoclonal antibodies. *Biochem Biophys Res Commun 228:115*.
24. Boshell, M., E. N. Lalani, L. Pemberton, J. Burchell, S. Gendler, and J. Taylor-Papadimitriou. 1992. The product of the human MUC1 gene when secreted by mouse cells transfected with the full-length cDNA lacks the cytoplasmic tail. *Biochem Biophys Res Commun 185:1*.
25. Hilkens, J., Ligtenberg, M.J.L., Litvinov, S., Vos, H.L., Gennissen, A.M.C., Buys, F., Hageman, P. 1991. Structure, processing, differential glycosylation and biology of

episialin. In *Breast Epithelial Antigens: Molecular Biology to Clinical Applications*. R. L. Ceriani, ed. Plenum Press, New York, p. 25.
26. Thathiah, A., C. P. Blobel, and D. D. Carson. 2003. Tumor Necrosis Factor-alpha Converting Enzyme/ADAM 17 Mediates MUC1 Shedding. *J Biol Chem 278:3386*.
27. Julian, J., and D. D. Carson. 2002. Formation of MUC1 metabolic complex is conserved in tumor-derived and normal epithelial cells. *Biochem Biophys Res Commun 293:1183*.
28. Hanisch, F. G., and S. Muller. 2000. MUC1: the polymorphic appearance of a human mucin. *Glycobiology 10:439*.
29. Wandall, H. H., H. Hassan, E. Mirgorodskaya, A. K. Kristensen, P. Roepstorff, E. P. Bennett, P. A. Nielsen, M. A. Hollingsworth, J. Burchell, J. Taylor-Papadimitriou, and H. Clausen. 1997. Substrate specificities of three members of the human UDP-N-acetyl-alpha-D-galactosamine:Polypeptide N-acetylgalactosaminyltransferase family, GalNAc-T1, -T2, and -T3. *J Biol Chem 272:23503*.
30. Muller, S., S. Goletz, N. Packer, A. Gooley, A. M. Lawson, and F. G. Hanisch. 1997. Localization of O-glycosylation sites on glycopeptide fragments from lactation-associated MUC1. All putative sites within the tandem repeat are glycosylation targets in vivo. *J Biol Chem 272:24780*.
31. Bennett, E. P., H. Hassan, U. Mandel, E. Mirgorodskaya, P. Roepstorff, J. Burchell, J. Taylor-Papadimitriou, M. A. Hollingsworth, G. Merkx, A. G. van Kessel, H. Eiberg, R. Steffensen, and H. Clausen. 1998. Cloning of a human UDP-N-acetyl-alpha-D-Galactosamine:polypeptide N-acetylgalactosaminyltransferase that complements other GalNAc-transferases in complete O-glycosylation of the MUC1 tandem repeat. *J Biol Chem 273:30472*.
32. Hanisch, F. G., S. Muller, H. Hassan, H. Clausen, N. Zachara, A. A. Gooley, H. Paulsen, K. Alving, and J. Peter-Katalinic. 1999. Dynamic epigenetic regulation of initial O-glycosylation by UDP-N-Acetylgalactosamine:Peptide N-acetylgalactosaminyltransferases. site-specific glycosylation of MUC1 repeat peptide influences the substrate qualities at adjacent or distant Ser/Thr positions. *J Biol Chem 274:9946*.
33. Dalziel, M., C. Whitehouse, I. McFarlane, I. Brockhausen, S. Gschmeissner, T. Schwientek, H. Clausen, J. M. Burchell, and J. Taylor-Papadimitriou. 2001. The relative activities of the C2GnT1 and ST3Gal-I glycosyltransferases determine O-glycan structure and expression of a tumor-associated epitope on MUC1. *J Biol Chem 276:11007*.
34. Hanisch, F. G., C. A. Reis, H. Clausen, and H. Paulsen. 2001. Evidence for glycosylation-dependent activities of polypeptide N-acetylgalactosaminyltransferases rGalNAc-T2 and -T4 on mucin glycopeptides. *Glycobiology 11:731*.
35. Butcher, E. C. 1991. Leukocyte-endothelial cell recognition: three (or more) steps to specificity and diversity. *Cell 67:1033*.
36. Carlos, T. M., and J. M. Harlan. 1994. Leukocyte-endothelial adhesion molecules. *Blood 84:2068*.
37. Springer, T. A. 1994. Traffic signals for lymphocyte recirculation and leukocyte emigration: the multistep paradigm. *Cell 76:301*.
38. Butcher, E. C., M. Williams, K. Youngman, L. Rott, and M. Briskin. 1999. Lymphocyte trafficking and regional immunity. *Adv Immunol 72:209*.
39. Fabbri, M., E. Bianchi, L. Fumagalli, and R. Pardi. 1999. Regulation of lymphocyte traffic by adhesion molecules. *Inflamm Res 48:239*.

40. von Andrian, U. H., and C. R. Mackay. 2000. T-cell function and migration. Two sides of the same coin. *N Engl J Med 343:1020*.
41. Kunkel, E. J., and E. C. Butcher. 2002. Chemokines and the tissue-specific migration of lymphocytes. *Immunity 16:1*.
42. Vestweber, D. 2003. Lymphocyte trafficking through blood and lymphatic vessels: more than just selectins, chemokines and integrins. *Eur J Immunol 33:1361*.
43. Jones, D. A., C. W. Smith, and L. V. McIntire. 1996. Leucocyte adhesion under flow conditions: principles important in tissue engineering. *Biomaterials 17:337*.
44. Etzioni, A., C. M. Doerschuk, and J. M. Harlan. 1999. Of man and mouse: leukocyte and endothelial adhesion molecule deficiencies. *Blood 94:3281*.
45. Imhof, B. A., B. Engelhardt, and M. Vadas. 2001. Novel mechanisms of the transendothelial migration of leukocytes. *Trends Immunol 22:411*.
46. Ley, K. 2003. The role of selectins in inflammation and disease. *Trends Mol Med 9:263*.
47. Kansas, G. S. 1996. Selectins and their ligands: current concepts and controversies. *Blood 88:3259*.
48. Watson, M. L., S. F. Kingsmore, G. I. Johnston, M. H. Siegelman, M. M. Le Beau, R. S. Lemons, N. S. Bora, T. A. Howard, I. L. Weissman, R. P. McEver, and et al. 1990. Genomic organization of the selectin family of leukocyte adhesion molecules on human and mouse chromosome 1. *J Exp Med 172:263*.
49. Ellies, L. G., M. Sperandio, G. H. Underhill, J. Yousif, M. Smith, J. J. Priatel, G. S. Kansas, K. Ley, and J. D. Marth. 2002. Sialyltransferase specificity in selectin ligand formation. *Blood 100:3618*.
50. Kanamori, A., N. Kojima, K. Uchimura, T. Muramatsu, T. Tamatani, M. C. Berndt, G. S. Kansas, and R. Kannagi. 2002. Distinct sulfation requirements of selectins disclosed using cells that support rolling mediated by all three selectins under shear flow. L-selectin prefers carbohydrate 6-sulfation totyrosine sulfation, whereas p-selectin does not. *J Biol Chem 277:32578*.
51. Vestweber, D., and J. E. Blanks. 1999. Mechanisms that regulate the function of the selectins and their ligands. *Physiol Rev 79:181*.
52. Puri, K. D., and T. A. Springer. 1996. A schiff base with mildly oxidized carbohydrate ligands stabilizes L-selectin and not P-selectin or E-selectin rolling adhesions in shear flow. *J Biol Chem 271:5404*.
53. Erbe, D. V., S. R. Watson, L. G. Presta, B. A. Wolitzky, C. Foxall, B. K. Brandley, and L. A. Lasky. 1993. P- and E-selectin use common sites for carbohydrate ligand recognition and cell adhesion. *J Cell Biol 120:1227*.
54. Bevilacqua, M. P., and R. M. Nelson. 1993. Selectins. *J Clin Invest 91:379*.
55. Bevilacqua, M. P., S. Stengelin, M. A. Gimbrone, Jr., and B. Seed. 1989. Endothelial leukocyte adhesion molecule 1: an inducible receptor for neutrophils related to complement regulatory proteins and lectins. *Science 243:1160*.
56. Erbe, D. V., B. A. Wolitzky, L. G. Presta, C. R. Norton, R. J. Ramos, D. K. Burns, J. M. Rumberger, B. N. Rao, C. Foxall, B. K. Brandley, and et al. 1992. Identification of an E-selectin region critical for carbohydrate recognition and cell adhesion. *J Cell Biol 119:215*.
57. Graves, B. J., R. L. Crowther, C. Chandran, J. M. Rumberger, S. Li, K. S. Huang, D. H. Presky, P. C. Familletti, B. A. Wolitzky, and D. K. Burns. 1994. Insight into E-

selectin/ligand interaction from the crystal structure and mutagenesis of the lec/EGF domains. *Nature 367:532*.
58. Weis, W. I. 1994. Lectins on a roll: the structure of E-selectin. *Structure 2:147*.
59. Martin, M. J., T. Feizi, C. Leteux, D. Pavlovic, V. E. Piskarev, and W. Chai. 2002. An investigation of the interactions of E-selectin with fuco-oligosaccharides of the blood group family. *Glycobiology 12:829*.
60. Maly, P., A. Thall, B. Petryniak, C. E. Rogers, P. L. Smith, R. M. Marks, R. J. Kelly, K. M. Gersten, G. Cheng, T. L. Saunders, S. A. Camper, R. T. Camphausen, F. X. Sullivan, Y. Isogai, O. Hindsgaul, U. H. von Andrian, and J. B. Lowe. 1996. The alpha(1,3)fucosyltransferase Fuc-TVII controls leukocyte trafficking through an essential role in L-, E-, and P-selectin ligand biosynthesis. *Cell 86:643*.
61. Lorenzon, P., E. Vecile, E. Nardon, E. Ferrero, J. M. Harlan, F. Tedesco, and A. Dobrina. 1998. Endothelial cell E- and P-selectin and vascular cell adhesion molecule-1 function as signaling receptors. *J Cell Biol 142:1381*.
62. Yoshida, M., W. F. Westlin, N. Wang, D. E. Ingber, A. Rosenzweig, N. Resnick, and M. A. Gimbrone, Jr. 1996. Leukocyte adhesion to vascular endothelium induces E-selectin linkage to the actin cytoskeleton. *J Cell Biol 133:445*.
63. Holness, C. L., and D. L. Simmons. 1994. Structural motifs for recognition and adhesion in members of the immunoglobulin superfamily. *J Cell Sci 107 (Pt 8):2065*.
64. Elangbam, C. S., C. W. Qualls, Jr., and R. R. Dahlgren. 1997. Cell adhesion molecules--update. *Vet Pathol 34:61*.
65. Wang, J., and T. A. Springer. 1998. Structural specializations of immunoglobulin superfamily members for adhesion to integrins and viruses. *Immunol Rev 163:197*.
66. Voraberger, G., R. Schafer, and C. Stratowa. 1991. Cloning of the human gene for intercellular adhesion molecule 1 and analysis of its 5'-regulatory region. Induction by cytokines and phorbol ester. *J Immunol 147:2777*.
67. Staunton, D. E., S. D. Marlin, C. Stratowa, M. L. Dustin, and T. A. Springer. 1988. Primary structure of ICAM-1 demonstrates interaction between members of the immunoglobulin and integrin supergene families. *Cell 52:925*.
68. Simmons, D., M. W. Makgoba, and B. Seed. 1988. ICAM, an adhesion ligand of LFA-1, is homologous to the neural cell adhesion molecule NCAM. *Nature 331:624*.
69. van de Stolpe, A., and P. T. van der Saag. 1996. Intercellular adhesion molecule-1. *J Mol Med 74:13*.
70. Miller, J., R. Knorr, M. Ferrone, R. Houdei, C. P. Carron, and M. L. Dustin. 1995. Intercellular adhesion molecule-1 dimerization and its consequences for adhesion mediated by lymphocyte function associated-1. *J Exp Med 182:1231*.
71. Bella, J., P. R. Kolatkar, C. W. Marlor, J. M. Greve, and M. G. Rossmann. 1998. The structure of the two amino-terminal domains of human ICAM-1 suggests how it functions as a rhinovirus receptor and as an LFA-1 integrin ligand. *Proc Natl Acad Sci U S A 95:4140*.
72. Casasnovas, J. M., T. Stehle, J. H. Liu, J. H. Wang, and T. A. Springer. 1998. A dimeric crystal structure for the N-terminal two domains of intercellular adhesion molecule-1. *Proc Natl Acad Sci U S A 95:4134*.
73. Pober, J. S., and R. S. Cotran. 1990. Cytokines and endothelial cell biology. *Physiol Rev 70:427*.

74. Hubbard, A. K., and R. Rothlein. 2000. Intercellular adhesion molecule-1 (ICAM-1) expression and cell signaling cascades. *Free Radic Biol Med 28:1379*.
75. Rothlein, R., M. L. Dustin, S. D. Marlin, and T. A. Springer. 1986. A human intercellular adhesion molecule (ICAM-1) distinct from LFA-1. *J Immunol 137:1270*.
76. Marlin, S. D., and T. A. Springer. 1987. Purified intercellular adhesion molecule-1 (ICAM-1) is a ligand for lymphocyte function-associated antigen 1 (LFA-1). *Cell 51:813*.
77. Diamond, M. S., D. E. Staunton, S. D. Marlin, and T. A. Springer. 1991. Binding of the integrin Mac-1 (CD11b/CD18) to the third immunoglobulin-like domain of ICAM-1 (CD54) and its regulation by glycosylation. *Cell 65:961*.
78. Wang, Q., and C. M. Doerschuk. 2002. The signaling pathways induced by neutrophil-endothelial cell adhesion. *Antioxid Redox Signal 4:39*.
79. Lawson, C., M. Ainsworth, M. Yacoub, and M. Rose. 1999. Ligation of ICAM-1 on endothelial cells leads to expression of VCAM-1 via a nuclear factor-kappaB-independent mechanism. *J Immunol 162:2990*.
80. Sano, H., N. Nakagawa, R. Chiba, K. Kurasawa, Y. Saito, and I. Iwamoto. 1998. Cross-linking of intercellular adhesion molecule-1 induces interleukin-8 and RANTES production through the activation of MAP kinases in human vascular endothelial cells. *Biochem Biophys Res Commun 250:694*.
81. Lowe, J. B. 2002. Glycosylation in the control of selectin counter-receptor structure and function. *Immunol Rev 186:19*.
82. Daniels, M. A., K. A. Hogquist, and S. C. Jameson. 2002. Sweet 'n' sour: the impact of differential glycosylation on T cell responses. *Nat Immunol 3:903*.
83. Moore, K. L., N. L. Stults, S. Diaz, D. F. Smith, R. D. Cummings, A. Varki, and R. P. McEver. 1992. Identification of a specific glycoprotein ligand for P-selectin (CD62) on myeloid cells. *J Cell Biol 118:445*.
84. Sako, D., X. J. Chang, K. M. Barone, G. Vachino, H. M. White, G. Shaw, G. M. Veldman, K. M. Bean, T. J. Ahern, B. Furie, and et al. 1993. Expression cloning of a functional glycoprotein ligand for P-selectin. *Cell 75:1179*.
85. Asa, D., L. Raycroft, L. Ma, P. A. Aeed, P. S. Kaytes, A. P. Elhammer, and J. G. Geng. 1995. The P-selectin glycoprotein ligand functions as a common human leukocyte ligand for P- and E-selectins. *J Biol Chem 270:11662*.
86. Li, F., P. P. Wilkins, S. Crawley, J. Weinstein, R. D. Cummings, and R. P. McEver. 1996. Post-translational modifications of recombinant P-selectin glycoprotein ligand-1 required for binding to P- and E-selectin. *J Biol Chem 271:3255*.
87. Wilkins, P. P., K. L. Moore, R. P. McEver, and R. D. Cummings. 1995. Tyrosine sulfation of P-selectin glycoprotein ligand-1 is required for high affinity binding to P-selectin. *J Biol Chem 270:22677*.
88. Pouyani, T., and B. Seed. 1995. PSGL-1 recognition of P-selectin is controlled by a tyrosine sulfation consensus at the PSGL-1 amino terminus. *Cell 83:333*.
89. Wilkins, P. P., R. P. McEver, and R. D. Cummings. 1996. Structures of the O-glycans on P-selectin glycoprotein ligand-1 from HL-60 cells. *J Biol Chem 271:18732*.
90. Somers, W. S., J. Tang, G. D. Shaw, and R. T. Camphausen. 2000. Insights into the molecular basis of leukocyte tethering and rolling revealed by structures of P- and E-selectin bound to SLe(X) and PSGL-1. *Cell 103:467*.
91. Snapp, K. R., C. E. Heitzig, L. G. Ellies, J. D. Marth, and G. S. Kansas. 2001. Differential requirements for the O-linked branching enzyme core 2 beta1-6-N-

glucosaminyltransferase in biosynthesis of ligands for E-selectin and P-selectin. *Blood 97:3806*.
92. Knibbs, R. N., R. A. Craig, S. Natsuka, A. Chang, M. Cameron, J. B. Lowe, and L. M. Stoolman. 1996. The fucosyltransferase FucT-VII regulates E-selectin ligand synthesis in human T cells. *J Cell Biol 133:911*.
93. Knibbs, R. N., R. A. Craig, P. Maly, P. L. Smith, F. M. Wolber, N. E. Faulkner, J. B. Lowe, and L. M. Stoolman. 1998. Alpha(1,3)-fucosyltransferase VII-dependent synthesis of P- and E-selectin ligands on cultured T lymphoblasts. *J Immunol 161:6305*.
94. Borges, E., W. Tietz, M. Steegmaier, T. Moll, R. Hallmann, A. Hamann, and D. Vestweber. 1997. P-selectin glycoprotein ligand-1 (PSGL-1) on T helper 1 but not on T helper 2 cells binds to P-selectin and supports migration into inflamed skin. *J Exp Med 185:573*.
95. Lim, Y. C., L. Henault, A. J. Wagers, G. S. Kansas, F. W. Luscinskas, and A. H. Lichtman. 1999. Expression of functional selectin ligands on Th cells is differentially regulated by IL-12 and IL-4. *J Immunol 162:3193*.
96. Carlow, D. A., S. Y. Corbel, M. J. Williams, and H. J. Ziltener. 2001. IL-2, -4, and -15 differentially regulate O-glycan branching and P-selectin ligand formation in activated CD8 T cells. *J Immunol 167:6841*.
97. Lim, Y. C., H. Xie, C. E. Come, S. I. Alexander, M. J. Grusby, A. H. Lichtman, and F. W. Luscinskas. 2001. IL-12, STAT4-dependent up-regulation of CD4(+) T cell core 2 beta-1,6-n-acetylglucosaminyltransferase, an enzyme essential for biosynthesis of P-selectin ligands. *J Immunol 167:4476*.
98. White, S. J., G. H. Underhill, M. H. Kaplan, and G. S. Kansas. 2001. Cutting edge: differential requirements for Stat4 in expression of glycosyltransferases responsible for selectin ligand formation in Th1 cells. *J Immunol 167:628*.
99. Barry, S. M., D. G. Zisoulis, J. H. Neal, N. A. Clipstone, and G. S. Kansas. 2003. Induction of FucT-VII by the Ras/MAP kinase cascade in Jurkat T cells. *Blood*.
100. Hogg, N., R. Henderson, B. Leitinger, A. McDowall, J. Porter, and P. Stanley. 2002. Mechanisms contributing to the activity of integrins on leukocytes. *Immunol Rev 186:164*.
101. Leitinger, B., and N. Hogg. 2000. From crystal clear ligand binding to designer I domains. *Nat Struct Biol 7:614*.
102. Hogg, N., and B. Leitinger. 2001. Shape and shift changes related to the function of leukocyte integrins LFA-1 and Mac-1. *J Leukoc Biol 69:893*.
103. Plow, E. F., T. A. Haas, L. Zhang, J. Loftus, and J. W. Smith. 2000. Ligand binding to integrins. *J Biol Chem 275:21785*.
104. Harris, E. S., T. M. McIntyre, S. M. Prescott, and G. A. Zimmerman. 2000. The leukocyte integrins. *J Biol Chem 275:23409*.
105. Rossetti, G., M. Collinge, J. R. Bender, R. Molteni, and R. Pardi. 2002. Integrin-dependent regulation of gene expression in leukocytes. *Immunol Rev 186:189*.
106. Leitinger, B., and N. Hogg. 2000. Effects of I domain deletion on the function of the beta2 integrin lymphocyte function-associated antigen-1. *Mol Biol Cell 11:677*.
107. van Kooyk, Y., and C. G. Figdor. 2000. Avidity regulation of integrins: the driving force in leukocyte adhesion. *Curr Opin Cell Biol 12:542*.
108. Constantin, G., M. Majeed, C. Giagulli, L. Piccio, J. Y. Kim, E. C. Butcher, and C. Laudanna. 2000. Chemokines trigger immediate beta2 integrin affinity and mobility

changes: differential regulation and roles in lymphocyte arrest under flow. *Immunity 13:759*.
109. Bianchi, E., S. Denti, A. Granata, G. Bossi, J. Geginat, A. Villa, L. Rogge, and R. Pardi. 2000. Integrin LFA-1 interacts with the transcriptional co-activator JAB1 to modulate AP-1 activity. *Nature 404:617*.
110. Porter, J. C., M. Bracke, A. Smith, D. Davies, and N. Hogg. 2002. Signaling through integrin LFA-1 leads to filamentous actin polymerization and remodeling, resulting in enhanced T cell adhesion. *J Immunol 168:6330*.
111. Rodriguez-Fernandez, J. L., M. Gomez, A. Luque, N. Hogg, F. Sanchez-Madrid, and C. Cabanas. 1999. The interaction of activated integrin lymphocyte function-associated antigen 1 with ligand intercellular adhesion molecule 1 induces activation and redistribution of focal adhesion kinase and proline-rich tyrosine kinase 2 in T lymphocytes. *Mol Biol Cell 10:1891*.
112. Schlaepfer, D. D., and T. Hunter. 1998. Integrin signalling and tyrosine phosphorylation: just the FAKs? *Trends Cell Biol 8:151*.
113. Porter, J. C., and N. Hogg. 1997. Integrin cross talk: activation of lymphocyte function-associated antigen-1 on human T cells alters alpha4beta1- and alpha5beta1-mediated function. *J Cell Biol 138:1437*.
114. Sanchez-Madrid, F., and M. A. del Pozo. 1999. Leukocyte polarization in cell migration and immune interactions. *Embo J 18:501*.
115. Gomez-Mouton, C., J. L. Abad, E. Mira, R. A. Lacalle, E. Gallardo, S. Jimenez-Baranda, I. Illa, A. Bernad, S. Manes, and A. C. Martinez. 2001. Segregation of leading-edge and uropod components into specific lipid rafts during T cell polarization. *Proc Natl Acad Sci U S A 98:9642*.
116. Serrador, J. M., M. Nieto, and F. Sanchez-Madrid. 1999. Cytoskeletal rearrangement during migration and activation of T lymphocytes. *Trends Cell Biol 9:228*.
117. Fais, S., and W. Malorni. 2003. Leukocyte uropod formation and membrane/cytoskeleton linkage in immune interactions. *J Leukoc Biol 73:556*.
118. Pelletier, A. J., L. J. van der Laan, P. Hildbrand, M. A. Siani, D. A. Thompson, P. E. Dawson, B. E. Torbett, and D. R. Salomon. 2000. Presentation of chemokine SDF-1 alpha by fibronectin mediates directed migration of T cells. *Blood 96:2682*.
119. Nieto, M., J. M. Frade, D. Sancho, M. Mellado, A. C. Martinez, and F. Sanchez-Madrid. 1997. Polarization of chemokine receptors to the leading edge during lymphocyte chemotaxis. *J Exp Med 186:153*.
120. del Pozo, M. A., C. Cabanas, M. C. Montoya, A. Ager, P. Sanchez-Mateos, and F. Sanchez-Madrid. 1997. ICAMs redistributed by chemokines to cellular uropods as a mechanism for recruitment of T lymphocytes. *J Cell Biol 137:493*.
121. del Pozo, M. A., P. Sanchez-Mateos, M. Nieto, and F. Sanchez-Madrid. 1995. Chemokines regulate cellular polarization and adhesion receptor redistribution during lymphocyte interaction with endothelium and extracellular matrix. Involvement of cAMP signaling pathway. *J Cell Biol 131:495*.
122. Ratner, S., W. S. Sherrod, and D. Lichlyter. 1997. Microtubule retraction into the uropod and its role in T cell polarization and motility. *J Immunol 159:1063*.
123. Serrador, J. M., J. L. Alonso-Lebrero, M. A. del Pozo, H. Furthmayr, R. Schwartz-Albiez, J. Calvo, F. Lozano, and F. Sanchez-Madrid. 1997. Moesin interacts with the

cytoplasmic region of intercellular adhesion molecule-3 and is redistributed to the uropod of T lymphocytes during cell polarization. *J Cell Biol 138:1409*.

124. Rowse, G. J., R. M. Tempero, M. L. VanLith, M. A. Hollingsworth, and S. J. Gendler. 1998. Tolerance and immunity to MUC1 in a human MUC1 transgenic murine model. *Cancer Res 58:315*.
125. Finn, O. J., K. R. Jerome, R. A. Henderson, G. Pecher, N. Domenech, J. Magarian-Blander, and S. M. Barratt-Boyes. 1995. MUC-1 epithelial tumor mucin-based immunity and cancer vaccines. *Immunol Rev 145:61*.
126. Lloyd, K. O., J. Burchell, V. Kudryashov, B. W. Yin, and J. Taylor-Papadimitriou. 1996. Comparison of O-linked carbohydrate chains in MUC-1 mucin from normal breast epithelial cell lines and breast carcinoma cell lines. Demonstration of simpler and fewer glycan chains in tumor cells. *J Biol Chem 271:33325*.
127. Agrawal, B., M. A. Reddish, M. J. Krantz, and B. M. Longenecker. 1995. Does pregnancy immunize against breast cancer? *Cancer Res 55:2257*.
128. Jerome, K. R., D. L. Barnd, K. M. Bendt, C. M. Boyer, J. Taylor-Papadimitriou, I. F. McKenzie, R. C. Bast, Jr., and O. J. Finn. 1991. Cytotoxic T-lymphocytes derived from patients with breast adenocarcinoma recognize an epitope present on the protein core of a mucin molecule preferentially expressed by malignant cells. *Cancer Res 51:2908*.
129. Feuerer, M., P. Beckhove, L. Bai, E. F. Solomayer, G. Bastert, I. J. Diel, C. Pedain, M. Oberniedermayr, V. Schirrmacher, and V. Umansky. 2001. Therapy of human tumors in NOD/SCID mice with patient-derived reactivated memory T cells from bone marrow. *Nat Med 7:452*.
130. Brossart, P., S. Wirths, G. Stuhler, V. L. Reichardt, L. Kanz, and W. Brugger. 2000. Induction of cytotoxic T-lymphocyte responses in vivo after vaccinations with peptide-pulsed dendritic cells. *Blood 96:3102*.
131. Kotera, Y., J. D. Fontenot, G. Pecher, R. S. Metzgar, and O. J. Finn. 1994. Humoral immunity against a tandem repeat epitope of human mucin MUC-1 in sera from breast, pancreatic, and colon cancer patients. *Cancer Res 54:2856*.
132. von Mensdorff-Pouilly, S., A. A. Verstraeten, P. Kenemans, F. G. Snijdewint, A. Kok, G. J. Van Kamp, M. A. Paul, P. J. Van Diest, S. Meijer, and J. Hilgers. 2000. Survival in early breast cancer patients is favorably influenced by a natural humoral immune response to polymorphic epithelial mucin. *J Clin Oncol 18:574*.
133. Domenech, N., R. A. Henderson, and O. J. Finn. 1995. Identification of an HLA-A11-restricted epitope from the tandem repeat domain of the epithelial tumor antigen mucin. *J Immunol 155:4766*.
134. Brossart, P., K. S. Heinrich, G. Stuhler, L. Behnke, V. L. Reichardt, S. Stevanovic, A. Muhm, H. G. Rammensee, L. Kanz, and W. Brugger. 1999. Identification of HLA-A2-restricted T-cell epitopes derived from the MUC1 tumor antigen for broadly applicable vaccine therapies. *Blood 93:4309*.
135. Carmon, L., K. M. El-Shami, A. Paz, S. Pascolo, E. Tzehoval, B. Tirosh, R. Koren, M. Feldman, M. Fridkin, F. A. Lemonnier, and L. Eisenbach. 2000. Novel breast-tumor-associated MUC1-derived peptides: characterization in Db-/- x beta2 microglobulin (beta2m) null mice transgenic for a chimeric HLA-A2.1/Db-beta2 microglobulin single chain. *Int J Cancer 85:391*.
136. Heukamp, L. C., S. H. van der Burg, J. W. Drijfhout, C. J. Melief, J. Taylor-Papadimitriou, and R. Offringa. 2001. Identification of three non-VNTR MUC1-derived

HLA-A*0201-restricted T-cell epitopes that induce protective anti-tumor immunity in HLA-A2/K(b)-transgenic mice. *Int J Cancer 91:385*.

137. Graham, R. A., J. M. Burchell, P. Beverley, and J. Taylor-Papadimitriou. 1996. Intramuscular immunisation with MUC1 cDNA can protect C57 mice challenged with MUC1-expressing syngeneic mouse tumour cells. *Int J Cancer 65:664*.
138. Tempero, R. M., M. L. VanLith, K. Morikane, G. J. Rowse, S. J. Gendler, and M. A. Hollingsworth. 1998. CD4+ lymphocytes provide MUC1-specific tumor immunity in vivo that is undetectable in vitro and is absent in MUC1 transgenic mice. *J Immunol 161:5500*.
139. Acres, B., V. Apostolopoulos, J. M. Balloul, D. Wreschner, P. X. Xing, D. Ali-Hadji, N. Bizouarne, M. P. Kieny, and I. F. McKenzie. 2000. MUC1-specific immune responses in human MUC1 transgenic mice immunized with various human MUC1 vaccines. *Cancer Immunol Immunother 48:588*.
140. Soares, M. M., V. Mehta, and O. J. Finn. 2001. Three different vaccines based on the 140-amino acid MUC1 peptide with seven tandemly repeated tumor-specific epitopes elicit distinct immune effector mechanisms in wild-type versus MUC1-transgenic mice with different potential for tumor rejection. *J Immunol 166:6555*.
141. Agrawal, B., M. J. Krantz, J. Parker, and B. M. Longenecker. 1998. Expression of MUC1 mucin on activated human T cells: implications for a role of MUC1 in normal immune regulation. *Cancer Res 58:4079*.
142. Chang, J. F., H. L. Zhao, J. Phillips, and G. Greenburg. 2000. The epithelial mucin, MUC1, is expressed on resting T lymphocytes and can function as a negative regulator of T cell activation. *Cell Immunol 201:83*.
143. Treon, S. P., P. Maimonis, D. Bua, G. Young, N. Raje, J. Mollick, D. Chauhan, Y. T. Tai, T. Hideshima, Y. Shima, J. Hilgers, S. von Mensdorff-Pouilly, A. R. Belch, L. M. Pilarski, and K. C. Anderson. 2000. Elevated soluble MUC1 levels and decreased anti-MUC1 antibody levels in patients with multiple myeloma. *Blood 96:3147*.
144. Delsol, G., K. C. Gatter, H. Stein, W. N. Erber, K. A. Pulford, K. Zinne, and D. Y. Mason. 1984. Human lymphoid cells express epithelial membrane antigen. Implications for diagnosis of human neoplasms. *Lancet 2:1124*.
145. Chadburn, A., G. Inghirami, and D. M. Knowles. 1992. The kinetics and temporal expression of T-cell activation-associated antigens CD15 (LeuM1), CD30 (Ki-1), EMA, and CD11c (LeuM5) by benign activated T cells. *Hematol Pathol 6:193*.
146. Fattorossi, A., A. Battaglia, P. Malinconico, A. Stoler, L. Andreocci, D. Parente, A. Coscarella, N. Maggiano, A. Perillo, L. Pierelli, and G. Scambia. 2002. Constitutive and inducible expression of the epithelial antigen MUC1 (CD227) in human T cells. *Exp Cell Res 280:107*.
147. Wykes, M., K. P. MacDonald, M. Tran, R. J. Quin, P. X. Xing, S. J. Gendler, D. N. Hart, and M. A. McGuckin. 2002. MUC1 epithelial mucin (CD227) is expressed by activated dendritic cells. *J Leukoc Biol 72:692*.
148. Correa, I., T. Plunkett, A. Vlad, A. Mungul, J. Candelora-Kettel, J. M. Burchell, J. Taylor-Papadimitriou, and O. J. Finn. 2003. Form and pattern of MUC1 expression on T cells activated in vivo or in vitro suggests a function in T-cell migration. *Immunology 108:32*.
149. Blockzjil, A., K. Nilsson, and O. Nilsson. 1998. Epitope characterization of MUC1 antibodies. *Tumour Biol 19 Suppl 1:46*.

150. Burchell, J., and J. Taylor-Papadimitriou. 1993. Effect of modification of carbohydrate side chains on the reactivity of antibodies with core-protein epitopes of the MUC1 gene product. *Epithelial Cell Biol 2:155*.
151. Wang, X. Y., J. R. Ostberg, and E. A. Repasky. 1999. Effect of fever-like whole-body hyperthermia on lymphocyte spectrin distribution, protein kinase C activity, and uropod formation. *J Immunol 162:3378*.
152. Lee, J. K., and E. A. Repasky. 1987. Cytoskeletal polarity in mammalian lymphocytes in situ. *Cell Tissue Res 247:195*.
153. Maki, W., R. E. Morales, V. A. Carroll, W. G. Telford, R. N. Knibbs, L. M. Stoolman, and S. T. Hwang. 2002. CCR6 colocalizes with CD18 and enhances adhesion to activated endothelial cells in CCR6-transduced Jurkat T cells. *J Immunol 169:2346*.
154. Hilkens, J., and M. Boer. 1998. Monoclonal antibodies against the nonmucin domain of MUC1/episialin. *Tumour Biol 19 Suppl 1:67*.
155. Bierhuizen, M. F., and M. Fukuda. 1992. Expression cloning of a cDNA encoding UDP-GlcNAc:Gal beta 1-3-GalNAc-R (GlcNAc to GalNAc) beta 1-6GlcNAc transferase by gene transfer into CHO cells expressing polyoma large tumor antigen. *Proc Natl Acad Sci U S A 89:9326*.
156. Bierhuizen, M. F., M. G. Mattei, and M. Fukuda. 1993. Expression of the developmental I antigen by a cloned human cDNA encoding a member of a beta-1,6-N-acetylglucosaminyltransferase gene family. *Genes Dev 7:468*.
157. Schwientek, T., J. C. Yeh, S. B. Levery, B. Keck, G. Merkx, A. G. van Kessel, M. Fukuda, and H. Clausen. 2000. Control of O-glycan branch formation. Molecular cloning and characterization of a novel thymus-associated core 2 beta1, 6-n-acetylglucosaminyltransferase. *J Biol Chem 275:11106*.
158. Zotter, S., P. C. Hageman, A. Lossnitzer, W. J. Mooi, and J. Hilgers. 1988. Tissue and tumour distribution of human polymorphic epithelial mucin. *Cancer Rev 11-12:55*.
159. Girling, A., J. Bartkova, J. Burchell, S. Gendler, C. Gillett, and J. Taylor-Papadimitriou. 1989. A core protein epitope of the polymorphic epithelial mucin detected by the monoclonal antibody SM-3 is selectively exposed in a range of primary carcinomas. *Int J Cancer 43:1072*.
160. Peat, N., S. J. Gendler, N. Lalani, T. Duhig, and J. Taylor-Papadimitriou. 1992. Tissue-specific expression of a human polymorphic epithelial mucin (MUC1) in transgenic mice. *Cancer Res 52:1954*.
161. Sikut, R., A. Sikut, K. Zhang, D. Baeckstrom, and G. C. Hansson. 1998. Reactivity of antibodies with highly glycosylated MUC1 mucins from colon carcinoma cells and bile. *Tumour Biol 19 Suppl 1:122*.
162. Hanisch, F. G., G. Uhlenbruck, J. Peter-Katalinic, H. Egge, J. Dabrowski, and U. Dabrowski. 1989. Structures of neutral O-linked polylactosaminoglycans on human skim milk mucins. A novel type of linearly extended poly-N-acetyllactosamine backbones with Gal beta(1-4)GlcNAc beta(1-6) repeating units. *J Biol Chem 264:872*.
163. Hull, S. R., A. Bright, K. L. Carraway, M. Abe, D. F. Hayes, and D. W. Kufe. 1989. Oligosaccharide differences in the DF3 sialomucin antigen from normal human milk and the BT-20 human breast carcinoma cell line. *Cancer Commun 1:261*.
164. Piller, F., V. Piller, R. I. Fox, and M. Fukuda. 1988. Human T-lymphocyte activation is associated with changes in O-glycan biosynthesis. *J Biol Chem 263:15146*.

165. Epenetos, A. A., V. Hird, H. Lambert, P. Mason, and C. Coulter. 2000. Long term survival of patients with advanced ovarian cancer treated with intraperitoneal radioimmunotherapy. *Int J Gynecol Cancer 10:44*.
166. Vezys, V., S. Olson, and L. Lefrancois. 2000. Expression of intestine-specific antigen reveals novel pathways of CD8 T cell tolerance induction. *Immunity 12:505*.
167. Agrawal, B., M. J. Krantz, M. A. Reddish, and B. M. Longenecker. 1998. Cancer-associated MUC1 mucin inhibits human T-cell proliferation, which is reversible by IL-2. *Nat Med 4:43*.
168. Chan, A. K., D. C. Lockhart, W. von Bernstorff, R. A. Spanjaard, H. G. Joo, T. J. Eberlein, and P. S. Goedegebuure. 1999. Soluble MUC1 secreted by human epithelial cancer cells mediates immune suppression by blocking T-cell activation. *Int J Cancer 82:721*.
169. Paul, S., N. Bizouarne, A. Paul, M. R. Price, G. C. Hansson, M. P. Kieny, and R. B. Acres. 1999. Lack of evidence for an immunosuppressive role for MUC1. *Cancer Immunol Immunother 48:22*.
170. van de Wiel-van Kemenade, E., M. J. Ligtenberg, A. J. de Boer, F. Buijs, H. L. Vos, C. J. Melief, J. Hilkens, and C. G. Figdor. 1993. Episialin (MUC1) inhibits cytotoxic lymphocyte-target cell interaction. *J Immunol 151:767*.
171. Kondo, K., N. Kohno, A. Yokoyama, and K. Hiwada. 1998. Decreased MUC1 expression induces E-cadherin-mediated cell adhesion of breast cancer cell lines. *Cancer Res 58:2014*.
172. McDermott, K. M., P. R. Crocker, A. Harris, M. D. Burdick, Y. Hinoda, T. Hayashi, K. Imai, and M. A. Hollingsworth. 2001. Overexpression of MUC1 reconfigures the binding properties of tumor cells. *Int J Cancer 94:783*.
173. Wesseling, J., S. W. van der Valk, H. L. Vos, A. Sonnenberg, and J. Hilkens. 1995. Episialin (MUC1) overexpression inhibits integrin-mediated cell adhesion to extracellular matrix components. *J Cell Biol 129:255*.
174. Lowin-Kropf, B., V. S. Shapiro, and A. Weiss. 1998. Cytoskeletal polarization of T cells is regulated by an immunoreceptor tyrosine-based activation motif-dependent mechanism. *J Cell Biol 140:861*.
175. Hyduk, S. J., and M. I. Cybulsky. 2002. Alpha 4 integrin signaling activates phosphatidylinositol 3-kinase and stimulates T cell adhesion to intercellular adhesion molecule-1 to a similar extent as CD3, but induces a distinct rearrangement of the actin cytoskeleton. *J Immunol 168:696*.
176. del Pozo, M. A., M. Vicente-Manzanares, R. Tejedor, J. M. Serrador, and F. Sanchez-Madrid. 1999. Rho GTPases control migration and polarization of adhesion molecules and cytoskeletal ERM components in T lymphocytes. *Eur J Immunol 29:3609*.
177. Campanero, M. R., P. Sanchez-Mateos, M. A. del Pozo, and F. Sanchez-Madrid. 1994. ICAM-3 regulates lymphocyte morphology and integrin-mediated T cell interaction with endothelial cell and extracellular matrix ligands. *J Cell Biol 127:867*.
178. Okabe, S., S. Fukuda, and H. E. Broxmeyer. 2002. Activation of Wiskott-Aldrich syndrome protein and its association with other proteins by stromal cell-derived factor-1alpha is associated with cell migration in a T-lymphocyte line. *Exp Hematol 30:761*.
179. Sanchez-Mateos, P., M. R. Campanero, M. A. del Pozo, and F. Sanchez-Madrid. 1995. Regulatory role of CD43 leukosialin on integrin-mediated T-cell adhesion to endothelial

and extracellular matrix ligands and its polar redistribution to a cellular uropod. *Blood 86:2228*.
180. Rosenman, S. J., A. A. Ganji, T. F. Tedder, and W. M. Gallatin. 1993. Syn-capping of human T lymphocyte adhesion/activation molecules and their redistribution during interaction with endothelial cells. *J Leukoc Biol 53:1*.
181. Ramachandran, V., M. U. Nollert, H. Qiu, W. J. Liu, R. D. Cummings, C. Zhu, and R. P. McEver. 1999. Tyrosine replacement in P-selectin glycoprotein ligand-1 affects distinct kinetic and mechanical properties of bonds with P- and L-selectin. *Proc Natl Acad Sci U S A 96:13771*.
182. Wesseling, J., S. W. van der Valk, and J. Hilkens. 1996. A mechanism for inhibition of E-cadherin-mediated cell-cell adhesion by the membrane-associated mucin episialin/MUC1. *Mol Biol Cell 7:565*.
183. Nath, D., A. Hartnell, L. Happerfield, D. W. Miles, J. Burchell, J. Taylor-Papadimitriou, and P. R. Crocker. 1999. Macrophage-tumour cell interactions: identification of MUC1 on breast cancer cells as a potential counter-receptor for the macrophage-restricted receptor, sialoadhesin. *Immunology 98:213*.
184. Kohem, C. L., R. I. Brezinschek, H. Wisbey, C. Tortorella, P. E. Lipsky, and N. Oppenheimer-Marks. 1996. Enrichment of differentiated CD45RBdim,CD27- memory T cells in the peripheral blood, synovial fluid, and synovial tissue of patients with rheumatoid arthritis. *Arthritis Rheum 39:844*.
185. To, S. S., P. M. Newman, V. J. Hyland, B. G. Robinson, and L. Schrieber. 1996. Regulation of adhesion molecule expression by human synovial microvascular endothelial cells in vitro. *Arthritis Rheum 39:467*.
186. Hilkens, J., M. J. Ligtenberg, H. L. Vos, and S. V. Litvinov. 1992. Cell membrane-associated mucins and their adhesion-modulating property. *Trends Biochem Sci 17:359*.
187. Ligtenberg, M. J., F. Buijs, H. L. Vos, and J. Hilkens. 1992. Suppression of cellular aggregation by high levels of episialin. *Cancer Res 52:2318*.
188. Hudson, M. J., G. W. Stamp, M. A. Hollingsworth, M. Pignatelli, and E. N. Lalani. 1996. MUC1 expressed in PanC1 cells decreases adhesion to type 1 collagen but increases contraction in collagen lattices. *Am J Pathol 148:951*.
189. Regimbald, L. H., L. M. Pilarski, B. M. Longenecker, M. A. Reddish, G. Zimmermann, and J. C. Hugh. 1996. The breast mucin MUCI as a novel adhesion ligand for endothelial intercellular adhesion molecule 1 in breast cancer. *Cancer Res 56:4244*.
190. Kam, J. L., L. H. Regimbald, J. H. Hilgers, P. Hoffman, M. J. Krantz, B. M. Longenecker, and J. C. Hugh. 1998. MUC1 synthetic peptide inhibition of intercellular adhesion molecule-1 and MUC1 binding requires six tandem repeats. *Cancer Res 58:5577*.
191. Pandey, P., S. Kharbanda, and D. Kufe. 1995. Association of the DF3/MUC1 breast cancer antigen with Grb2 and the Sos/Ras exchange protein. *Cancer Res 55:4000*.
192. Quin, R. J., and M. A. McGuckin. 2000. Phosphorylation of the cytoplasmic domain of the MUC1 mucin correlates with changes in cell-cell adhesion. *Int J Cancer 87:499*.
193. Zrihan-Licht, S., A. Baruch, O. Elroy-Stein, I. Keydar, and D. H. Wreschner. 1994. Tyrosine phosphorylation of the MUC1 breast cancer membrane proteins. Cytokine receptor-like molecules. *FEBS Lett 356:130*.

194. Meerzaman, D., P. X. Xing, and K. C. Kim. 2000. Construction and characterization of a chimeric receptor containing the cytoplasmic domain of MUC1 mucin. *Am J Physiol Lung Cell Mol Physiol 278:L625*.
195. Yamamoto, M., A. Bharti, Y. Li, and D. Kufe. 1997. Interaction of the DF3/MUC1 breast carcinoma-associated antigen and beta-catenin in cell adhesion. *J Biol Chem 272:12492*.
196. Schroeder, J. A., M. C. Thompson, M. M. Gardner, and S. J. Gendler. 2001. Transgenic MUC1 interacts with epidermal growth factor receptor and correlates with mitogen-activated protein kinase activation in the mouse mammary gland. *J Biol Chem 276:13057*.
197. Li, Y., H. Kuwahara, J. Ren, G. Wen, and D. Kufe. 2001. The c-Src tyrosine kinase regulates signaling of the human DF3/MUC1 carcinoma-associated antigen with GSK3 beta and beta-catenin. *J Biol Chem 276:6061*.
198. Li, Y., J. Ren, W. Yu, Q. Li, H. Kuwahara, L. Yin, K. L. Carraway, 3rd, and D. Kufe. 2001. The epidermal growth factor receptor regulates interaction of the human DF3/MUC1 carcinoma antigen with c-Src and beta-catenin. *J Biol Chem 276:35239*.
199. Gonzaez-Guerrico, A. M., E. G. Cafferata, M. Radrizzani, F. Marcucci, D. Gruenert, O. H. Pivetta, R. R. Favaloro, R. Laguens, S. V. Perrone, G. C. Gallo, and T. A. Santa-Coloma. 2002. Tyrosine kinase c-Src constitutes a bridge between cystic fibrosis transmembrane regulator channel failure and MUC1 overexpression in cystic fibrosis. *J Biol Chem 277:17239*.
200. Meerzaman, D., P. S. Shapiro, and K. C. Kim. 2001. Involvement of the MAP kinase ERK2 in MUC1 mucin signaling. *Am J Physiol Lung Cell Mol Physiol 281:L86*.
201. Li, Y., and D. Kufe. 2001. The Human DF3/MUC1 carcinoma-associated antigen signals nuclear localization of the catenin p120(ctn). *Biochem Biophys Res Commun 281:440*.
202. Schroeder, J. A., M. C. Adriance, M. C. Thompson, T. D. Camenisch, and S. J. Gendler. 2003. MUC1 alters beta-catenin-dependent tumor formation and promotes cellular invasion. *Oncogene 22:1324*.
203. Li, Y., A. Bharti, D. Chen, J. Gong, and D. Kufe. 1998. Interaction of glycogen synthase kinase 3beta with the DF3/MUC1 carcinoma-associated antigen and beta-catenin. *Mol Cell Biol 18:7216*.
204. Ren, J., Y. Li, and D. Kufe. 2002. Protein kinase C delta regulates function of the DF3/MUC1 carcinoma antigen in beta-catenin signaling. *J Biol Chem 277:17616*.
205. Li, Y., W. Chen, J. Ren, W. H. Yu, Q. Li, K. Yoshida, and D. Kufe. 2003. DF3/MUC1 signaling in multiple myeloma cells is regulated by interleukin-7. *Cancer Biol Ther 2:37*.
206. Wen, Y., T. C. Caffrey, M. J. Wheelock, K. R. Johnson, and M. A. Hollingsworth. 2003. Nuclear association of the cytoplasmic tail of MUC1 and {beta}-catenin. *J Biol Chem*.
207. Carraway, K. L., V. P. Ramsauer, B. Haq, and C. A. Carothers Carraway. 2003. Cell signaling through membrane mucins. *Bioessays 25:66*.
208. Yao, L., J. Pan, H. Setiadi, K. D. Patel, and R. P. McEver. 1996. Interleukin 4 or oncostatin M induces a prolonged increase in P-selectin mRNA and protein in human endothelial cells. *J Exp Med 184:81*.
209. Piedra, J., D. Martinez, J. Castano, S. Miravet, M. Dunach, and A. G. de Herreros. 2001. Regulation of beta-catenin structure and activity by tyrosine phosphorylation. *J Biol Chem 276:20436*.

210. Muller, T., A. Choidas, E. Reichmann, and A. Ullrich. 1999. Phosphorylation and free pool of beta-catenin are regulated by tyrosine kinases and tyrosine phosphatases during epithelial cell migration. *J Biol Chem 274:10173*.
211. Roura, S., S. Miravet, J. Piedra, A. Garcia de Herreros, and M. Dunach. 1999. Regulation of E-cadherin/Catenin association by tyrosine phosphorylation. *J Biol Chem 274:36734*.
212. Hayashi, T., T. Takahashi, S. Motoya, T. Ishida, F. Itoh, M. Adachi, Y. Hinoda, and K. Imai. 2001. MUC1 mucin core protein binds to the domain 1 of ICAM-1. *Digestion 63 Suppl 1:87*.
213. Zhang, K., D. Baeckstrom, H. Brevinge, and G. C. Hansson. 1997. Comparison of sialyl-Lewis a-carrying CD43 and MUC1 mucins secreted from a colon carcinoma cell line for E-selectin binding and inhibition of leukocyte adhesion. *Tumour Biol 18:175*.
214. Zhang, K., D. Baeckstrom, H. Brevinge, and G. C. Hansson. 1996. Secreted MUC1 mucins lacking their cytoplasmic part and carrying sialyl-Lewis a and x epitopes from a tumor cell line and sera of colon carcinoma patients can inhibit HL-60 leukocyte adhesion to E-selectin-expressing endothelial cells. *J Cell Biochem 60:538*.
215. Fernandez-Rodriguez, J., O. Dwir, R. Alon, and G. C. Hansson. 2001. Tumor cell MUC1 and CD43 are glycosylated differently with sialyl-Lewis a and x epitopes and show variable interactions with E-selectin under physiological flow conditions. *Glycoconj J 18:925*.
216. Favero, J., and V. Lafont. 1998. Effector pathways regulating T cell activation. *Biochem Pharmacol 56:1539*.
217. Tangemann, K., A. Bistrup, S. Hemmerich, and S. D. Rosen. 1999. Sulfation of a high endothelial venule-expressed ligand for L-selectin. Effects on tethering and rolling of lymphocytes. *J Exp Med 190:935*.
218. Jutila, M. A., S. Kurk, L. Jackiw, R. N. Knibbs, and L. M. Stoolman. 2002. L-selectin serves as an E-selectin ligand on cultured human T lymphoblasts. *J Immunol 169:1768*.
219. Weber, K. S., G. Ostermann, A. Zernecke, A. Schroder, L. B. Klickstein, and C. Weber. 2001. Dual role of H-Ras in regulation of lymphocyte function antigen-1 activity by stromal cell-derived factor-1alpha: implications for leukocyte transmigration. *Mol Biol Cell 12:3074*.
220. Bechard, D., A. Scherpereel, H. Hammad, T. Gentina, A. Tsicopoulos, M. Aumercier, J. Pestel, J. P. Dessaint, A. B. Tonnel, and P. Lassalle. 2001. Human endothelial-cell specific molecule-1 binds directly to the integrin CD11a/CD18 (LFA-1) and blocks binding to intercellular adhesion molecule-1. *J Immunol 167:3099*.
221. Liu, L., B. R. Schwartz, J. Tupper, N. Lin, R. K. Winn, and J. M. Harlan. 2002. The GTPase Rap1 regulates phorbol 12-myristate 13-acetate-stimulated but not ligand-induced beta 1 integrin-dependent leukocyte adhesion. *J Biol Chem 277:40893*.
222. Giblin, P. A., S. T. Hwang, T. R. Katsumoto, and S. D. Rosen. 1997. Ligation of L-selectin on T lymphocytes activates beta1 integrins and promotes adhesion to fibronectin. *J Immunol 159:3498*.
223. Sigal, A., D. A. Bleijs, V. Grabovsky, S. J. van Vliet, O. Dwir, C. G. Figdor, Y. van Kooyk, and R. Alon. 2000. The LFA-1 integrin supports rolling adhesions on ICAM-1 under physiological shear flow in a permissive cellular environment. *J Immunol 165:442*.
224. Chan, J. R., S. J. Hyduk, and M. I. Cybulsky. 2000. Alpha 4 beta 1 integrin/VCAM-1 interaction activates alpha L beta 2 integrin-mediated adhesion to ICAM-1 in human T cells. *J Immunol 164:746*.

225. Roy, S., C. K. Sen, H. Kobuchi, and L. Packer. 1998. Antioxidant regulation of phorbol ester-induced adhesion of human Jurkat T-cells to endothelial cells. *Free Radic Biol Med 25:229*.
226. Koga, T., K. Claycombe, and M. Meydani. 2002. Homocysteine increases monocyte and T-cell adhesion to human aortic endothelial cells. *Atherosclerosis 161:365*.
227. Piller, V., F. Piller, and M. Fukuda. 1990. Biosynthesis of truncated O-glycans in the T cell line Jurkat. Localization of O-glycan initiation. *J Biol Chem 265:9264*.
228. Ju, T., and R. D. Cummings. 2002. A unique molecular chaperone Cosmc required for activity of the mammalian core 1 beta 3-galactosyltransferase. *Proc Natl Acad Sci U S A 99:16613*.
229. Schlaepfer, D. D., S. K. Hanks, T. Hunter, and P. van der Geer. 1994. Integrin-mediated signal transduction linked to Ras pathway by GRB2 binding to focal adhesion kinase. *Nature 372:786*.
230. Cepek, K. L., D. L. Rimm, and M. B. Brenner. 1996. Expression of a candidate cadherin in T lymphocytes. *Proc Natl Acad Sci U S A 93:6567*.
231. Chung, E. J., S. G. Hwang, P. Nguyen, S. Lee, J. S. Kim, J. W. Kim, P. A. Henkart, D. P. Bottaro, L. Soon, P. Bonvini, S. J. Lee, J. E. Karp, H. J. Oh, J. S. Rubin, and J. B. Trepel. 2002. Regulation of leukemic cell adhesion, proliferation, and survival by beta-catenin. *Blood 100:982*.
232. Axelsson, B., R. Youseffi-Etemad, S. Hammarstrom, and P. Perlmann. 1988. Induction of aggregation and enhancement of proliferation and IL-2 secretion in human T cells by antibodies to CD43. *J Immunol 141:2912*.
233. Pedraza-Alva, G., L. B. Merida, S. J. Burakoff, and Y. Rosenstein. 1998. T cell activation through the CD43 molecule leads to Vav tyrosine phosphorylation and mitogen-activated protein kinase pathway activation. *J Biol Chem 273:14218*.
234. Pedraza-Alva, G., L. B. Merida, S. J. Burakoff, and Y. Rosenstein. 1996. CD43-specific activation of T cells induces association of CD43 to Fyn kinase. *J Biol Chem 271:27564*.
235. Kasinrerk, W., N. Tokrasinwit, S. Moonsom, and H. Stockinger. 2000. CD99 monoclonal antibody induce homotypic adhesion of Jurkat cells through protein tyrosine kinase and protein kinase C-dependent pathway. *Immunol Lett 71:33*.
236. Mukherjee, P., A. R. Ginardi, C. S. Madsen, C. J. Sterner, M. C. Adriance, M. J. Tevethia, and S. J. Gendler. 2000. Mice with spontaneous pancreatic cancer naturally develop MUC-1-specific CTLs that eradicate tumors when adoptively transferred. *J Immunol 165:3451*.
237. Spicer, A. P., G. Parry, S. Patton, and S. J. Gendler. 1991. Molecular cloning and analysis of the mouse homologue of the tumor-associated mucin, MUC1, reveals conservation of potential O-glycosylation sites, transmembrane, and cytoplasmic domains and a loss of minisatellite-like polymorphism. *J Biol Chem 266:15099*.
238. Vos, H. L., Y. de Vries, and J. Hilkens. 1991. The mouse episialin (Muc1) gene and its promoter: rapid evolution of the repetitive domain in the protein. *Biochem Biophys Res Commun 181:121*.
239. Kingsmore, S. F., A. P. Spicer, S. J. Gendler, and M. F. Seldin. 1995. Genetic mapping of the tumor-associated mucin 1 gene on mouse chromosome 3. *Mamm Genome 6:378*.
240. Braga, V. M., L. F. Pemberton, T. Duhig, and S. J. Gendler. 1992. Spatial and temporal expression of an epithelial mucin, Muc-1, during mouse development. *Development 115:427*.

241. Pimental, R. A., J. Julian, S. J. Gendler, and D. D. Carson. 1996. Synthesis and intracellular trafficking of Muc-1 and mucins by polarized mouse uterine epithelial cells. *J Biol Chem 271:28128*.
242. Jentoft, N. 1990. Why are proteins O-glycosylated? *Trends Biochem Sci 15:291*.
243. Chen, D., S. Koido, Y. Li, S. Gendler, and J. Gong. 2000. T cell suppression as a mechanism for tolerance to MUC1 antigen in MUC1 transgenic mice. *Breast Cancer Res Treat 60:107*.
244. Parry, G., J. Li, J. Stubbs, M. J. Bissell, C. Schmidhauser, A. P. Spicer, and S. J. Gendler. 1992. Studies of Muc-1 mucin expression and polarity in the mouse mammary gland demonstrate developmental regulation of Muc-1 glycosylation and establish the hormonal basis for mRNA expression. *J Cell Sci 101 (Pt 1):191*.
245. Braga, V. M., and S. J. Gendler. 1993. Modulation of Muc-1 mucin expression in the mouse uterus during the estrus cycle, early pregnancy and placentation. *J Cell Sci 105 (Pt 2):397*.
246. Xing, P. X., C. Lees, J. Lodding, J. Prenzoska, G. Poulos, M. Sandrin, S. Gendler, and I. F. McKenzie. 1998. Mouse mucin 1 (MUC1) defined by monoclonal antibodies. *Int J Cancer 76:875*.